NIST Technical Note
NIST TN 2303

# The Character of Burning Residential and Office Items

Anthony Hamins
Giovanni Di Cristina
Matthew Bundy
Tony Chakalis
Marco Fernandez
Ickchan Kim
Selvarajah Ramesh
Mauro Zammarano

This publication is available free of charge from:
https://doi.org/10.6028/NIST.TN.2303

NATIONAL INSTITUTE OF
STANDARDS AND TECHNOLOGY
U.S. DEPARTMENT OF COMMERCE

**NIST Technical Note**
**NIST TN 2303**


# The Character of Burning Residential and Office Items


Anthony Hamins
Giovanni Di Cristina
Matthew Bundy
Tony Chakalis
Marco Fernandez
Ickchan Kim
Selvarajah Ramesh
Mauro Zammarano
*Fire Research Division*
*Engineering Laboratory*



This publication is available free of charge from:
https://doi.org/10.6028/NIST.TN.2303

March 2025

U.S. Department of Commerce
*Howard Lutnick, Secretary*

National Institute of Standards and Technology
*Craig Burkhardt, Acting Under Secretary of Commerce for Standards and Technology and Acting NIST Director*

NIST TN 2303
March 2025



**Publication History**
Approved by the NIST Editorial Review Board on 2024-08-30

**How to Cite this NIST Technical Series Publication**
Hamins A, Di Cristina G, Bundy M, Chakalis T, Fernandez M, Kim I, Ramesh S, Zammarano M (2025) The Character of Burning Residential and Office Items. (National Institute of Standards and Technology, Gaithersburg, MD), NIST Technical Note (TN) NIST TN 2303. https://doi.org/10.6028/NIST.TN.2303

**Author ORCID iDs**
Anthony Hamins: 0000-0001-7531-4256
Giovanni Di Cristina Torres: 0000-0002-0799-3418
Matthew Bundy: 0000-0002-1138-0307
Tony Chakalis: 0009-0004-4331-7101
Marco Fernandez: 0000-0002-4227-8866
Ickchan Kim: 0000-0001-9089-0403
Selvarajah Ramesh: 0000-0002-9525-6767
Mauro Zammarano: 0000-0002-5145-7110

**Contacte Information:**
anthony.hamins@nist.gov

**Abstract**

This report of test describes a series of experiments that investigated the burning behavior of single items and assemblies commonly found in offices and residences, including chairs, sofas, mattresses with pillows and bedclothes, and some miscellaneous items such as laptops, bookshelves, and side tables. The measurements were conducted in the open under fully-ventilated and quasi-quiescent conditions. The global measurements reported include the transient, peak and total heat release rates, the yields of CO and soot, and the mass loss. The appearance of the fires was captured by video cameras from two orthogonal views. Measurements of the heat flux to the surroundings from the test specimens were used to estimate the radiative fraction of the fires. The data generated from the study are included in the NIST Fire Calorimetry Database (FCD), which links to this report.

**Keywords**
burning rate; commodity fires; fire calorimetry database; furniture fires; heat release rate; radiative emission

## Table of Contents

**List of Tables**



## List of Figures

**Acknowledgments**

The authors are grateful to Phillip Deardorff, Laurean DeLauter, and Artur Chernovsky of NIST for their outstanding technical support during the test series and to Lisa Scott and Greg Masenheimer of the Consumer Product Safety Commission (CPSC) for their expert guidance on conducting the mattress flammability standard test (16 CFR 1633). Thanks also go to Lisa Scott for very helpful discussions.

## 1. Introduction

This report of test describes a series of fire experiments that investigate the burning characteristics of single items and assemblies typically found in residences and offices, burning under fully-ventilated and quasi-quiescent conditions. This study expands the NIST Fire Calorimetry Database (FCD). This report contains only a cursory analysis of the results. A full analysis of the measurement results, characterizing the burning behavior of the specimens and the implications for fire safety and fire protection design will be addressed in future publications.

The FCD contains hundreds of measurement results of fire experiments conducted since 2017 at NIST's National Fire Research Laboratory (NFRL). The FCD is used by fire protection engineers to support engineering analysis including performance-based design, as well as by fire safety science researchers interested in calorimetric information about specific types of items. The test specimens contained in the database include a variety of single burning items, fully furnished rooms, controlled burners, well characterized fuels, and composite fuels typically of unknown composition. Table 1 lists the information typically provided in the FCD for each dataset. Accompanying information includes a summary of the measurement results, their uncertainty, and the experimental test conditions. An emphasis of the FCD is the accuracy of the transient heat release rate (HRR) measurement and its uncertainty [Bryant and Bundy 2019]. The data generated from this study is included in the FCD, which links to this report.

**Table 1. Parameters reported in the Fire Calorimetry Database (FCD)**

| FCD Items |
|---|
| brief description of the test specimen, including the type of fuel and its character |
| transient HRR [kW] |
| peak HRR [kW] |
| time to peak HRR [s] |
| total heat released [MJ] |
| quality confirmation of the HRR |
| initial specimen mass [kg] |
| mass change of the specimen [kg] |
| net effective heat of combustion [kJ/g] |
| $O_2$ consumed per change in mass [mol/g] |

| FCD Items |
|---|
| $CO_2$ yield [kg/kg] |
| CO yield [kg/kg] |
| soot yield [kg/kg] |
| test duration [min] |
| baseline exhaust flow [kg/s] |
| exhaust hood size [m] |
| effective exhaust duct diameter [m] |
| exhaust flow correction factor [-] |
| net heat of combustion (per unit mass of O2) [kJ/g] |
| net heat of combustion (per unit mass fuel) [kJ/g] |
| exhaust hood size [$m^2$] |

The items selected for characterization in this study are commonly found in offices and residences, such as upholstered furniture, which continues to be the leading cause of annual residential fire deaths in the U.S., causing about 570 deaths (about 22 % of the civilian deaths in home fires), 900 civilian injuries, and $357 million in direct property damage (averaged over 2013 to 2017) [Ahrens 2019]. After upholstered furniture, mattresses and bedding are the next leading items involved in civilian fire deaths [Ahrens 2019; 2021]. As furniture has changed with the use of thermoplastics in place of natural fibers, fires grow faster and larger [Kerber 2011]. The percentage of fires that begin with ignition of either upholstered furniture or mattresses and bedding in 2016 to 2020 more than doubled as compared to 1980 to 1984 with the death rate per 1,000 reported home fires over the last 40 years also increasing [Hall 2023]. Upholstered furniture and mattresses (or bedding) also frequently act as secondary fuel sources, operating as the key contributors to the spread of fire and casualties, even if they are not the initial items ignited [Ahrens 2021]. Considering items that contributed most to fire spread along with those that were the first item ignited, Ahrens [2021] found that the combination of upholstered furniture and mattress or bedding fires accounted for 34 percent of fire deaths in the 2013 to 2017 time period.

Over the last few decades, there have been many research studies on the flammability of modern furniture, demonstrating the complex nature of soft furnishing fires, the most hazardous of which involve flexible polyurethane foam (PUF) and thermoplastic fabrics. The fire behavior of items containing such materials includes transient phenomena involving ignition, fire-spread, heat release, liquefaction, dripping and pool fire formation, as well as compartment effects. Except for highly specific situations, prediction of the spread and growth of furniture fires is currently not practical and is the subject of active research [Brown 2018]. For this reason, a fire calorimetry database including items in the present marketplace are needed for fire protection engineering applications.

As the modern fire protection engineering field has developed over the last several decades, engineering design of buildings has moved from prescriptive to performance-based fire protection analysis and design of buildings (PFD). PFD is a process by which engineers develop fire protection measures that provide acceptable levels of safety without imposing unnecessary constraints on other aspects of building design and operation. PFD considers realistic fire scenarios and the response of the building contents, its occupants, fire protection systems, and the structure itself [Alvarez 2013]. The process involves postulated "design fires" that include specification of fire heat release rates for the occupancy type of interest. To accomplish PFD, full-scale data are commonly used because neither modeling, small-scale test results, nor a combination of the two can be reliably used to predict the complex fire behavior of an actual burning item, except for highly-researched and limited cases [Sundström 1995; Zammarano 2021]. There are simply too many physical, geometric, and design scenario attributes that can influence the burning behavior of a fire. These attributes include a specimen's material properties, its dimensions, its configuration, and how it is assembled among other issues [Babrauskas 1985; Sundström 1995; 2021; Zammarano, 2020]. The heat release rate data reported in this study can be useful in the application of PFD.

According to fire loss statistics from the National Fire Protection Association (NFPA), the majority of reported fires in public assemblies, educational, institutional, business, and residential settings are confined to the room of origin [Hall, 2023]. Thus, the burning character of a single item or assembly such as those tested here, can have a significant impact on the development of a fire and its heat release rate. Testing items in the open (not in a room) under well-ventilated conditions provides an understanding of how an item begins to burn if it was, for example, the first item ignited in a generic fire scenario such as in a room or compartment. This approach allows direct comparison of the burning character of different items burning under the same conditions.

According to the NFPA, soft furnishing fires including upholstered furniture and mattresses most often ignite with smoking materials, presumably mainly cigarettes [Hall, 2023]. Other prevalent ignition scenarios of soft furnishings involve small flames associated with candles or matches. As commodity products have transitioned to the heavy use of thermoplastics and synthetic polymers in general, studies of the fire behavior of soft furnishings manufactured before the 2000s are becoming less relevant. New HRR data is constantly needed as materials and assemblies available in the marketplace change.

This report is broken into five main sections. Four appendices contain photos of the experiment and plots of the transient load cell and heat release rate measurements.

## 1.1. Previous Work

Table 2 provides a brief survey of fire experiments over the last 25 years that have measured the transient HRR of residential and office items such as bedding and furniture burning as a single item in the open under well-ventilated conditions or within a compartment. The table notes the range of peak HRRs measured, which varies from about 150 kW to 6300 kW. This large range is due to the very different experimental configurations, geometries, and materials associated with each of the burning items. Babrauskas [2016] provides a compendium of studies over the last 30 years that characterize the HRR of a comprehensive variety of single burning items including those commonly found in both residences and offices. The transient HRR results for a wide variety of items are presented including soft furnishings such as chairs, sofas, and mattresses - many composed of PUF and thermoplastic fabrics. This study complements the results presented in the previous studies, providing HRR measurement results for items currently available in the marketplace.

**Table 2. Some previous studies measuring the heat release rate (HRR) of residential and office items.**

| Reference | Specimen | Compartment? | Peak HRR (kW) |
|---|---|---|---|
| Gratkowski [2020] | bed clothes | no | not reported |
| Bwalya [2015] | bed clothes | yes | 200 to 390 |
| Bwalya [2015] | bed assemblies | yes | 1800 to 6260 |
| Ohlemiller [2003, 2005] | mattresses | yes | 200 to 1000 |
| Bwalya [2015] | mattresses | yes | 1810 to 3800 |
| Sundström [2021] | mattresses | yes | 200 to 2000 |
| Sundström [2021] | chairs | yes | 200 to 1600 |
| Lock [2016] | upholstered chairs | no | 370 to 1910 |
| Mehta [2012] | upholstered chairs | no | 750 to 1850 |
| Morrisset [2024] | upholstered chairs | no | 145 to 320 |
| Bwalya [2015] | upholstered chairs | yes | 450 to 3360 |
| McKinnon [2021] | upholstered furniture | no | 660 to 2830 |
| Sundström [2021] | sofas | yes | 1400 to 2300 |
| Guillaume [2020] | sofas | no | 580 to 1510 |
| Bwalya [2015] | computer workstation | yes | 1800 |
| Blais [2015] | flat screen television | yes | 310 |

Mattresses or bedding and upholstered furniture have been the leading items first ignited in home structure fires for decades [Ahrens 2019]. And although the death toll from upholstered furniture and mattresses or bedding has fallen, the death rates per 1,000 reported fires beginning with these items in 2013 to 2017 is more than twice as high as in 1980 to 1984. The regulation of residential upholstered furniture in the USA has been changing. The Consumer Product Safety Commission (CPSC) enforces two fire safety standards for mattresses and one for upholstered furniture [16 CFR Part 1632; 16 CFR Part 1633; 16 CFR Part 1640]. In 2021, a cigarette ignition test enumerated in the state of California Technical Bulletin TB 117-2013 was adopted as a national standard referenced by 16 CFR Part 1640 [HR 133]. The mattress standards address both smoldering and flaming ignition, whereas the furniture standard only addresses the smoldering resistance of materials used in upholstered furniture. There are no regulatory requirements for the flammability of bedclothes.

Nazaré [2012] reported on the factors that can impact the behavior of a mattress fire such as the construction type, geometry, the mattress size, and the propensity of component materials to ignite and the rate at which they burn. Ohlemiller [2000, 2003, 2005] conducted important studies on the flammability of mattresses and bedclothes. A key aspect of Ohlemiller's research was to design gas burners that mimic the thermal load imposed on a mattress by burning bedclothes [Ohlemiller 2000]. The work led to the development of the test method that is the basis of 16 CFR Part 1633, the Standard for the Flammability (Open Flame) of Mattress Sets. Ohlemiller investigated the burning of bedclothes on a twin mattress that were contemporaneous at the time, including a single pillow, two sheets, a mattress pad, an acrylic blanket and a medium weight comforter. Various combinations of components were used that included (fitted and flat) sheets and a pillowcase made either of cotton or a 50/50 polyester/cotton blend. The composition of the comforters used in the study was a 50/50 polyester/cotton with 100 % polyester fiber fill. The combustion of polyester/cotton blended fabrics are known to be more hazardous than the individual components due to a scaffolding effect by which the cotton component chars to form a skeleton while the polyester melts, covering the skeleton, where it readily provides fuel for a fire. The blends ignite more easily, burn more intensely, and thermally decompose faster than the individual components [Xie 2024].

The 16 CFR 1633 regulation specifies the flammability performance requirements for a mattress that should be met before sale in the United States. The requirements specify that the peak HRR must be less than 200 kW during the 30 min test and that the total heat release be less than 10 MJ during the first 10 min of the test. Since the experiments were conducted on twin size mattresses, Ohlemiller [2005] cautioned that larger size beds could present a larger fire threat and thermal insult onto a mattress. Ohlemiller [2005] conducted tests on three types of custom-made mattresses with greatly reduced flammability relative to practice at the time, each using different types of barrier materials. A set of "heavy bedclothes" were ignited by a match-size flame. Ohlemiller [2005] found that even for the mattress type with the best fire resistance, the peak HRRs were large enough (greater than 200 kW) to pose a serious threat in a realistic bedroom context for the queen and, especially, the king size mattress with bedclothes. For all three mattress designs, the bedclothes fires yielded controlled fires for the twin size but runaway fires for the king size. The findings showed that mattress flammability as well as bed size played a significant role in fire hazard. There have been few experimental studies that have examined the HRR of modern bedding assemblies sold in the USA since the work of Ohlemiller.

There have been, however, many studies on the flammability performance of full-scale furniture, some conducted in a room and some in the open under fully ventilated conditions (see Table 2). Several of the studies investigated the fire performance of chairs constructed with specified fabrics and foams with and without fire barriers. Guillaume [2020] conducted experiments to evaluate the fire performance of sofas purchased in 27 countries across Europe. Only sofas from countries with regulations that require no ignition by a cigarette and a small flame, or no ignition by a cigarette, a small flame and wood crib, showed a noticeable improvement in fire performance. The rapid rise in the HRR of furniture fires occurs after the ignition of flammable liquid products beneath the burning object, where the liquefaction and dripping of PUF lead to the formation of a pool fire [Ohlemiller 1995; Sundström 1995, 2021; Zammarano 2020]. In the presence of a fire barrier fabric, the liquefaction of PUF is delayed due to reduced heat transfer from the flame to the padding material. Additionally, the liquid pyrolyzates must percolate through the fire barrier to reach the underside of the burning item before igniting. These mass and heat transfer processes are the primary mechanisms by which a fire barrier functions [Thompson 2021].

The way and extent by which the composition and thickness of padding material in the seat cushions of a sofa affects fire growth and pool fire formation has not been investigated to date. Similarly, a literature review suggests that there is only one study conducted 30 years ago that investigated the effect of flaming ignition location on fire development on a full-size upholstered chair. The sole conclusion of the study was that location can significantly affect fire growth [Mitler 1994]. To close these gaps, this study investigated igniting sofas at three distinct locations and varying the composition and thickness of the padding material in the seat cushions.

The experiments conducted in this study also complement previous studies and expand the [NIST Fire Calorimetry Database (FCD),] providing comprehensive calorimetric information (see Table 1) with known certainty as well as a video record of fires burning items commonly found in residences and offices. The next section describes the experimental apparatus and procedures.

## 2. Experimental Details

The experiments investigated the burning of items in the open under quasi-quiescent conditions (without an applied wind field). The experiments were conducted under two separate exhaust hood calorimeters at the National Fire Research Laboratory (NFRL). The sections below describe the setup, instrumentation, and procedures used in the experimental campaign.

### 2.1. Experimental Setup

Tests were run under a 3 m × 3 m canopy hood with a capacity of 500 kW or a 9 m × 12 m canopy exhaust hood with a 10 MW capacity. Both hoods were instrumented with oxygen consumption calorimetry. Details about calorimetry, measurement method, its calibration, and measurement uncertainty are documented in Bryant and Bundy [2019]. The exhaust flow was adjusted depending on the anticipated HRR. The exhaust flow ranged between 1 kg/s to 10 kg/s in the 500 kW hood and between 20 kg/s to 40 kg/s in the 10 MW hood. The exact exhaust flow for each test is listed in the FCD output.

Figure 1 shows the experimental layout for the 500 kW canopy hood. A large round exhaust duct (0.48 m diameter) was located 4.1 m above the floor. Side skirts located 1.8 m above the floor surrounded the exhaust hood. Below the side skirts, the experimental area on the east and north sides was surrounded by a double-layered, fine wire mesh screen (6 mesh/cm) to reduce ambient air currents. The test specimen was placed directly below the center of the exhaust duct.

Figure 2 shows the experimental set-up for the 9 m × 12 m hood, which was analogous. For practical reasons, mesh screens were not used under this hood. The 2.0 m diameter round exhaust duct was located 8.7 m above the floor. The side skirts were located 3.1 m above the floor.

### 2.2. Instrumentation

Measurements conducted as part of the experimental campaign described in this report included all the normally reported items in the FCD (see Table 1) plus the following:

- radiative heat flux to targets and an estimate of the radiative fraction of each fire;
- transient mass loss for Test 1 to Test 24;
- yield of hydrogen cyanide (HCN) determined via Fourier Transform Infrared Spectroscopy (FTIR) gas analysis of the extracted gas samples from the exhaust duct;
- video camera record from two orthogonal views.

The data acquisition rate was set at 1 Hz. A description of each of these measurements follows.

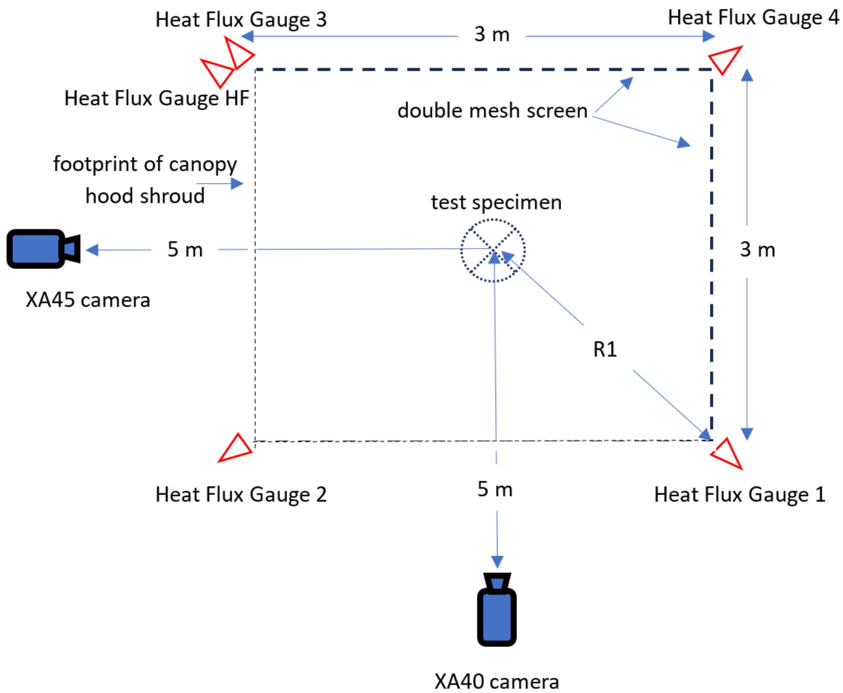


**Figure 1. Schematic of the experimental setup under the 3 m × 3 m exhaust hood and calorimeter.**

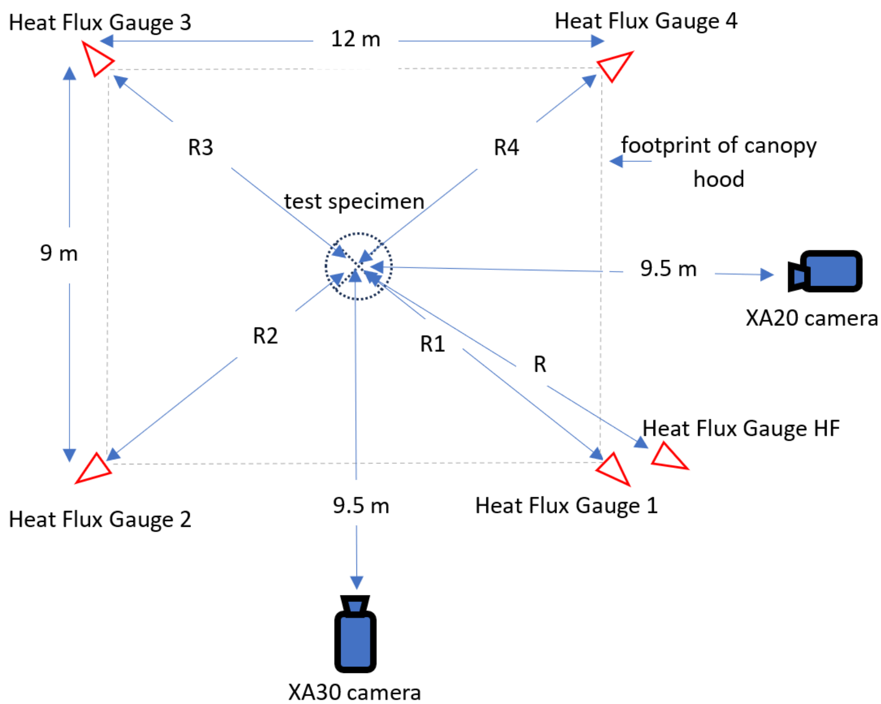


**Figure 2. Schematic of the experimental setup under the 9 m × 12 m exhaust hood and calorimeter.**

### 2.2.1. Radiative Heat Flux to Targets

Five water-cooled, wide-view angle (180°), thermopile-type, total heat flux sensors were directed towards the central axis of the fire. Four of the gauges (Huskeflux model SBG01) were located every 90 degrees about the fire at about the same distance from the center of the specimen. The gauges were placed at a radial distance of about 3 m (in the 3 m hood) and 6 m (in the 9 m x 12 m hood) from the center of the specimen, depending on the anticipated fire size and the available space (i.e., which canopy hood was being used). A fifth gauge (Medtherm 64 series heat flux transducer; designated as "HF") placed at a different distance than the other gauges was also used as noted in Table 3.

**Table 3. Heat flux gauge locations.**

| Test No. | Heat Flux Gauge | R (cm) | Z (cm) |
|---|---|---|---|
| 1 - 20 | HF | 300 | 100 |
| | HF1 | 302 | 100 |
| | HF2 | 300 | 100 |
| | HF3 | 298 | 100 |
| | HF4 | 203 | 100 |
| 21 - 48 | HF | 700 | 87 |
| | HF1 | 610 | 100 |
| | HF2 | 610 | 100 |
| | HF3 | 610 | 100 |
| | HF4 | 600 | 104 |

An estimate of the total radiative energy ($TRE_i$) measured over the entire burn at the $i^{th}$ heat flux gauge was determined by integrating the measured radiative heat flux over the entire duration of the fire at each of the measurement locations:

$$TRE_i = \int_0^{t_e} 4\pi \, R_i^2 \, \dot{q}_i'' \, dt \qquad (1)$$

where ($\dot{q}_i''$) is the radiative heat flux measured at a distance ($R_i$) from the fire at the $i^{th}$ gauge and $t_e$ is the time at the end of the test. For suitably far distances from the fire, the ratio of the average total radiated energy to the surroundings ($\overline{TRE_i}$) and the idealized total heat release rate can be used to estimate the radiative fraction ($\chi_{rad}$) of the fire as defined in Eq. 2:

$$\chi_{rad} = \frac{\overline{TRE_i}}{\Delta m \, H_c} \qquad (2)$$

where $\Delta m$ is the total mass loss, that is, the difference between the initial mass and final specimen mass and $H_c$ is the net heat of combustion of the fuel per unit mass of oxygen (taken here as 13.1 kJ/g ± 0.5 kJ/g) [Bryant and Bundy 2019], assuming water as a gaseous product.

### 2.2.2. Mass Loss

The mass before and after each experiment was always determined. For Test 1 to Test 24, the transient mass loss was determined using calibrated load cells (Test 1 to Test 20:RADWAG APP 60.R1; Test 21 to Test 24: Metler Toledo Jagxtreme). The test specimen was positioned on a metal pan sitting on the load cell. A piece of gypsum board (2 cm thick) was placed between the load cell and the pan to reduce heat transfer from the fire to the load cell.

### 2.2.3. Yields of Exhaust Products

The mass flows of CO, $CO_2$, and HCN in the exhaust stream was measured using gas analyzers and soot was determined using a laser transmission measurement across the exhaust duct following the method described by Bryant and Bundy [2019].

Bryant and Bundy [2019] describe the CO and $CO_2$ gas analysis measurement system, which is part of the calorimetry system. Gas was extracted from the exhaust duct stream and the transient concentrations of CO and $CO_2$ were measured using non-dispersive infrared analyzers.

A Thermo Scientific Antaris IGS Fourier Transform Infrared (FTIR) Gas Analyzer tapped into the exhaust sampling line (before the calorimetry conditioning system) to determine the concentration of trace gas species including HCN. A particulate filter was installed to prevent soot from entering the FTIR gas cell. The FTIR features a 10 m path length and 2 L volume. The FTIR provides information on the concentrations of many species including CO, $CO_2$, and HCN. For complex gas mixtures such as combustion gases, sensitivity is limited by spectral interferences, enabling practical detection of species concentrations as low as approximately 100 ppm. The time response of the FTIR measurements is on the order of 24 s.

From the velocity and temperature measurements made in the exhaust stream, the total transient exhaust mass flow rate was determined as a function of time. The species yields are the ratio of the integrated value of the transient species mass flows to the change in the specimen mass over the duration of the experiment. A detailed discussion on the determination of the species measurements and the yield calculations is provided in Di Cristina Torres [2024] and Bryant and Bundy [2019].

### 2.2.4. Video Record

Two video cameras (Canon models XA40 and XA45 for Test 1 to Test 20 and Canon models XA20 and XA30 for Test 21 to Test 48) recorded the fire at 30 frames/s and 1920 x 1104 resolution. The cameras captured videos of the specimens from orthogonal views as seen in Figs. 1 and 2. During the burning of sofas A and B (Tests 29, 30, 35, 36, 40 and 41), a webcam was also positioned underneath the sofa to provide a view of the formation of the liquid pool associated with liquefaction of the polyurethane foam cushions [Thompson 2021]. The cameras were positioned to capture the fires in their entirety. The camera to specimen distance was 5 m for Test 1 to Test 20 and 9.5 m for Test 21 to Test 48, while the camera height was kept at 1.5 m. Light-emitting diode (LED) lights were positioned at the same height with a distance of 4 m for Test 1 to Test 20 and 9.5 m for Test 21 to Test 48. The camera shutter speed was set to 1/60 s with a f 4.0 aperture stop. The cameras and instrumentation were synchronized to better than ±2 s [Bryant and Bundy 2019].

### 2.3. Test Specimens

Table 4 lists the residential and office specimens tested in this study. The specimens are listed in the following five categories: pillows, chairs, sofas, mattresses, and miscellaneous items. The initial mass of each test specimen is also listed. The combined expanded (k=2) uncertainty with a 95 % confidence level of the initial and final masses was 20 g, based on repeat measurements, calibration with standard weights, load cell manufacturer information, and sensitivity to the ambient temperature. Appendix A presents photos and a detailed description of the test specimens.

All the mattresses, bedclothes, pillows, sofa loveseats (Tests 29, 35, and 40), sofas with chaise (Tests 30, 36, and 41), and chairs used in Test 23 and Test 24 were purchased as new in 2023. The other chairs and sofas tested were used and estimated to be greater than 30 years old.

A brief description of the test specimens is provided in the next section by specimen category. See Appendix A for a full description of each of the test specimens along with photos overlaid with their dimensions.

#### 2.3.1. Pillows

Six types of pillows were tested individually and then in various group arrangements. The pillows can be described as follows:

- **Pillow A** was a low-density polyester pillow insert with polyester insert cover (50 cm × 50 cm or 20" × 20") covered by a polyester pillow cover.
- **Pillow B** was a PUF ("memory foam") insert with polyester insert cover (50 cm × 50 cm or 20" × 20") covered by a polyester pillow cover.
- **Pillow C** was a duck feather pillow insert with polyester insert cover (50 cm × 50 cm or 20" × 20") covered by a polyester pillow cover.
- **Pillow D** was a polypropylene pillow insert with polyester insert cover (50 cm × 76 cm or 20" × 30") covered by a polypropylene pillow cover.
- **Pillow E** was a down-filled pillow insert (50 cm × 50 cm or 20" × 20") with a cotton insert cover.
- **Pillow F** was a polyester pillow insert (50 cm × 50 cm or 20" × 20") with a shaggy wool pillow cover.

Pillows A to C and E to F were smaller "throw" pillows, whereas Pillow D was a larger "hotel" pillow about a factor of 1.5 more massive.

Pillows A and D were tested three times each (Tests 1, 7, 13, and Tests 4, 11, and 12, respectively) to establish experimental reproducibility. Pillow A was used as the first item ignited for all the sofa experiments (Tests 29, 30, 34 to 36, 40, and 41) and experiments testing the flammability of a laptop, a carpet, and a bookshelf (Tests 15, 28, and 33, respectively). Pillow D was used as the first item ignited in all the mattress tests except Test 42 and Test 43, which did not involve pillows.

Queen size mattresses are the most popular mattress type on the market [Trainer 2023]. Many mattresses are likely to have at least two pillows on them and some may have more than two pillows. For this reason, Test 8 to Test 10 considered the burning of two or more pillows.

### 2.3.2. Chairs

Eleven types of chairs were tested including wheeled chairs, armchairs, stackable chairs, and a beanbag chair. Two types of stackable chairs were tested, stacked in a group of 3 chairs. The chairs can be described as follows:

- Stackable **Chair A** was composed of a metal frame, two hard-plastic contoured seat-back layers, a contoured foam cushion and cover fabric.
- **Chair B** was composed of a wood fame, PUF cushions with blended polyester/cotton fiber batting and a woven-glass backing layer.
- **Chair C** was composed of a wood frame, PUF cushions, and woven fabric seat and back cover.
- Stackable **Chair D** was composed of a metal frame, wood seat and back layers, contoured foam cushions and cover fabric.
- Large desk **Armchair E** (wheels removed) was composed of a wood frame, cover fabric, PUF with cotton batting.
- Beanbag **Chair F** was filled with 9 mm long polystyrene pellets with a loose weave internal polyester cover and an outer polyester cover.
- High-back **Chair G** had a bent wood fame and thin PUF seat cushions with cover fabric identical to that used in [Di Cristina Torres, 2024].
- Large **Armchair H** was composed of a wood frame, PUF cushions, metal springs, thin fiberglass cloth over the foam, a blended cover fabric.
- Stackable **Chair I** with arms was composed of a metal frame, particle board seat and back, PUF seat and back cushions, and cover fabric.
- Wheeled office **Chair J** with arms was composed of a contoured hard plastic frame and backing, PUF seat and back cushions, and cover fabric.
- Wheeled office **Chair K** was composed of a hard plastic frame and arms, a PUF seat cushion and webbed backing.

The chair types were significantly different in terms of dimensions, shapes, and masses (see Appendix A and Table 6).

### 2.3.3. Mattresses

Three types of queen size (152 cm × 203 cm) mattresses were selected for testing based on their popularity (number of reviews) on a widely used Ecommerce marketplace as follows:

- **Mattress A** was a 15 cm thick, single-sided, innerspring mattress with a 12 cm innerspring core. Two layers of PUF (a 2 cm and a 1 cm layer) were situated above the contiguous (unpocketed) metal spring set. The core was encapsulated with a non-woven fire barrier fabric with a thickness of roughly 6 mm. The mattress was enclosed within a knit polyester/polyolefin outer ticking fabric (see Figure A53). Mattress A was used in Test 26 and Test 39.
- **Mattresses B** and **C** had a thickness of 15 cm and 30 cm, respectively, but were otherwise identical. They were both double-sided, flexible polyurethane foam (PUF) core mattresses enclosed by a stretchable knitted fire barrier cover fabric (“FR sock”) which was relatively thin (less than 1 mm), and a knitted polyester outer ticking fabric secured by a zipper on the ticking bottom panel (see Figure A54 and Figure A55). Mattress B was used in Test 31 and Test 37, and Mattress C was used in Tests 32, 38, and 42 to 44. In Test 44, the FR sock was removed.

The mattress tests were conducted with and without bedclothes. All mattress tests (except Test 42 and Test 43 which followed the 16 CFR 1633 test protocol using Mattress C) were conducted with two D pillows overhanging the edge of the mattress by approximately 2 cm.

A box spring foundation was not used in any of the mattress tests. Instead, the mattresses rested on a queen size, flat, steel-slatted, platform frame, which held the mattresses 46 cm above the floor as seen in Figure A26. The solid frame’s slats were separated by 13.5 cm to 14.0 cm, running along the width of the frame. The frame had nine rectangular support legs.

#### 2.3.3.1. Mattress Tests without Bedclothes

The burning of Mattresses A, B, and C without bedclothes — except for two D pillows which were used as the first item ignited — was investigated in Tests 26, 31, and 32, respectively. See the discussion on the ignition method in Section 2.4.

#### 2.3.3.2. Mattress Tests with Bedclothes

The burning of Mattresses A and B with bedclothes was investigated in Test 39 and Test 37, respectively. The bedclothes used in Test 39 included two D pillows (used as the first item ignited), a polyester mattress cover, a 2 cm thick PUF mattress topper, a polyester flat fitted sheet set, and a comforter composed of a polyester cover with polyester fiber fill. The same bedclothes set was used in Test 37, except without the mattress topper. See Appendix A for photos of these tests.

The burning of Mattress C with bedclothes was investigated in Test 38 and Test 44. The same bedclothes set used in Test 37 (see above) was used in Test 38 and Test 44. In Test 44, the mattress was modified by opening its zipper and removing the FR sock.

#### 2.3.3.3. Standard Mattress Flammability Test

Mattress C was tested following the general terms of the 16 CFR 1633 standard mattress flammability test [16 CFR 1633].[1] As specified by the test method, no bedclothes or pillows were present during this test. The test involves subjecting a mattress to top and side burner flames in a specified arrangement for 70 s and 50 s, respectively, providing a total fire energy release of 1.71 MJ. To meet the performance requirements of the 16 CFR 1633 test, the peak HRR during the test must be maintained less than 200 kW during the entire 30 min test and the total heat release at 10 min must be less than 15 MJ [16 CFR 1633].

### 2.3.4. Sofas

Three types of sofas were tested.

- **Sofa A** was a three-person sofa with low armrests, pocket springs, and deep seat foam cushions with a polyester cover fabric.
- **Sofa B** was nearly identical to the structure of Sofa A with the addition of a chaise lounge on its left side (facing the front of the sofa). The chaise section had a relatively large mass, such that Sofa B was about 40 kg heavier than Sofa A (see Table 4).
- **Sofa C** was a used piece of furniture estimated to be greater than 30 years old.

In one series of sofa experiments (Tests 35, 29, and 40), three identical Sofa A specimens were tested, each with the seat cushions modified such that they contained 1, 2, or 3 three layers of PUF as described in Table 4 and the captions of Figure A 35, Figure A29, and Figure A40, respectively.

In another series of sofa experiments (Tests 30, 36, and 41), three identical B Sofas were tested using three different ignition locations (see Figure A30, Figure A36, and Figure A41, respectively), where one A pillow was either positioned on the right arm rest (Test 30), on top of the middle of the sofa seat cushions (Test 36), or on the floor behind the middle of the sofa's back (Test 41).

### 2.3.5. Miscellaneous Items

Several miscellaneous residential and office items were tested including laptops, a side table, a carpet, and a bookshelf. Many of the specimens selected for study were identical to those tested

1. The experiments were conducted under the expert guidance of Consumer Product Safety Commission (CPSC) staff who regularly conduct the 16 CFR 1633 test protocol.

in a series of room fire experiments by Di Cristina Torres [2024], including Pillow A (Test 1), a side table (Test 18), a bentwood armchair (Test 24), a bookshelf (Test 33), and the sofas with chaise (Tests 30, 36, and 41).

Pillow A was used to promote ignition and fire growth in Test 15 (a laptop computer), Test 28 (a carpet), and Test 33 (a bookshelf). Furthermore, Laptop B in Test 15 was folded 45 degrees and supported by two 6 mm diameter metal rods approximately 2 cm above one A pillow. This arrangement prevented the laptop from compressing the pillow. Appendix A presents photos of all the test configurations, including the relative positions of the pillows and the test specimens.

**Table 4. List of test specimens and their initial mass. The combined expanded (k=2) uncertainty of the mass was 0.7 g for Test 1 to Test 25 and 20 g for Test 26 to Test 48. Appendix A presents photos and a detailed description of the specimens.**

| Test No. | Test Specimens | Mass (kg) |
|---|---|---|
| | **Pillows** | |
| 1 | **Pillow A** (repeat of Tests 7 and 13; used in Di Cristina Torres [2024]) | 0.581 |
| 7 | **Pillow A** (repeat of Tests 1 and 13) | 0.574 |
| 13 | **Pillow A** (repeat of Tests 1 and 7) | 0.577 |
| 9 | **Four A** pillows (arranged as seen in Figure A49 of Appendix A) | 2.294 |
| 2 | **Pillow B** | 1.167 |
| 3 | **Pillow C** | 1.042 |
| 4 | **Pillow D** (repeat of Tests 11 and 12) | 0.893 |
| 11 | **Pillow D** (repeat of Tests 4 and 12) | 0.890 |
| 12 | **Pillow D** (repeat of Tests 4 and 11) | 0.896 |
| 8 | **Two D Pillows** (arranged as seen in Figure A8 of Appendix A) | 1.788 |
| 10 | **Four D Pillows** (arranged as seen in Figure A10 of Appendix A) | 3.577 |
| 5 | **Pillow E** | 0.964 |
| 6 | **Pillow F** | 0.742 |
| | **Chairs** | |
| 16 | Stackable **Chair A** (repeat of Test 21 but under the 3 m × 3 m hood) | 9.677 |
| 21 | Stackable **Chair A** (repeat of Test 16 but under the 9 m × 12 m hood) | 9.703 |
| 25 | Three stacked **A Chairs** (identical to those used in Tests 16 and 21) | 29.008 |
| 17 | **Chair B** | 7.424 |
| 19 | **Chair C** | 7.187 |
| 20 | Stackable **Chair D** | 7.279 |
| 47 | **Three** stackable **D chairs** (identical to those used in Test 20) | 23.148 |
| 22 | Large desk **Armchair E** | 10.042 |
| 23 | Beanbag **Chair F** | 2.513 |
| 24 | High-back **Chair G** | 8.872 |
| 27 | Large **Armchair H** | 26.594 |

| Test No. | Test Specimens | Mass (kg) |
|---|---|---|
| 45 | **Three** stackable **I Chairs** | 20.126 |
| 46 | Wheeled office **Chair J** | 17.876 |
| 48 | Wheeled office **Chair K** | 12.368 |
| | **Mattresses** | |
| 26 | **Mattress A** with **two D Pillows** | 25.052 |
| 39 | **Mattress A** with **two D Pillows** (identical to Test 26 with the addition of bedclothes) | 33.086 |
| 31 | **Mattress B** with **two D Pillows** | 16.934 |
| 37 | **Mattress B** with **two D Pillows** (identical to Test 31 but with the same bedclothes as Test 39 but without the mattress topper) | 20.685 |
| 32 | **Mattress C** with **two D Pillows** | 27.534 |
| 38 | **Mattress C** with **two D Pillows** (identical to Test 32 but with the same bedclothes as Test 37) | 31.114 |
| 42 | **Mattress C** without pillows or bedclothes, undergoing the 16 CFR 1633 test protocol | 26.390 |
| 43 | **Mattress C** without pillows or bedclothes (repeat of Test 42) | 26.390 |
| 44 | **Mattress C** with **two D Pillows** (identical to Test 38 but with the mattress' FR sock removed) | 30.890 |
| | **Sofas** | |
| 29 | **Sofa A** with **two A Pillows** (similar to Tests 35 and 40, but with modified seat cushions that included 2 layers of PUF as presented in Figure A49) | 57.638 |
| 35 | **Sofa A** with **two A Pillows** (similar to Tests 29 and 40 but with modified seat cushions that included one layer of PUF as described in Figure A51) | 56.725 |
| 40 | **Sofa A** with **two A Pillows** (similar to Tests 29 and 40, but with modified seat cushions that included three layers of PUF as described in Figure A52) | 58.874 |
| 30 | **Sofa B** with chaise (identical to Tests 36 and 41, but with **two A Pillows** positioned on the armrests) | 96.582 |
| 36 | **Sofa B** with chaise (identical to Tests 30 and 41, but with **two A Pillows** positioned in the middle of the sofa) | 97.393 |
| 41 | **Sofa B** with chaise (identical to Tests 30 and 36, but with **two A Pillows,** one positioned on the left armrest and one behind the middle of the sofa on the floor) | 97.960 |
| 34 | **Sofa C** with **two A Pillows** | 50.849 |
| | **Miscellaneous items** | |
| 14 | **Laptop A** folded at 45 degrees | 1.330 |
| 15 | **Laptop B** folded at 45 degrees positioned over **one A Pillow** | 2.754 |
| 18 | **Side Table** (identical to that used in Di Cristina Torres [2024]) | 3.202 |
| 28 | Polypropylene **Carpet** with **two A Pillows** | 5.489 |
| 33 | **Bookshelf** with **one A Pillow** (identical to that used in Di Cristina Torres [2024]) | 19.540 |

## 2.4. Ignition Method

Table 5 provides a summary of the process used to ignite the specimens for each of the tests. The table lists the igniter power, duration, the total energy applied to ignite the specimen, and if a pillow was used to promote ignition of the primary specimen. The igniter typically used a 89 mL/min propane flow emanating from a ¼ inch (6 mm) outer diameter copper tube, yielding a flame about 1.5 cm in length with a HRR of 128 W. The igniter flame impinged on the specimen for 30 s or longer as seen in Table 5. In some cases, longer ignition durations and/or higher propane flows were used to promote ignition and sustained burning. For the sofa and mattress tests, the igniter flame was positioned next to Pillow A or Pillow D, which acted as an ignition source for the test specimen.

In the first 13 tests, the pillows were angled at 45 degrees and the igniter flame was positioned approximately 1 cm below the middle of the bottom of the pillow as seen in the images in Appendix A. When multiple pillows were tested, the igniter was typically placed between the pillows, where they touched as seen for example in Figure A8.

Ignition of the chairs was achieved by placing the igniter in the chair's crevice (when present) between the chair seat and back cushions. If an air gap existed between the seat and back cushions, then the igniter was placed such that it was 1 cm below the (front side) bottom of the back cushion.

As stated above, all mattress tests (except Test 42 and Test 43) were conducted with two D pillows overhanging the edge of the mattress by about 2 cm. Ignition of the mattresses was achieved by placing the igniter flame approximately 2 cm inside the edge of the mattress and 1 cm above it, just below the intersection of the two pillows (see Figure A31).

In all of the sofa experiments, two A pillows were positioned on top of the sofa or next to it and one of the pillows was used as the first item ignited by the propane igniter.

**Table 5. The average igniter power, duration and total energy applied to the specimen. Uncertainties are reported as the combined expanded (k = 2) uncertainty, representing a 95 % confidence interval.**

| Test No. | Igniter Power (W) | Igniter Duration (s) | Igniter Energy (kJ) | Pillow used to ignite primary object? |
|---|---|---|---|---|
| **Pillows** | | | | |
| 1 | 128 ± 1 % | 90 ± 2 % | 11.6 ± 3 % | No |
| 2 | 128 ± 1 % | 30 ± 7 % | 3.9 ± 7 % | No |
| 3 | 128 ± 1 % | 30 ± 7 % | 3.9 ± 7 % | No |
| 4 | 128 ± 1 % | 30 ± 7 % | 3.9 ± 7 % | No |
| 5 | 128 ± 1 % | 30 ± 7 % | 3.9 ± 7 % | No |
| 6 | 128 ± 1 % | 22 ± 9 % | 2.8 ± 9 % | No |
| 7 | 128 ± 1 % | 30 ± 7 % | 3.9 ± 7 % | No |
| 8 | 128 ± 1 % | 105 ± 7 % | 13.5 ± 2 % | No |
| 9 | 128 ± 1 % | 30 ± 7 % | 3.9 ± 7 % | No |
| 10 | 128 ± 1 % | 31 ± 7 % | 4.0 ± 7 % | No |
| 11 | 128 ± 1 % | 31 ± 7 % | 4.0 ± 7 % | No |

| Test No. | Igniter Power (W) | Igniter Duration (s) | Igniter Energy (kJ) | Pillow used to ignite primary object? |
|---|---|---|---|---|
| 12 | 128 ± 1 % | 30 ± 7 % | 3.9 ± 7 % | No |
| 13 | 128 ± 1 % | 30 ± 7 % | 3.9 ± 7 % | No |
| **Chairs** | | | | |
| 16 | 128 ± 1 % | 75 ± 3 % | 9.6 ± 3 % | No |
| 17 | 128 ± 1 % | 30 ± 7 % | 3.9 ± 7 % | No |
| 19 | 128 ± 1 % | 30 ± 7 % | 3.9 ± 7 % | No |
| 20 | 128 ± 1 % | 30 ± 7 % | 3.9 ± 7 % | No |
| 21 | 256± 1 % | 60 ± 3 % | 14.4 ± 4 % | No |
| 22 | 128 ± 1 % | 40 ± 5 % | 5.1 ± 5 % | No |
| 23 | 128 ± 1 % | 23 ± 9 % | 3.0 ± 9 % | No |
| 24 | 128 ± 1 % | 30 ± 7 % | 3.9 ± 7 % | No |
| 25 | 128 ± 1 % | 63 ± 3 % | 8.1 ± 3 % | No |
| 27 | 128 ± 1 % | 27 ± 7 % | 3.5 ± 8 % | No |
| 45 | 128 ± 1 % | 30 ± 7 % | 3.9 ± 7 % | No |
| 46 | 128 ± 1 % | 60 ± 3 % | 7.7 ± 4 % | No |
| 47 | 128 ± 1 % | 30 ± 7 % | 3.9 ± 7 % | No |
| 48 | 128 ± 1 % | 65 ± 3 % | 8.3 ± 3 % | No |
| **Mattresses** | | | | |
| 26 | 128 ± 1 % | 22 ± 9 % | 2.8 ± 9 % | Two D Pillows |
| 31 | 128 ± 1 % | 30 ± 7 % | 3.9 ± 7 % | Two D Pillows |
| 32 | 128 ± 1 % | 30 ± 7 % | 3.9 ± 7 % | Two D Pillows |
| 37 | 128 ± 1 % | 30 ± 7 % | 3.9 ± 7 % | Two D Pillows |
| 38 | 128 ± 1 % | 30 ± 7 % | 3.9 ± 7 % | Two D Pillows |
| 39 | 128 ± 1 % | 30 ± 7 % | 3.9 ± 7 % | Two D Pillows |
| 42 | A* | 70 ± 1 % | 1706 ± 5 % | No |
| 43 | A* | 70 ± 1 % | 1706 ± 5 % | No |
| 44 | 128 ± 1 % | 30 ± 7 % | 3.9 ± 7 % | Two D Pillows |
| **Sofas** | | | | |
| 29 | 128 ± 1 % | 30 ± 7 % | 3.9 ± 7 % | One A Pillow |
| 30 | 128 ± 1 % | 30 ± 7 % | 3.9 ± 7 % | One A Pillow |
| 34 | 128 ± 1 % | 30 ± 7 % | 3.9 ± 7 % | One A Pillow |
| 35 | 128 ± 1 % | 30 ± 7 % | 3.9 ± 7 % | One A Pillow |
| 36 | 128± 1 % | 43 ± 5 % | 5.5 ± 5 % | One A Pillow |
| 40 | 128± 1 % | 34 ± 9 % | 4.4 ± 9 % | One A Pillow |
| 41 | 128 ± 1 % | 33 ± 7 % | 4.2 ± 7 % | One A Pillow |
| **Miscellaneous items** | | | | |
| 14 | B* | 305 ± 0.3 % | 98.9 ± 2 % | No |
| 15 | 128 ± 1 % | 30 ± 7 % | 3.9 ± 7 % | One A Pillow |
| 18 | 128 ± 1 % | 156 ± 3 % | 20.0 ± 2 % | No |

| Test No. | Igniter Power (W) | Igniter Duration (s) | Igniter Energy (kJ) | Pillow used to ignite primary object? |
|---|---|---|---|---|
| 28 | 128 ± 1 % | 30 ± 7 % | 3.9 ± 7 % | One A Pillow |
| 33 | 128 ± 1 % | 30 ± 7 % | 3.9 ± 7 % | One A Pillow |

*The igniter power was increased over time (*t*) as follows:
A (Tests 42, 43): 9.15 kW ± 1 % (side burner) for $t < 50$ s; 17.84 kW ± 1 % (top burner) for $t < 70$ s
B (Test 14): 128 W ± 1 % for $t < 90$ s; 256 W ± 1 % for 90 s < $t$ < 180 s; 512 W ± 1 % for 180 s < $t$ < 305 s

## 2.5. Test Duration

The specimens were typically allowed to burn to near completion. For some relatively long duration experiments, data acquisition was stopped, and the fire was suppressed when the measured transient HRR was approximately less than 1 percent to 2 percent of the peak HRR.

## 3. Results and Discussion

Table 6 presents a summary of the experimental results organized by specimen category and include the specimen label, the test number, the total specimen mass loss, the residual mass loss, test duration, peak HRR, time to peak HRR, total heat released, and the effective heat of combustion (HOC). The values and uncertainties of each of the parameters listed in Table 6 are provided in the NIST Fire Calorimetry Database (FCD) by test number. The table is grouped by the similitude of the specimens (see Table 4 and Appendix A for a detailed description of the specimens Appendix C shows the measured mass loss as a function of time for Tests 1 to Test 24. Appendix D presents the transient heat release rate measurements for all the tests.

The discussion below emphasizes the measured amount of total heat released (THR) by the fire, its peak HRR, and the net heat of combustion (HOC). The peak HRR provides an idea of the fire size whereas the latter is an indicator of fire hazard — as the peak HRR significantly influences the rate of fire spread and growth [Babrauskas, 1992]. In general, examination of the HOC is a simple way to compare the energy released per unit mass for different materials and configurations.

### 3.1. Pillows

Table 6 shows that the peak HRR for the individual pillows varied from 20 kW to 101 kW, which occurred in less than 3 min after ignition. Pillows A and D were tested three times each, since they were of particular interest. They were used as the first item ignited in most of the experiments, including those investigating the burning of sofas, mattresses, and miscellaneous items such as a bookshelf, a laptop, and a side table. The average THR of Pillow D was almost 10 MJ, about twice that of Pillow A (see Table 6), whereas its total mass was only about 50 % larger than Pillow A. This discrepancy can be attributed to differences in the percentage of the specimen that burned as seen in the values of the residual mass. Consistent with this notion, the average values of the measured HOC for the two pillow types are within 1 % of each other. The HOC for all pillow types was about 17 kJ/g except for pillows B, C, and E. Pillows B and E have somewhat smaller values of HOC. Their inserts were composed of feathers, not thermoplastics. Pillow C, which was composed of memory foam (presumably PUF), had a significantly larger HOC (about 23 kJ/g) and similar to the HOC of PUF (equal to about 26 kJ/g) [Krämer 2010].

### 3.2. Chairs

Table 6 shows that the peak HRRs, the residual masses, and the HOC values for the individual chairs covered a wide range. The HRRs varied from 118 kW for stackable Chair D (Test 20) to 1733 kW for large Armchair K (Test 27), the residual mass was as large as 99 % or as small as nearly zero, and the HOC varied by greater than a factor of 3. This is attributed to the fact that the chairs were extremely different in terms of their shapes, dimensions, masses, age, assembly, and probably composition. As expected, examination of the results showed that both the peak HRR and the THR roughly increased with mass loss. The largest THR measured was for large armchair H, which was composed of a wood frame, PUF cushions, metal springs, and thin fiberglass cloth. Of the chairs, the mass of Chair H was the largest.

Test 47 considered three stacked D Chairs (see Figure A27). The measured HOC was 17.9 kJ/g ± 1.3 kJ/g, whereas the single D chair (Test 20) yielded a HOC value equal to 20.2 kJ/g ± 1.3 kJ/g, which was within experimental uncertainty. The peak HRR was 118 kW or roughly one-third of the single burning D Chair (Test 45). The set of three stackable I chairs (Test 45) yielded a peak HRR of 282 kW, significantly less than the 377 kW peak HRR of the three D chairs (Test 47). This was consistent with the mass of PUF in the chair, which was more than 5 times larger for Chair D (586 g) than for Chair I (112 g).

## 3.3. Mattresses

Table 6 shows that the mattress fires varied widely in terms of the peak HRR and the total heat release. Tests of Mattress A consistently resulted in smaller peak HRRs than tests with either Mattress B or Mattress C. All the tests involved mattresses with two D pillows. Note that innerspring Mattress A included less combustible mass than foam core Mattresses B and C and used a different type of fire barrier fabric. The video recordings of the tests provide insight on the behavior of the fires (see the NIST Fire Calorimetry Database (FCD)). After igniting the pillows, the fire spread about the pillows and then onto the mattresses. The largest flames associated with the tests involving Mattress A (Test 26 and Test 39) appeared to be from the pillows and bedclothes. Tests using Mattress B (Test 31 and Test 37) and Mattress C (Test 32 and Test 38) appeared to behave very differently than the tests involving Mattress A. As the flames spread across the pillows, the volume of the pillows appeared to diminish, likely due to liquefaction of its thermoplastic contents. Large flames appeared on the surface of the mattresses, spreading away from the pillows towards the edges of the mattresses. As the flames spread, the top of the mattresses appeared to char and burn away, exposing the PUF core. Concurrently, flaming drips of molten material fell from the mattress onto the floor, yielding pool fires that grew in size as they heated the bottom of the mattresses, and the molten dripping intensified. The peak HRRs occurred only after the pool fires under the mattresses were present as seen on the test videos available on the NIST Fire Calorimetry Database (FCD).

The peak HRR for mattresses without bedclothes (but with two D pillows) ranged from 0.2 MW for Mattress A (Test 26) to 0.9 MW for Mattress B (Test 31) and 2.8 MW for Mattress C (Test 32). The total energy release followed the same order as the peak HRR with Mattress A yielding a peak HRR of 0.2 MW at 4.7 min after ignition (Test 26) followed by Mattress B with a peak HRR of 0.9 MW at 12.5 min (Test 31), and Mattress C with a peak HRR of 2.8 MW at 16.5 min.

For tests burning mattresses with bedclothes (and two pillows), the peak HRRs followed the same order as the tests without bedclothes. The peak HRR of Mattress A was 0.2 MW at 4.4 min after ignition (Test 39) followed by Mattress B yielding a peak HRR of 3.4 MW at 11.9 min (Test 37), and Mattress C yielding a peak HRR of 4.6 MW at 12.8 min (Test 38). Table 6 shows that this same trend was measured for the total energy released.

The total energy released for the tests with bedclothes was larger than the tests without bedclothes by 16 MJ, 89 MJ, and 90 MJ for Mattresses A, B, and C, respectively. The peak HRRs followed a similar trend. For the fires using Mattress A, the peak HRR was nearly the same with and without (Test 32 and Test 26, respectively) bedclothes. For Mattresses B, the difference in the peak HRRS with and without bedclothes was 2.5 MW (Test 31 and Test 37, respectively), whereas for Mattress C, the difference in the peak HRR was 1.8 MW (Test 32 and Test 38, respectively). The presence of the bedclothes served to increase the thermal insult onto the mattress. These results suggest that the fire barrier fabrics used in Mattress A effectively shielded the flammable PUF core from the fire generated by the bedclothes so its burning rate was only marginally affected by the fire impinging on it, whereas this was not the case for the thinner fire barrier fabric (FR sock) of Mattress B and C with its expected higher thermal conductivity.

A series of tests investigated the flammability of Mattress C (see Section 2.3.3 for a description of the mattresses). Test 42 and Test 43 investigated the ability of the mattress to meet the 16 CFR 1633 flammability test. The results showed that Mattress C passed the 16 CFR 1633 test with a peak HRR of less than 200 kW for 30 min and a total energy release of less than 10 MJ over the first 10 min after the prescribed ignition sequence [16 CFR 1633]. Mattress C was also tested to determine its burning behavior without bedclothes, but with two D pillows (Test 32). This test yielded a peak HRR of 2.8 MW ± 0.1 MW after 16.6 min, exceeding the 16 CFR 1633 allowable HRR. Test 38 investigated the effect of bedclothes (in addition to the pillows) on the burning behavior of Mattress C, leading to a peak HRR of 4.6 MW ± 0.2 MW after 12.8 min, almost 50 % larger in peak fire size and 25 % faster than the no bedclothes case (Test 32).

The last experiment in the series (Test 44) investigated the effect of removing the FR sock from Mattress C with the same bedclothes and pillows as in Test 38. In this case, the barrier was cut and removed and the polyester ticking zipped back into place. The peak HRR in Test 44 was measured as 7.1 MW ± 0.4 MW, which occurred less than 8 min after ignition. This was the largest HRR measured for the Mattress C fires. It's useful to consider the time when the Mattress C fires reached 1.2 MW, which can be considered an indicator of the time available for safe egress for locations beyond the room of fire origin.[2] The times to reach 1.2 MW for the

2. Flashover is estimated to occur after about 3 min for fires larger than 1.2 MW based on the calculation method provided by Karlsson and Quintiere [2000] for a typical residential master bedroom (4.3 m by 4.8 m x 2.4) with 1.6 cm thick gypsum walls and a 0.8 m by 2.0 m open door.

Mattress C tests were 13.4 min (Test 32), 11.8 min (Test 38), and 6.6 min (Test 44). The results of the latter test indicate that the FR sock helped increase the time available for safe egress. The FR sock, however, would not reduce the risk of room flashover for a typical size bedroom, but it would delay its occurrence.

The 16 CFR 1633 test is a performance standard and therefore does not prescribe design elements. Many mattress designs, including Mattresses A, B, and C, use a fire barrier fabric to protect the inner fuel load from the exterior ignition source. As described above, a comparison of Test 44 with Test 38 shows the significant impact a fire barrier can have on the burning behavior of a mattress and the resultant improvement in available egress time.

Although there has been no recent comprehensive study on the flammability of mattresses in the marketplace, CPSC reported that for the 5-year period ending in 2017 (their most recent publication on this topic), about 37 % of mattresses tested for compliance did not pass the 16 CFR 1633 test [Scott 2018]. The CPSC report was careful to note that CPSC mattress surveillance testing does not represent a statistical survey of the marketplace. Failing the 16 CFR 1633 test protocol, however, is not the key issue at hand. In this study, Mattress C passed the 16 CFR 1633 test protocol, but when a couple of pillows were placed on top of the mattress without additional bedclothes and ignited with a 2 cm (87 W) propane flame for 30 s to mimic a possible ignition scenario, the resulting fire (Test 32) yielded a total energy release of 647 MJ and a peak HRR of 2.8 MW, far exceeding the 200 kW peak HRR limit of the 16 CFR 1633 protocol by more than an order of magnitude. As a reference, Test 8 burning two D pillows led to a peak HRR of 81 kW and a total energy release of 9.7 MJ, which is a relatively small value compared to the Test 32 fire, which involved Mattress C with two D pillows, but larger than the ignition source used in 16 CFR 1633 [2025]. These results suggest that the barrier in Mattress B and C performs well with the ignition flame used in 16 CFR 1633 but its effectiveness decreases in the presence of bedclothes and pillows, which once burning, represent a larger ignition source than that applied in 16 CFR 1633.

Mattress B was half as thick as Mattress C. Its burning behavior in Test 31 and Test 37 were similar to those of Mattress C (Test 32 and Test 38, respectively) with the observation of a pool fire under the mattresses before the peak HRR was obtained and with HOC values within about 10 % of each other. As expected, the THR and peak HRRs of Mattress B (with its smaller mass) were smaller than that of Mattress C. Fires on either of these mattresses would likely have led to flashover in a typical residential bedroom.[2]

### 3.4. Sofas

Three types of sofas were tested. Ignition was initiated using a pillow on the sofa armrest for Tests 29, 30, and 34. Table 6 shows that even though it had the smallest mass burned, Sofa C (Test 34) displayed the largest peak HRR, which was greater than 4 MW and larger than the peak HRR during Test 29 and Test 30. Pool fires were observed under all three sofas at about the same time, beginning at 4.30 min for Sofa A in Test 29, at 4.67 min for Sofa C in Test 34, and at 4.70 min for Sofa B in Test 34. The observation of the pool fire typically was associated with the occurrence of a rapid rise and inflection point in the HRR curve (see Appendix D). As expected, the sofas with the largest mass (Test 30) led to the largest total energy release.

The results of Tests 30, 36, and 41 show that the initial ignition location of identical sofas can lead to fires with significantly different fire sizes and times to peak HRR. Test 36 with an A pillow positioned on top of the middle of the sofa seat cushions led to a peak HRR of 5 MW in 5.9 min, whereas Test 41 with Pillow A positioned behind the middle of the sofa's back lead to a peak HRR of 4 MW in 10.7 min. Test 30 with a pillow ignited over the armrest led to a HRR of about 3 MW in 9.2 min. These three arrangements with the same specimens led to three completely different HRR profiles, whereas the total heat released in the fires was the same within less than 1 %.

In another series of experiments (Tests 35, 29, and 40), three identical A sofas were tested, each with the seat cushions modified such that they contained 1, 2, or 3 three layers of PUF, respectively (see Table 4 and the captions of the associated figures in Appendix A for a detailed description of the specimens). The video results show that the cushion with 1 layer of PUF (Test 35) had by far the fastest breakthrough (2.98 min after ignition) of melted/flaming liquid through the cushions, leading to a pool fire underneath the sofa, as compared to over 4 min for the tests with 2 layers and 3 layers of PUF in the cushions (Test 29 and Test 40). Consistent with this trend, the peak HRR occurred later in the burn during Test 40. In addition, the peak HRR was largest for the sofa with three layers of PUF. As expected, the time to pool formation increased with thickness of the PUF in the cushion because more time and heat is required to liquify the PUF before dripping can be generated. Also, with an increase in PUF thickness the size of the pool fire and, hence the peak HRR, increases.

### 3.5. Miscellaneous Items

The miscellaneous items included 2 laptops (LTA and LTB), a side table (TBL), a carpet (CPT), and a bookshelf (BS). The peak HRRs varied from essentially zero for the laptop (Test 14) to 148 kW for a polypropylene carpet with two A pillows (Test 28). Post-test inspection of the specimens indicated only small amounts of burned material in Test 14 and Test 18 and little burning beyond pillow A in Test 15 and Test 33.

**Table 6. Summary of test results including the specimen label, test number, total specimen mass loss, residual mass, test duration, peak heat release rate (HRR), time to peak HRR, total energy released, and the net effective heat of combustion (HOC). The uncertainty of each of the parameters is provided by Bryant and Bundy [2019] and is listed in the NIST Fire Calorimetry Database (FCD).**

| | Test No. | Mass Loss [kg] | Residual Mass % | Test Duration [min] | Peak HRR [kW] | Time to Peak HRR [min] | THR [MJ] | HOC (kJ/g) |
|---|---|---|---|---|---|---|---|---|
| **Pillows** | | | | | | | | |
| A | 1 | 0.262 | 55 | 8.63 | 48.6 | 2.20 | 4.4 | 16.8 |
| A | 7 | 0.301 | 48 | 6.95 | 70.4 | 1.82 | 5.2 | 17.2 |
| A | 13 | 0.317 | 45 | 7.17 | 72.9 | 2.15 | 5.4 | 17.1 |
| 4A | 9 | 0.991 | 57 | 11.03 | 109.2 | 2.88 | 16.9 | 17.1 |
| B | 2 | 1.043 | 11 | 16.27 | 86.9 | 5.53 | 24.4 | 23.4 |
| C | 3 | 0.717 | 31 | 20.30 | 20.1 | 14.33 | 10.9 | 15.2 |
| D | 4 | 0.567 | 37 | 11.07 | 81.7 | 3.13 | 9.7 | 17.0 |
| D | 11 | 0.592 | 33 | 16.48 | 93.6 | 3.42 | 10.0 | 17.0 |
| D | 12 | 0.584 | 35 | 11.92 | 101.2 | 2.42 | 10.0 | 17.2 |
| 2D | 8 | 0.878 | 51 | 16.73 | 80.5 | 4.68 | 14.8 | 16.9 |
| 4D | 10 | 2.335 | 35 | 13.15 | 191.9 | 5.30 | 40.1 | 17.2 |
| E | 5 | 0.609 | 37 | 35.95 | 23.6 | 15.30 | 9.5 | 15.6 |
| F | 6 | 0.321 | 57 | 20.02 | 27.1 | 3.67 | 5.4 | 17.0 |
| **Chairs** | | | | | | | | |
| A | 16 | 3.241 | 67 | 62.80 | 621 | 19.08 | 115 | 35.5 |
| A | 21 | 2.969 | 69 | 49.33 | 690 | 28.90 | 96.0 | 32.4 |
| 3A | 25 | 9.41 | 68 | 80.37 | 766 | 49.07 | 319 | 34.0 |
| B | 17 | 1.889 | 75 | 16.68 | 447 | 3.47 | 39.0 | 20.6 |
| C | 19 | 1.362 | 81 | 16.82 | 414 | 3.95 | 25.0 | 18.2 |
| D | 20 | 2.066 | 72 | 42.57 | 118 | 9.98 | 42.0 | 20.2 |
| 3D | 47 | 6.414 | 72 | 30.13 | 377 | 4.95 | 115 | 17.9 |
| E | 22 | 3.700 | 63 | 27.48 | 421 | 9.68 | 49.0 | 13.3 |
| F | 23 | 2.338 | 7 | 17.77 | 221 | 3.35 | 59.0 | 25.2 |
| G | 24 | 2.442 | 72 | 10.50 | 366 | 2.33 | 43.0 | 17.7 |
| H | 27 | 22.312 | 16 | 25.40 | 1733 | 3.48 | 381 | 17.1 |
| I | 45 | 7.754 | 61 | 29.93 | 282 | 10.78 | 132 | 17.0 |
| J | 46 | 6.992 | 61 | 40.27 | 563 | 9.98 | 259 | 37.1 |
| K | 48 | 0.106 | 99 | 5.98 | 18.8 | 3.32 | 1.4 | 13.4 |
| **Mattresses** | | | | | | | | |
| A | 26 | 5.080 | 80 | 48.48 | 164 | 4.73 | 83.0 | 16.3 |
| A | 39 | 8.730 | 74 | 33.92 | 189 | 4.37 | 99.0 | 11.3 |
| B | 31 | 15.730 | 7 | 46.98 | 897 | 12.52 | 353 | 22.5 |
| B | 37 | 19.377 | 6 | 20.13 | 3408 | 11.88 | 442 | 22.8 |
| C | 32 | 26.034 | 5 | 20.42 | 2819 | 16.57 | 647 | 24.9 |

| | Test No. | Mass Loss [kg] | Residual Mass % | Test Duration [min] | Peak HRR [kW] | Time to Peak HRR [min] | THR [MJ] | HOC (kJ/g) |
|---|---|---|---|---|---|---|---|---|
| C | 38 | 29.414 | 5 | 19.08 | 4563 | 12.77 | 737 | 25.1 |
| C | 42 | A | A | 7.73 | 34.1 | 0.75 | 1.9 | A |
| C | 43 | A | A | 19.18 | 37.4 | 0.73 | 2.0 | A |
| C | 44 | 28.975 | 6 | 14.40 | 7148 | 7.90 | 696 | 24.0 |
| **Sofas** | | | | | | | | |
| A | 29 | 52.116 | 10 | 34.67 | 1984 | 6.25 | 811 | 15.6 |
| A | 30 | 77.888 | 19 | 36.85 | 2994 | 9.20 | 1426 | 18.3 |
| A | 34 | 34.191 | 33 | 30.22 | 4021 | 6.08 | 633 | 18.5 |
| B | 35 | 48.107 | 15 | 43.17 | 1823 | 6.35 | 838 | 17.4 |
| B | 36 | 77.541 | 20 | 35.00 | 5153 | 5.88 | 1412 | 18.2 |
| B | 40 | 49.738 | 16 | 36.10 | 2217 | 6.57 | 891 | 17.9 |
| C | 41 | 77.132 | 21 | 39.30 | 4036 | 10.67 | 1413 | 18.3 |
| **Miscellaneous items** | | | | | | | | |
| LTA | 14 | 0.008 | A | 6.05 | 1.31 | 3.83 | 0.19 | A |
| LTB | 15 | 0.371 | 87 | 25.18 | 23.8 | 4.18 | 5.9 | 16.0 |
| TBL | 18 | 0.042 | A | 18.03 | 2.22 | 6.88 | 0.93 | A |
| CPT | 28 | 3.3125 | 40 | 20.50 | 145.8 | 3.05 | 23.2 | 7.0 |
| BS | 33 | 1.164 | 94 | 8.45 | 79.2 | 2.40 | 6.9 | 5.9 |

A: Mass loss and HRR occurred only when the igniter flame impinged on the specimen.

### 3.6. Heat Flux, Total Radiated Energy, and Radiative Fraction

The heat flux measured by each of the radiometers is shown in Appendix B. The results for Test 1 to Test 20 show larger values for heat flux gauge HF4 compared to the rest of the gauges due to its closer proximity to the specimen as seen in Table 3. Otherwise, the heat flux measurements were similar with only minor differences among the gauges for Test 1 to Test 20. For Test 21 to Test 48, the measured heat flux among all gauges was usually similar. During some tests, however, the view was obstructed depending on the gauge's orientation relative to the specimen's configuration and the exact location of the ignition event. The radiated energy is an important consideration in terms of fire spread to nearby flammable items.

Table 7 lists the measured total radiated energy (TRE) over the duration of the tests as defined in Equation 1 for each of the radiometers. The combined expanded (k = 2) uncertainty of the TRE measurements was 17 % with contributions from uncertainty in the data acquisition system ($u_c$ = 0.08 %), the heat flux gauge calibration, ($u_c$ = 4.5 %), the background signal ($u_c$ = 5 %) which changed as the surroundings were heated by the fire, and the distance to the specimen ($u_c$ = 1 %). The table also lists the radiative fraction ($\chi_{rad}$), which was estimated using the TRE measurement results and Equation 2 (see Section 2.2.1). The value of $\chi_{rad}$ does not represent all the energy radiated by the specimen as some fraction is directed back to the specimen's surface. It does, however, represent an estimate of the fraction of energy radiated by the burning specimen to the surroundings. The average value of $\chi_{rad}$ for the pillows, chairs, mattresses, and sofas was 0.47 ± 0.07, 0.40 ± 0.09, 0.45 ± 0.03, and 0.43 ± 0.07, respectively. The average value overall was 0.44 ± 0.08, where the uncertainty represents the standard deviation of the five measurements. The combined expanded (k = 2) uncertainty of the $\chi_{rad}$ measurements is estimated as 18 %.

**Table 7. The total radiated energy determined from the heat flux gauges and the radiative fraction. The combined expanded (k = 2) uncertainties of total radiated energy ($TRE_i$) and $\chi_{rad}$ are 17 % and 18 %, respectively.**

| Test | TRE [kJ] | TRE1 [kJ] | TRE2 [kJ] | TRE3 [kJ] | TRE4 [kJ] | $\chi_{rad}$ |
|---|---|---|---|---|---|---|
| **Pillows** | | | | | | |
| 1 | na | na | na | na | na | na |
| 2 | 9598 | 11446 | 10859 | 11499 | 13808 | 0.47 |
| 3 | 1997 | 3941 | 3055 | 2722 | 3442 | 0.28 |
| 4 | 4597 | 4088 | 4610 | 5673 | 5483 | 0.50 |
| 5 | 2977 | 2777 | 2750 | 4570 | 4856 | 0.38 |
| 6 | 1360 | 3483 | 2354 | 1686 | 2494 | 0.42 |
| 7 | 2266 | 2425 | 2749 | 2722 | 2712 | 0.50 |
| 8 | 6882 | 5702 | 6635 | 8034 | 7875 | 0.47 |
| 9 | 7415 | 7669 | 8520 | 8628 | 9153 | 0.49 |
| 10 | 20523 | 19026 | 22575 | 23755 | 20590 | 0.53 |
| 11 | 5861 | 4811 | 4847 | 6078 | 5594 | 0.54 |
| 12 | 5579 | 4579 | 4883 | 6209 | 4733 | 0.52 |
| 13 | 2577 | 2724 | 2612 | 2892 | 2652 | 0.50 |
| **Chairs** | | | | | | |
| 16 | 53127 | 61149 | 55710 | 60470 | 68840 | 0.52 |
| 17 | 13451 | 14154 | 14341 | 15296 | 15785 | 0.37 |
| 19 | 8747 | 9662 | 9353 | 9531 | 10731 | 0.38 |
| 20 | 14350 | 17410 | 15709 | 16458 | 17344 | 0.39 |
| 21 | 59299 | 44416 | 44374 | 39666 | 48437 | 0.49 |
| 22 | 19454 | 17235 | 15914 | 20492 | 26161 | 0.41 |
| 23 | 33165 | 32946 | 32540 | 38588 | 29623 | 0.57 |
| 24 | 14612 | 11451 | 19769 | 18393 | 12884 | 0.36 |
| 25 | 169344 | 139639 | 119048 | 144466 | 149217 | 0.45 |
| 27 | 178476 | 172129 | 172445 | 176430 | 172722 | 0.46 |
| 45 | 42364 | 36833 | 39783 | 37653 | 29420 | 0.28 |
| 46 | 87449 | 78245 | 87007 | 93975 | 72144 | 0.32 |
| 47 | 34492 | 28794 | 24953 | 32062 | 28233 | 0.26 |
| 48 | na | na | na | na | na | na |
| **Mattresses** | | | | | | |

| Test | TRE [kJ] | TRE1 [kJ] | TRE2 [kJ] | TRE3 [kJ] | TRE4 [kJ] | $\chi_{rad}$ |
|---|---|---|---|---|---|---|
| 26 | 39279 | 35147 | 38555 | 38152 | 31447 | 0.44 |
| 31 | 139107 | 136984 | 154081 | 145417 | 121828 | 0.40 |
| 32 | 326326 | 316913 | 297227 | 338276 | 268341 | 0.48 |
| 37 | 191952 | 186654 | 201747 | 199522 | 164147 | 0.43 |
| 38 | 311525 | 300121 | 366593 | 370472 | 343450 | 0.46 |
| 39 | 54739 | 51026 | 42236 | 54332 | 43759 | 0.50 |
| 42 | na | na | na | na | na | na |
| 43 | na | na | na | na | na | na |
| 44 | 268753 | 237444 | 238221 | 246421 | 181296 | 0.34 |
| **Sofas** | | | | | | |
| 29 | 378853 | 367176 | 388143 | 391178 | 365012 | 0.47 |
| 30 | 611702 | 592295 | 690969 | 796666 | 593615 | 0.46 |
| 34 | 293315 | 290679 | 298863 | 295899 | 301875 | 0.47 |
| 35 | 419828 | 414812 | 403077 | 421923 | 419285 | 0.50 |
| 36 | 677235 | 660746 | 642343 | 675586 | 642517 | 0.47 |
| 40 | 337841 | 298179 | 298945 | 313535 | 288753 | 0.35 |
| 41 | 475921 | 422628 | 435118 | 543781 | 394881 | 0.32 |
| **Miscellaneous items** | | | | | | |
| 14 | B | A | A | A | A | na |
| 15 | 2851 | 2212 | 1909 | 2488 | 2306 | 0.40 |
| 18 | B | A | A | A | A | Na |
| 28 | 9503 | 8888 | 12466 | 7894 | 6599 | 0.39 |
| 33 | 5847 | 8390 | 1522 | 2491 | 2912 | 00.61 |

na: Data not available
A: Mass loss and HRR occurred only when the igniter flame impinged on the specimen
B: Below detection limits

## 3.7. Yields

Table 8 lists the total soot, CO, and HCN yields on a mass basis, which varied from about 0.01 to 0.05, from 0.01 to 0.08, and from 0.0001 to 0.0057, respectively. The largest soot yield was measured as 0.19 ± 0.03 during Test 23, which was the beanbag chair filled with expanded polystyrene pellets. For all the tests, the average values of the soot and CO yields were 0.032 ± 0.28 and 0.32 ± 0.14, respectively.

A cursory analysis of the data showed that that the soot yield was generally larger than the CO yield for the pillows and smaller for the sofas. The yields for the sofas were very consistent since there were only 3 types of sofas and two of them (Sofa A and B) were very similar in terms of their structure. No generalization can be made about the ratio of soot to CO for the chairs or mattresses. In some tests, the CO yields were larger than the soot yields and, in some tests, the opposite was true. The HCN yield was always smaller than the CO yield by a factor of about 800 on average. HCN was especially large in several tests, including Mattress A (Test 26 and Test 39), Chairs A, C, D, G, and K (Tests 21, 19, 20, 24, and 45, respectively), as well as Laptop A (Test 15) and the Side Table (Test 18). For the latter two tests, sustained burning did not occur when the igniter flame was removed.

**Table 8: Soot, Carbon Monoxide (CO), and Hydrogen Cyanide (HCN) yields. Uncertainties shown are the expanded (k = 2) uncertainties, which represent a 95 % confidence interval.**

| Test | Soot Yield [kg/kg] | CO Yield [kg/kg] | HCN Yield x $10^3$ [kg/kg] |
|---|---|---|---|
| **Pillows** | | | |
| 1 | 0.053 ± 0.009 | 0.035 ± 0.004 | - |
| 2 | 0.030 ± 0.004 | 0.023 ± 0.001 | - |
| 3 | 0.021 ± 0.004 | 0.030 ± 0.002 | - |
| 4 | 0.045 ± 0.006 | 0.026 ± 0.002 | - |
| 5 | 0.012 ± 0.003 | 0.026 ± 0.002 | - |
| 6 | 0.021 ± 0.005 | 0.024 ± 0.002 | - |
| 7 | 0.053 ± 0.009 | 0.032 ± 0.003 | - |
| 8 | 0.030 ± 0.006 | 0.025 ± 0.001 | - |
| 9 | 0.050 ± 0.006 | 0.030 ± 0.001 | - |
| 10 | 0.043 ± 0.006 | 0.025 ± 0.001 | - |
| 11 | 0.044 ± 0.006 | 0.028 ± 0.002 | 0.17 ± 0.06 |
| 12 | 0.041 ± 0.006 | 0.028 ± 0.002 | 0.21 ± 0.03 |
| 13 | 0.053 ± 0.008 | 0.034 ± 0.003 | 0.12 ± 0.03 |
| **Chairs** | | | |
| 16 | 0.061 ± 0.009 | 0.034 ± 0.001 | 0.40 ± 0.08 |
| 17 | 0.017 ± 0.002 | 0.028 ± 0.001 | 0.32 ± 0.04 |
| 19 | 0.022 ± 0.003 | 0.035 ± 0.001 | 2.06 ± 0.15 |
| 20 | 0.013 ± 0.002 | 0.052 ± 0.002 | 1.32 ± 0.08 |
| 21 | 0.060 ± 0.009 | 0.030 ± 0.001 | 1.38 ± 0.11 |
| 22 | 0.019 ± 0.01 | 0.053 ± 0.002 | 0.40 ± 0.04 |
| 23 | 0.185 ± 0.026 | 0.060 ± 0.002 | 0.29 ± 0.04 |
| 24 | 0.014 ± 0.003 | 0.014 ± 0.001 | 1.04 ± 0.48 |
| 25 | 0.081 ± 0.014 | 0.036 ± 0.0022 | 0.29 ± 0.03 |
| 27 | 0.013 ± 0.002 | 0.033 ± 0.001 | 0.14 ± 0.02 |
| 45 | 0.008 ± 0.004 | 0.035 ± 0.001 | 0.67 ± 0.04 |
| 46 | 0.045 ± 0.015 | 0.023 ± 0.001 | 0.57 ± 0.08 |
| 47 | 0.010 ± 0.006 | 0.032 ± 0.001 | 1.13 ± 0.18 |
| 48 | 0.004 ± 0.002 | 0.009 ± 0.012 | 5.71 ± 0.64 |
| **Mattresses** | | | |
| 26 | 0.034 ± 0.011 | 0.076 ± 0.003 | 2.00 ± 0.12 |
| 31 | 0.025 ± 0.003 | 0.024 ± 0.001 | 0.65 ± 0.05 |
| 32 | 0.036 ± 0.006 | 0.025 ± 0.001 | 0.77 ± 0.05 |

| Test | Soot Yield [kg/kg] | CO Yield [kg/kg] | HCN Yield x $10^3$ [kg/kg] |
|---|---|---|---|
| 37 | 0.032 ± 0.004 | 0.020 ± 0.001 | 0.64 ± 0.05 |
| 38 | 0.038 ± 0.005 | 0.024 ± 0.001 | 0.98 ± 0.06 |
| 39 | 0.027 ± 0.009 | 0.039 ± 0.001 | 1.00 ± 0.08 |
| 42 | - | - | - |
| 43 | - | - | - |
| 44 | 0.038 ± 0.006 | 0.018 ± 0.001 | 0.89 ± 0.09 |
| **Sofas** | | | |
| 29 | 0.014 ± 0.003 | 0.030 ± 0.001 | 0.20 ± 0.02 |
| 30 | 0.017 ± 0.003 | 0.033 ± 0.001 | 0.25 ± 0.03 |
| 34 | 0.014 ± 0.002 | 0.036 ± 0.001 | 0.37 ± 0.04 |
| 35 | 0.016 ± 0.003 | 0.037 ± 0.001 | 0.24 ± 0.05 |
| 36 | 0.020 ± 0.004 | 0.032 ± 0.001 | 0.21 ± 0.03 |
| 40 | 0.016 ± 0.003 | 0.031 ± 0.001 | 0.22 ± 0.14 |
| 41 | 0.019 ± 0.003 | 0.032 ± 0.001 | 0.22 ± 0.02 |
| **Miscellaneous items** | | | |
| 14 | - | - | - |
| 15 | 0.057 ± 0.01 | 0.061 ± 0.005 | 1.29 ± 0.17 |
| 18 | 0.010 ± 0.008 | 0.060 ± 0.043 | 2.86 ± 0.47 |
| 28 | 0.015 ± 0.002 | 0.012 ± 0.040 | 0.46 ± 0.05 |
| 33 | 0.016 ± 0.005 | 0.015 ± 0.001 | 1.04 ± 0.09 |

## 4. Summary and Conclusions

This report of test describes a series of experiments that investigate the burning behavior of single items and assemblies commonly found in offices and residences, including chairs, sofas, mattresses with pillows and bedclothes, and some miscellaneous items such as laptops, bookshelves, and side tables. The measurements reported include the transient, peak, and total heat release rates, the yields of carbon monoxide (CO), hydrogen cyanide (HCN), and soot, and the transient mass loss. The appearance of the fires was captured by video cameras from two orthogonal views. Measurements of the heat flux to the surroundings from the specimens were used to estimate the radiative fraction of the fires. The results provide unique calorimetric data which can be useful for development of design fire scenarios by fire protection engineers. The data generated from the study will be available on the NIST Fire Calorimetry Database (FCD), which will link to this report. The measurement results characterize the global combustion properties of the specimens and offer insight on the burning behavior of the fires.

General findings from the study include the following:

- The difference in the peak heat release rate (HRR) among items of similar function was significant:
  - the peak HRR for individual pillows varied by more than a factor of 4, from 20 kW to 87 kW, and was a function of pillow size and composition;
  - the peak HRR among identical sofas with different ignition scenarios varied by a factor of 1.7 from 3 MW to 5 MW as a function of ignition location and seat cushion composition;
  - The peak HRR for fires burning Mattresses C (a 30 cm thick queen size mattress using flexible polyurethane foam (PUF) as padding with a knitted fire barrier) with bedclothes and two pillows (4.5 MW) was a factor of 25 larger than the peak HRR (189 kW) of Mattress A (a 15 cm coil-spring queen size mattress with a non-woven fire barrier) with bedclothes and two pillows.
- Three identical A sofas were tested, each with the seat cushions modified such that they contained 1 layer, 2 layers, or 3 three layers of polyurethane foam (PUF). The time to pool formation was about one min longer as the thickness of the PUF in the cushion increased because more time and heat was required to liquify the PUF before dripping occurred. With increased PUF cushion thickness, the size of the pool fire and the peak HRR also increased.
- The average value of the radiative fraction for all the specimens was 0.43 ± 0.08 with little difference among the different specimen categories.

- The total soot and CO yields varied from about 0.01 to 0.05 and from 0.01 to 0.08, respectively. The largest soot yield was measured as 0.19 ± 0.03 during the burning of a beanbag chair filled with expanded polystyrene pellets.

The experiments with Mattress C show that relatively large fires can occur on a mattress that meets the 16 CFR 1633 mattress flammability standard. The purpose of 16 CFR 1633 is to establish flammability requirements that all mattress sets must meet before sale or introduction into commerce in an effort to reduce deaths and injuries associated with mattress fires by limiting the size of the fire generated by a mattress set. The 16 CFR 1633 test protocol was specifically designed to present a thermal insult onto a mattress that represents the effect of flaming bedclothes [Ohlemiller 2003]. Whereas the experiments showed that Mattress C met the 16 CFR 1633 test, fire experiments starting with bedclothes or just two pillows on Mattress C led to a very large fire — much larger than needed to cause flashover of a typical residential bedroom. Comparing the experimental results (in the presence of bedclothes) with and without the fire barrier cover fabric (FR sock) of Mattress C showed that a barrier material can significantly reduce the value of the peak HRR as well as delay its incidence.[3] The results indicate that the thermal insult from the 16 CFR 1633 burner (1.7 MJ) may underestimate the risk posed by likely scenarios involving contemporary bedding materials, such as sleeping pillows with thermoplastic fill and covers, which on their own generate about 10 MJ of energy. Use of this type of material was less prevalent when the standard was established in the 2000s but has since become more common in the consumer marketplace. The results suggest that further testing and research is needed to investigate popular mattress types and bedding currently available in the marketplace in terms of the 16 CFR 1633 regulation.

The experiments reported here represent the first stage of a multi-phase project. A full analysis of the measurements reported here will be provided in future publications. Additional experiments will address items associated with other types of spaces and scenarios relevant to fire protection engineering design.

3. The 16 CFR 1633 accounts for many factors when assessing life safety, including the available safe egress time.

## 5. References

[1] 16 CFR 1632, Title 16, Chapter II, Subchapter D, Part 1632 (2025) Standard for the flammability of upholstered furniture. https://www.ecfr.gov/current/title-16/chapter-II/subchapter-D/part-1632

[2] 16 CFR 1633, Title 16, Chapter II, Subchapter D, Part 1633 (2025) Standard for the flammability (open flame) of mattress sets. https://www.ecfr.gov/current/title-16/chapter-II/subchapter-D/part-1633

[3] 16 CFR 1640, Title 16, Chapter II, Subchapter D, Part 1640 (2025) Standard for the flammability of upholstered furniture. https://www.ecfr.gov/current/title-16/part-1640

[4] Ahrens M (2019) Home structure fires, *National Fire Protection Association*, Quincy, MA, 2019.

[5] Ahrens M (2021) Soft furnishing fires: they're still a problem, *Fire and Materials* 45, 8–16. https://doi.org/10.1002/fam.2874

[6] Alvarez A, Meachum B, Dembsey NA, Thomas JR (2013) Twenty years of performance based fire protection design: challenges faced and a look ahead. *Journal of Fire Protection Engineering* 23, 249–276.

[7] Babrauskas V (2016) Heat Release Rates, Chap 26 in *The SFPE Handbook of Fire Protection Engineering*, Ed.: Hurley M (New York, NY, Springer) Vol. 1, 5th Ed., 799-904.

[8] Babrauskas V, Krasny J (1985) Fire behavior of upholstered furniture (NBS Monograph 173), *NIST Interagency/Internal Report (NISTIR)*, National Institute of Standards and Technology, Gaithersburg, MD. https://tsapps.nist.gov/publication/get_pdf.cfm?pub_id=101655

[9] Babrauskas V, Peacock RD (1992) Heat release rates: the single most important variable in fire hazard, *Fire Safety Journal* 18, 255-272. https://doi.org/10.1016/0379-7112(92)90019-9

[10] Blais M, Carpenter K (2015) Combustion characteristics of flat panel televisions with and without fire retardants in the Casing, *Fire Technology* 51, 19–40. https://doi.org/10.1007/s10694-014-0420-7

[11] Brown A, Bruns M, Gollner M, Hewson J, Maragkos G, Marshall A, McDermott A, Merci B, Rogaume T, Stoliarov S, Torero JL, Trouve A, Wang A, Weckman E (2018) Proceedings of the first workshop organized by the IAFSS working group on measurement and computation of fire phenomena (MaCFP *), Fire safety Journal* 101, 1–17.

[12] Bryant R, Bundy M (2019) The NIST 20 MW calorimetry measurement system for large-fire research, *NIST Technical Note (NIST TN) 2077*, National Institute of Standards and Technology, Gaithersburg MD. https://doi.org/10.6028/NIST.TN.2077

[13] British Standard (BS) 5852 (2006) Methods of test for assessment of the ignitability of upholstered seating by smouldering and flaming ignition sources. https://www.en-standard.eu/bs-5852-2006-methods-of-test-for-assessment-of-the-ignitability-of-upholstered-seating-by-smouldering-and-flaming-ignition-sources/

[14] British Standard (BS) 13823 (2010) Reaction to fire tests for building products. Building products excluding floorings exposed to the thermal attack by a single burning item. Appendix E. https://www.en-standard.eu/bs-en-13823-2020-a1-2022-reaction-to-fire-tests-for-building-products-building-products-excluding-floorings-exposed-to-the-thermal-attack-by-a-single-burning-item/

[15] Bwalya A, Gibb, E, Lougheed G, Kashef A (2015) Heat release rates of modern residential furnishings during combustion in a room calorimeter, *Fire Materials* 39, 685–716. https://doi.org/10.1002/fam.2259

[16] Mehta S (2012) Upholstered furniture full scale chair tests – open flame ignition results and analysis, *Memorandum*, Consumer Product Safety Commission. Upholstered Furniture Full Scale Chair Tests - Open Flame Ignition Results and Analysis (4019) | CPSC.gov

[17] Lock A (2012) Upholstered furniture full scale chair tests – open flame ignition results and analysis, *Memorandum*, Consumer Product Safety Commission. Upholstered Furniture Flammability (cpsc.gov)

[18] Di Cristina Torres G, Falkenstein-Smith R, Kim I, Wessies S, Bundy M, Zammarano M (2024) Towards fire safe and flame-retardant-free upholstered furniture, *Proc Combust Inst* 40, 105399 https://doi.org/10.1016/j.proci.2024.105399

[19] Fire Calorimetry Database (FCD) National Institute of Standards and Technology, Gaithersburg, MD. https://www.nist.gov/el/fcd

[20] Gratkowski MT (2021) Bedding ignition, vertical flame spread and subsequent thermal impact on underlying mattress, *Fire Materials* 45, 28-36. https://doi.org/10.1002/fam.2834

[21] Guillaume E, de Feijter R, van Gelderen L (2020) An overview and experimental analysis of furniture fire safety regulations in Europe, *Fire Materials* 44, 624–639. https://doi.org/10.1002/fam.2826

[22] Hall S (2023) Home structure fires, *National Fire Protection Association*, Quincy, MA. https://content.nfpa.org/-/media/Project/Storefront/Catalog/Files/Research/NFPA-Research/Building-and-life-safety/oshomes.pdf?rev=604068f107bc42afa6a7582bbe043a2d

[23] H.R. 133 (2021) Consolidated Appropriations Act. Public Law No. 116-260. https://www.congress.gov/bill/116th-congress/house-bill/133/text

[24] Karlsson B, Quintiere JG (2000) Enclosure Fire Dynamics, CRC Press, Boca Raton, FL. https://doi.org/10.1201/9781420050219

[25] Kerber S (2012) Analysis of changing residential fire dynamics and its implications on firefighter operational timeframes, *Fire Technology* 48, 865-891. https://doi.org/10.1007/s10694-011-0249-2

[26] Krämer RH, Zammarano M, Linteris GT, Gedde UW, Gilman JW (2010) Heat release and structural collapse of flexible polyurethane foam, *Polymer Degradation and Stability* 95, 1115-1122. https://doi.org/10.1016/j.polymdegradstab.2010.02.019.

[27] McKinnon M, Willi J, Madrzykowski D (2021) Examination of fire dynamics analysis techniques: assessment of predictive fire algorithms and models. *Underwriters Laboratory (UL) Firefighter Safety Research Institute*. https://fireinvestigation.fsri.org/docs/Assessment_of_Predictive_Fire_Algorithms_and_Models.pdf

[28] Mitler HE, Tu KM (1994) Effect of ignition location on heat release rate of burning upholstered furniture. NIST Internal Report (NIST IR) 5499, National Institute of Standards and Technology, Gaithersburg, MD.

[29] Morrisset D, Reep J, Ojwang I, Hadden RM, Law A (2024) Repeat fire tests of upholstered furniture: variability and experimental observations, *Fire Technology* 60, 1453–1476. https://doi.org/10.1007/s10694-023-01523-3

[30] Nazaré S, Davis RD, Butler K (2012) Assessment of factors affecting fire performance of mattresses: a review. *Fire Science Reviews* 1, 2. https://doi.org/10.1186/2193-0414-1-2

[31] Ohlemiller, T, Shields JR, McLane RA, Gann RG (2000). Flammability assessment methodology for mattresses, *NIST Internal Report (NIST IR) 6497*. National Institute of Standards and Technology, Gaithersburg, MD. https://www.nist.gov/publications/flammability-assessment-methodology-mattresses-nistir-6497

[32] Ohlemiller T (2003) Flammability test of full-scale mattresses: gas burners versus burning bedclothes, *NIST Internal Report (NIST IR) 7006*. National Institute of Standards and Technology, Gaithersburg, MD. https://www.nist.gov/publications/flammability-tests-full-scale-mattresses-gas-burners-versus-burning-bedclothes

[33] Ohlemiller T (2005) A study of size effects in the fire performance of beds, *Technical Note (NIST TN) 1465*, National Institute of Standards and Technology, Gaithersburg, MD. https://www.nist.gov/publications/study-size-effects-fire-performance-beds

[34] Scott L (2018) CPSC and the mattress industry, the latest from the CPSC, *International Sleep Products Association (ISPA) EXPO*, Charlotte, NC. [ISPA-Mattress-Training-March-2018-Final.pdf (cpsc.gov)]()

[35] Sundström B (1995) Combustion behaviour of upholstered furniture (CBUF): fire safety of upholstered furniture - the final report of the CBUF research program. Director-General Science, Research and Development (Measurements and Testing) of the European Commission. *Report EUR 16477 EN, 1995*.

[36] Sundström B (2021) Combustion behaviour of upholstered furniture. Important findings, practical use, and implications, *Fire Materials* 45, 97-113. https://doi.org/10.1002/fam.2920

[37] Thompson A, Kim I, Hamins A, Bundy M, Zammarano M (2021), Performance and failure mechanism of fire barriers in full-scale chair mock-ups, *Fire Materials 46*, 329-346. https://doi.org/10.1002/fam.3007

[38] Trainer R (2023) President, International Sleep Products Association, *Email to M. Zammarano of NIST,* 7 November 2023, National Institute of Standards and Technology, Gaithersburg, MD.

[39] Xie L, Shao Y, Duan H, Sun J, Ma J, Qi D, Li J (2024) Flammability and combustion behavior of the polyester/cotton blended fabric via an independent flame-retardation for two components strategy, *Polymer Degradation Stability* 220, 110638, https://doi.org/10.1016/j.polymdegradstab.2023.110638

[40] Zammarano M, Hoehler M, Shields J, Thompson A, Kim I, Leventon I, Bundy M (2020) Full-scale experiments to demonstrate flammability risk of residential upholstered furniture and mitigation using barrier fabric, *Technical Note (NIST TN) 2129*, National Institute of Standards and Technology, Gaithersburg, MD https://doi.org/10.6028/NIST.TN.2129

[41] Zammarano M, Shields J, Leventon I, Kim I, Nazare S, Thompson A, Davis R, Chernovsky A, Bundy, M (2021) Reduced-Scale test to assess the effect of fire barriers on the flaming combustion of cored composites: An upholstery-material case study, *Fire Materials* 45, 0308-0501 https://doi.org/10.1002/fam.2910

## Appendix A. Photos and Descriptions of the Test Specimens

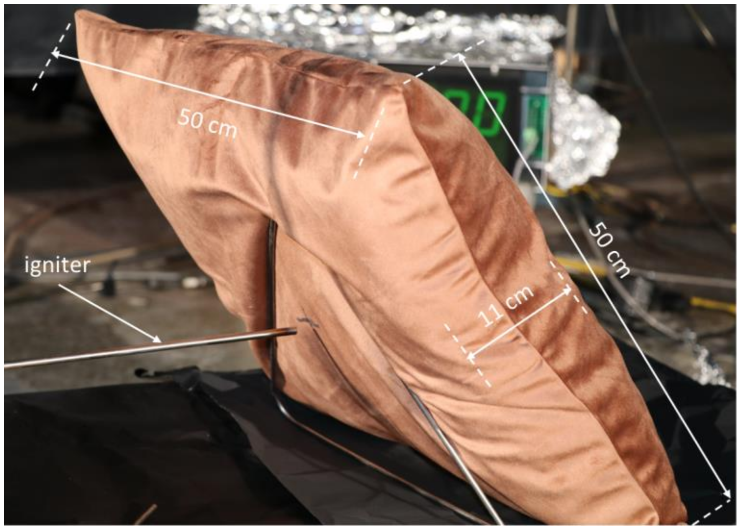


**Figure A1. Test 1 photo with dimensions of Pillow A.**

Figure A1 shows a photo of Test 1 burning Pillow A, which was composed of a low-density polyester pillow insert with polyester inset cover inside a polyester pillow cover. The pillow assembly was tilted at 45 degrees with the igniter flame 1 cm from the middle of the pillow bottom.


**Figure A2. Test 2 photo with dimensions of Pillow B.**

Figure A2 shows a photo of Test 2 burning Pillow B, which was composed of a PUF ("memory foam") insert with polyester insert cover inside a polyester pillow cover. The pillow assembly was tilted at 45 degrees with the igniter flame 1 cm from the middle of the pillow bottom.


**Figure A3. Test 3 photo with dimensions of Pillow C.**

Figure A3 shows a photo of Test 3 burning Pillow C, which was composed of a duck feather pillow insert with polyester insert cover inside a polyester pillow cover. The pillow assembly was tilted at 45 degrees with the igniter flame 1 cm from the middle of the pillow bottom.


**Figure A4. Test 4 photo with dimensions of Pillow D.**

Figure A4 shows a photo of Test 4, a repeat of Tests 11 and 12, burning Pillow D, which was composed of a polypropylene pillow insert with polyester insert cover inside a polypropylene pillow cover. The pillow was tilted at 45 degrees with the igniter flame positioned 1 cm from the middle of the pillow bottom.

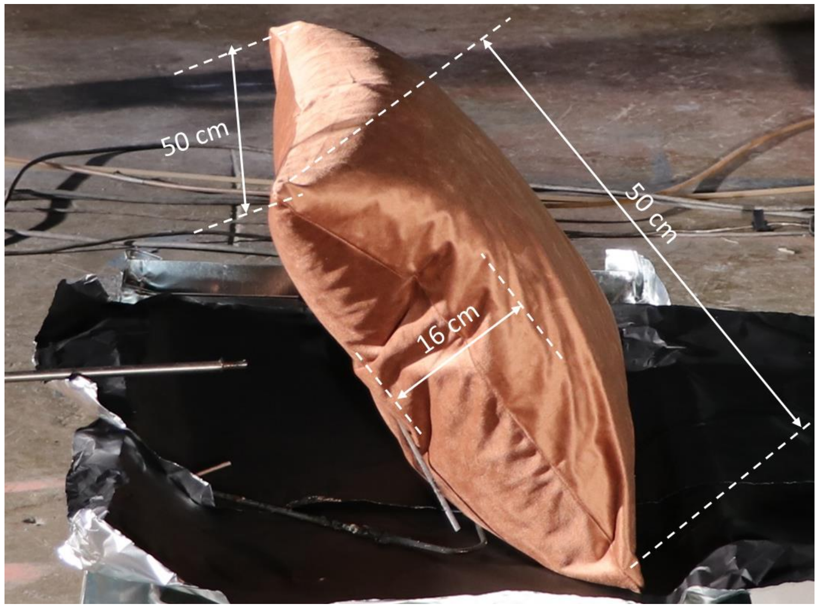


**Figure A5. Test 5 photo with dimensions of Pillow E.**

Figure A5 shows a photo of Test 5 burning Pillow E, which was composed of a down-filled pillow insert in a cotton cover tilted at 45 degrees with the igniter flame near the middle of the pillow bottom.

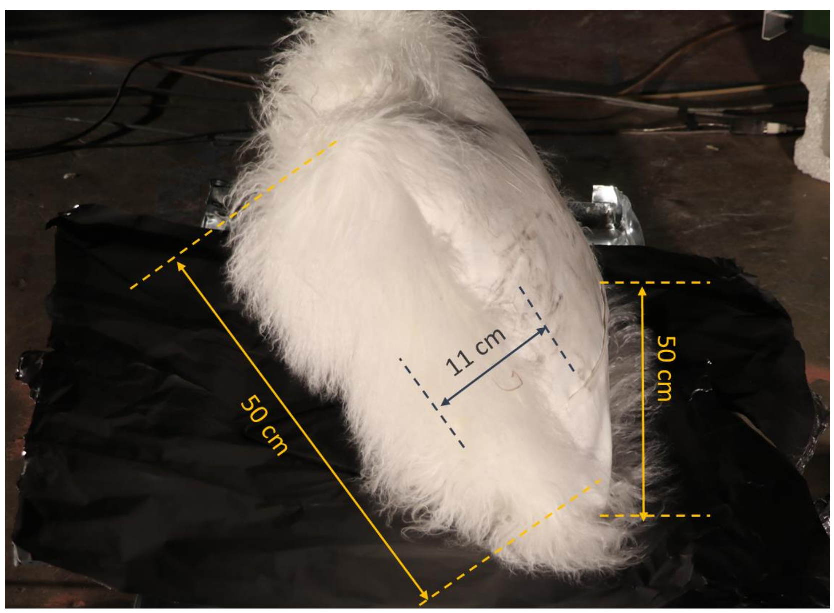


**Figure A6. Test 6 photo with dimensions of Pillow F.**

Figure A6 shows a photo of Test 6 burning Pillow F, which was composed of a polyester pillow insert inside a shaggy wool pillow cover tilted at 45 degrees, with the igniter flame near the middle of the bottom of the pillow.


**Figure A7. Test 7 photo with dimensions of Pillow A.**

Figure A7 shows a photo of Test 7, a repeat of Test 1 and Test 13, burning Pillow A, which was composed of a of a low-density polyester pillow insert inside a polyester cover tilted at 45 degrees with the igniter flame 1 cm from the middle of the bottom of the pillow.

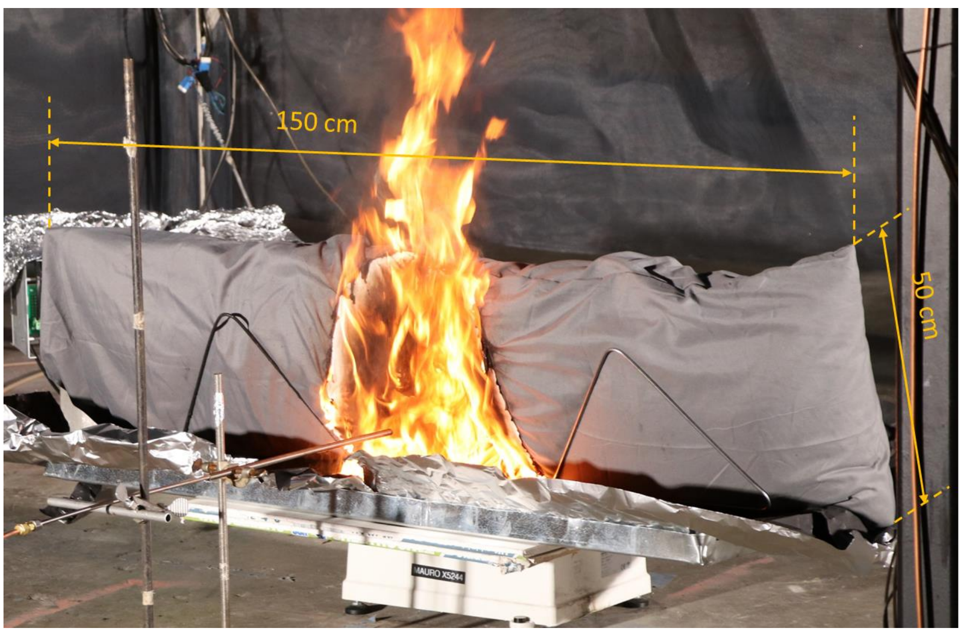


**Figure A8. Test 8 photo with dimensions of two D  pillows.**

Figure A8 shows a photo of Test 8 burning two D pillows, identical to those used in Test 4. Each pillow was composed of a polypropylene pillow insert inside a polyester cover. The pillows were tilted at 45 degrees. Ignition was initiated at the middle of the bottom of the pillows' intersection.

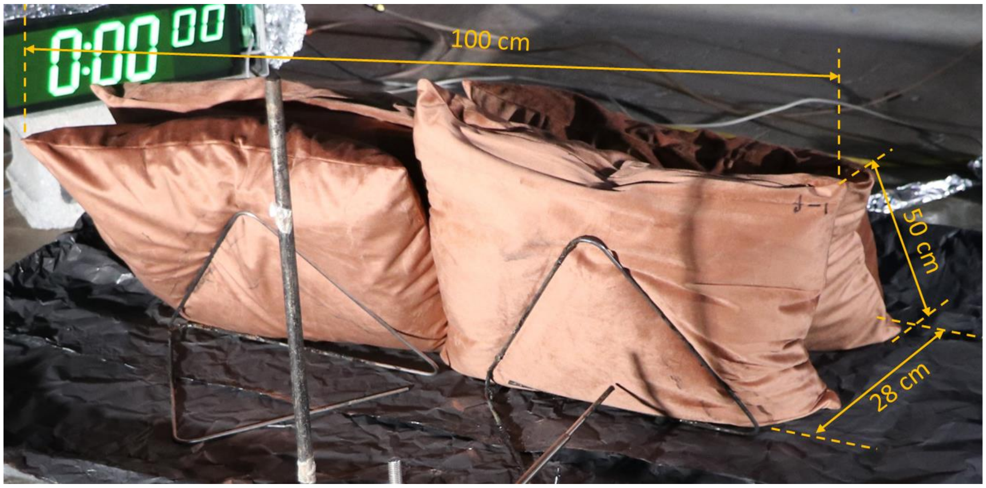


**Figure A9. Test 9 photo with dimensions of four A pillows.**

Figure A9 shows a photo of Test 9 using four A pillows identical to those used in Test 1, each composed of a low-density polyester pillow insert inside a polyester cover. The pillows were tilted at 45 degrees with ignition initiated at the middle of the bottom of the pillows' intersection.


**Figure A10. Test 10 photo with dimensions of four D pillows.**

Figure A10 shows a photo of Test 10 using four D pillows identical to those used in Test 4 and Test 7, each composed of a polypropylene pillow insert inside a polyester cover. The pillows were tilted at 45 degrees and ignition was initiated at the middle of the bottom of the pillows' intersection.


**Figure A11. Test 11 photo with dimensions of Pillow D.**

Figure A11 shows Test 11, a repeat of Test 4 and Test 12, burning Pillow D, which was composed of a polypropylene pillow insert with a polyester insert cover inside a polypropylene pillow cover. The pillow was tilted at 45 degrees with the igniter flame positioned 1 cm from the middle of the pillow bottom.

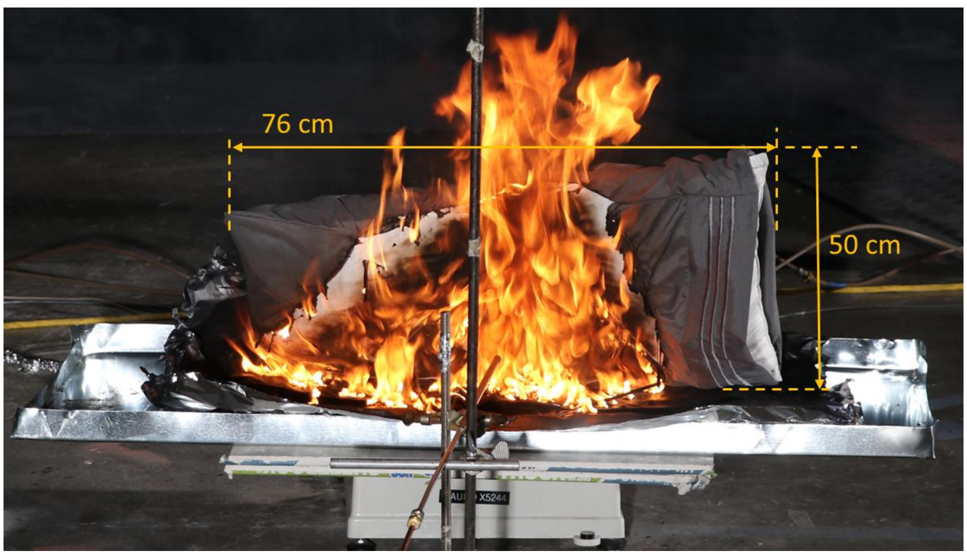


**Figure A12. Test 12 photo with dimensions of Pillow D.**

Figure A12 shows a photo of Test 12, a repeat of Test 4 and Test 11, burning Pillow D, which was composed of a polypropylene pillow insert with a polyester insert cover inside a polypropylene pillow cover. The pillow was tilted at 45 degrees with the igniter flame positioned 1 cm from the middle of the pillow bottom.

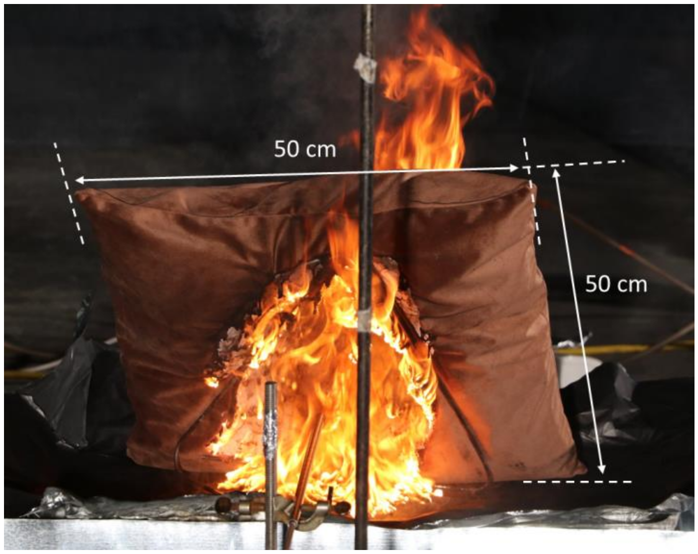


**Figure A13. Test 13 photo with dimensions of Pillow A.**

Figure A13 shows a photo of Test 13, a repeat of Test 1 and Test 7, burning Pillow A, which was composed of a of a low-density polyester pillow insert inside a polyester cover tilted at 45 degrees with the igniter flame 1 cm from the middle of the bottom of the pillow.


**Figure A14. Test 14 photo with dimensions of Laptop A.**

Figure A14 shows a photo of Test 14, using Laptop A, after ignition was attempted at the middle of the screen which had been folded at 45 degrees. Fire spread did not occur.


**Figure A15. Test 15 photo with dimensions of Laptop B folded at 45 degrees after ignition of the front of Pillow A.**

Figure A15 shows a photo of Test 15 using Laptop B folded at 45 degrees positioned just above Pillow A. Two metal rods prevented the laptop from compressing the pillow. The pillow was observed to burn, whereas the laptop did not appear to ignite.

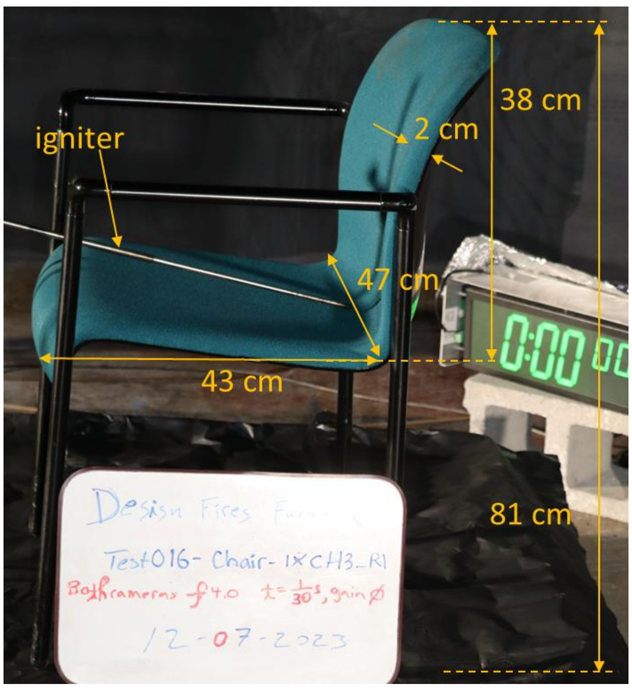


**Figure A16. Test 16 photo with dimensions of Chair A.**

Figure A16 shows a photo of Test 16 using Chair A composed of a metal frame, two hard-plastic contoured seat-back layers, a contoured foam cushion, and cover fabric with the igniter 1 cm from the crevice between the bottom and back cushions.

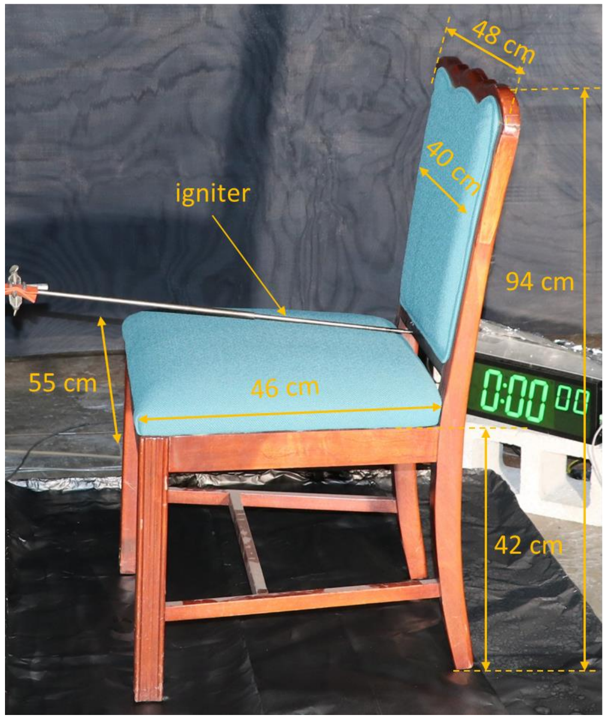


**Figure A17. Test 17 photo with dimensions of Chair B.**

Figure A17 shows a photo of Test 17 using Chair B composed of a wood fame, PUF cushions with blended polyester/cotton fiber batting and a woven-glass backing layer with the igniter 1 cm below the bottom of the back cushion.

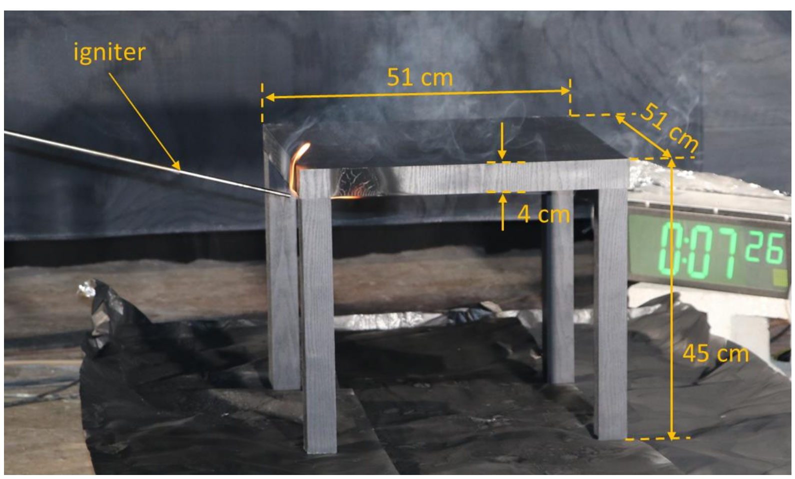


**Figure A18. Test 18 photo with dimensions of the compressed particleboard side table.**

Figure A18 shows a photo of Test 18 of the compressed particleboard side table with the igniter about 1 cm below the table bottom and 5 cm from its edge. The table did not ignite even after many minutes of an imposed flame.


**Figure A19. Test 19 photo with dimensions of Chair C.**

Figure A19 shows a photo of Test 19 using Chair C. which was composed of a wood fame, PUF cushions, and woven fabric seat and back cover ignited at the bottom of the back cushion.

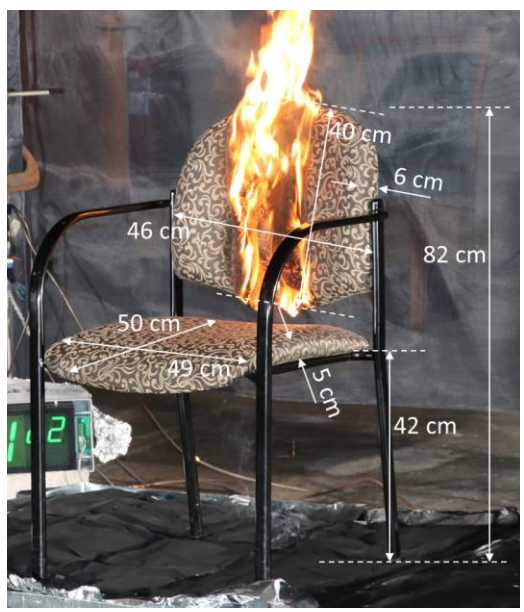


**Figure A20. Test 20 photo with dimensions of Chair D.**

Figure A20 shows a photo of Test 20 burning Chair D, which was a stackable chair composed of a metal frame, wood back layers, contoured foam cushions, and cover fabrics ignited at the bottom of the middle of the chair back.

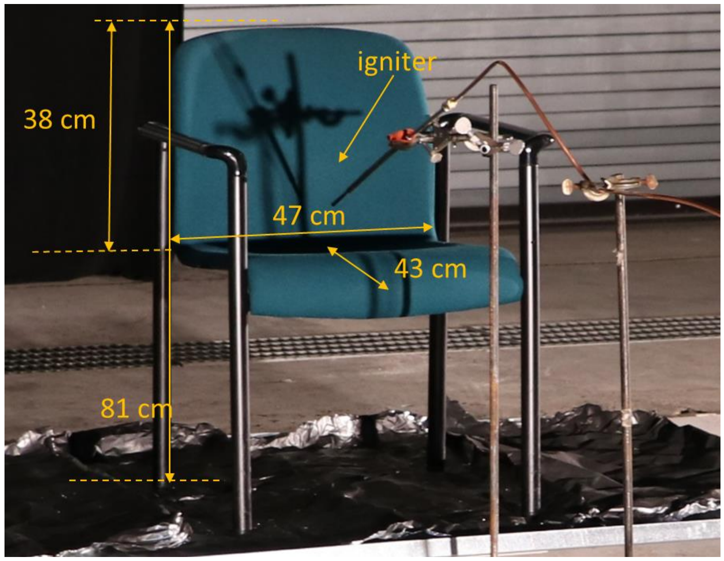


**Figure A21. Test 21 photo with dimensions of Chair A.**

Figure A21 shows a photo of Test 21 burning Chair A composed of a metal frame, two hard-plastic contoured seat-back layers, a contoured foam cushion, and cover fabric, which was ignited with a 1 cm flame in the crevice between the bottom and back cushions. This test was a repeat of Test 16, but under the 9 m × 12 m exhaust hood and calorimeter.

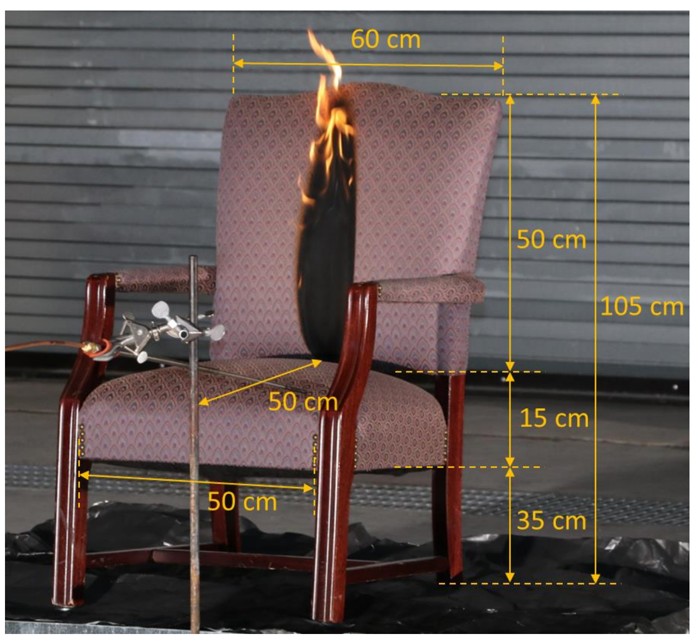


**Figure A22. Test 22 photo with dimensions of large desk armchair E.**

Figure A22 shows a photo of Test 22 burning large Armchair E (wheels removed) composed of a wood frame, PUF, and a cotton batting, which was ignited by a 1 cm flame at the bottom of the middle of the chair back.


**Figure A23. Test 23 photo with dimensions of a 122 cm beanbag Chair F.**

Figure A23 shows a photo of Test 23 burning beanbag Chair F filled with 9 mm long polystyrene pellets in a loose weave internal cover and an outer polyester cover, which was ignited with a 1 cm flame at the bottom of a crevice created by sitting in the chair.

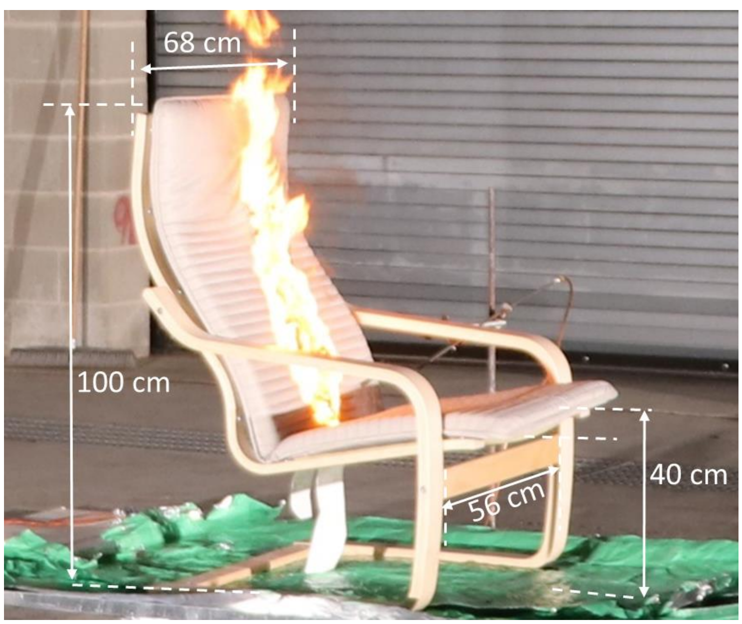


**Figure A24. Test 24 photo with dimensions of high-back Chair G.**

Figure A24 shows a photo of Test 24 burning beanbag high-back Chair G with a bent wood frame and thin PUF cushions and cover fabric ignited with a 1 cm flame at the bottom of the middle of the back cushion.

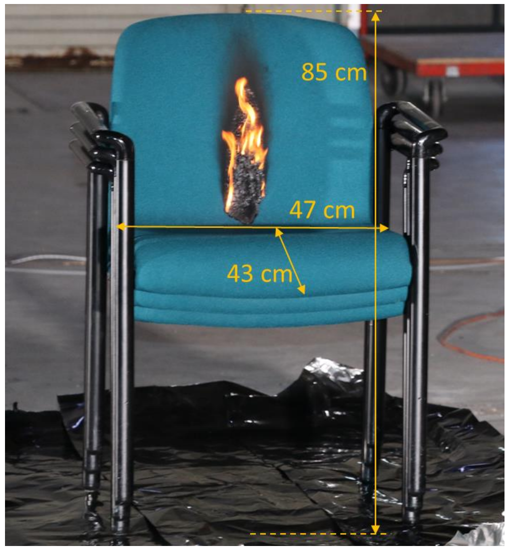


**Figure A 25. Test 25 photo with dimensions of three stacked A chairs.**

Figure A25 shows a photo of Test 25 burning three stacked A chairs (identical to those used in Test 16 and Test 21), each composed of a metal frame, two hard-plastic contoured seat-back layers, a contoured foam cushion, and cover fabric, which was ignited by a 1 cm flame at the middle of the bottom of the back cushion from the top chair in the stack.


**Figure A26. Test 26 photo with dimensions of Mattress A with two D pillows.**

Figure A26 shows a photo of Test 26 burning Mattress A, a 15 cm thick, queen size innerspring mattress, resting on a metal frame 46 cm above the floor. The mattress was single-sided with a 12 cm innerspring core. Two layers of PUF were situated above the contiguous (unpocketed) metal spring set. The core was covered with non-woven fire barrier fabric on all sides and enclosed by a polyester outer ticking fabric (see the diagram in Figure A53). Two D pillows overhung the end of the mattress by about 2 cm. The igniter flame was positioned about 2 cm inside the edge of the mattress and 1 cm above it, just below the intersection of the pillows. The experiment was identical to Test 39 except there were no bedclothes or mattress topper.


**Figure A27. Test 27 photo with dimensions of large armchair H composed of a wood frame, PUF cushions, metal springs, and thin fiberglass cloth.**

Figure A27 shows a photo of Test 27 using large armchair H which was composed of a wood frame, PUF cushions, metal springs, and thin fiberglass cloth. The 1 cm igniter flame was positioned just above the crevice between the seat and back cushions.

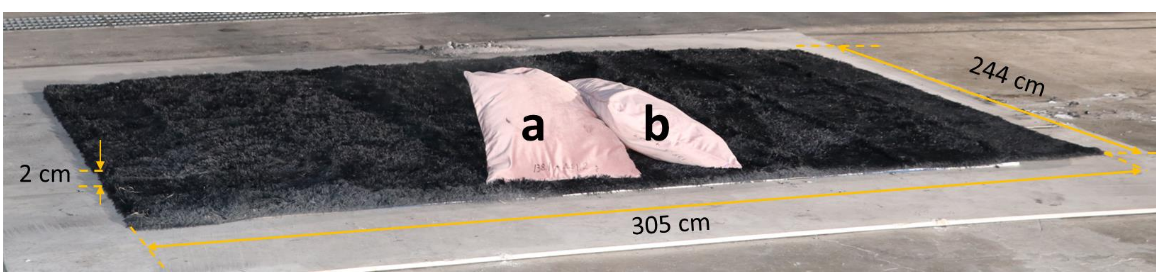


**Figure A28. Test 28 photo with dimensions of a 244 cm × 305 cm polypropylene carpet with two A pillows (identical to those used in Test 1) tilted at about 45 degrees.**

Figure A28 shows a photo of Test 28 using a polypropylene carpet with two A pillows (identical to those used in Test 1) tilted at about 45 degrees. Ignition was initiated at the middle of the bottom of the left pillow labeled “a” in the photo.

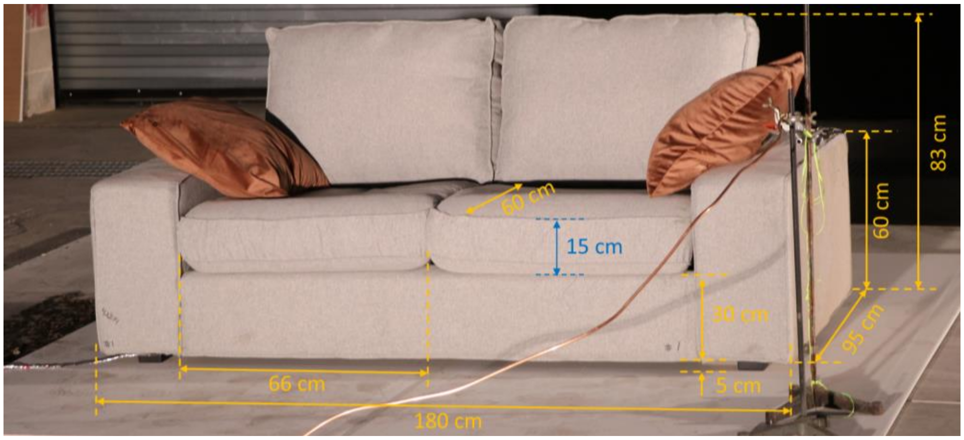


**Figure A29. Test 29 photo with dimensions of Sofa A with two A pillows and modified seat cushion inserts with spring sets removed.**

Figure A29 shows a photo of Test 29 using Sofa A, which was identical to Test 35 and Test 40 but with modified seat cushion inserts with 2 layers of PUF and the seat cushion spring set removed (see Figure A49). Two A pillows rested on the edges of the seat cushions and armrests positioned at about 45 degrees. The igniter was positioned just above the right armrest, 1 cm below the middle of the right pillow. The sofa was composed of polyester (PE) batting, fiber, and fabrics, PUF, fiberboard, plywood, solid wood, and particle board.


**Figure A30. Test 30 photo with dimensions of chaise Sofa B with two A pillows on the armrests.**

Figure A30 shows a photo of Test 30 of Sofa B with chaise identical to Tests 36 and 41 but with two A pillows, each positioned on one of the armrests at about 45 degrees. The igniter was positioned just above the right armrest, 1 cm below the middle of the right pillow. The loveseat cushion inserts were composed of a horizontal layer of low-density polyester batting, two horizontal layers of PUF, a spring set, and high-density polyester batting (see Figure A49 and associated discussion). The back cushion inserts were composed of polyester fiber. The seat and back cushion inserts were covered by a low-density polyester insert cover and cover fabric. The sofa back and armrest frames consisted of fiberboard, plywood, solid wood, and particle board. Sofa B was identical to that used by Di Cristina Torres [2024].

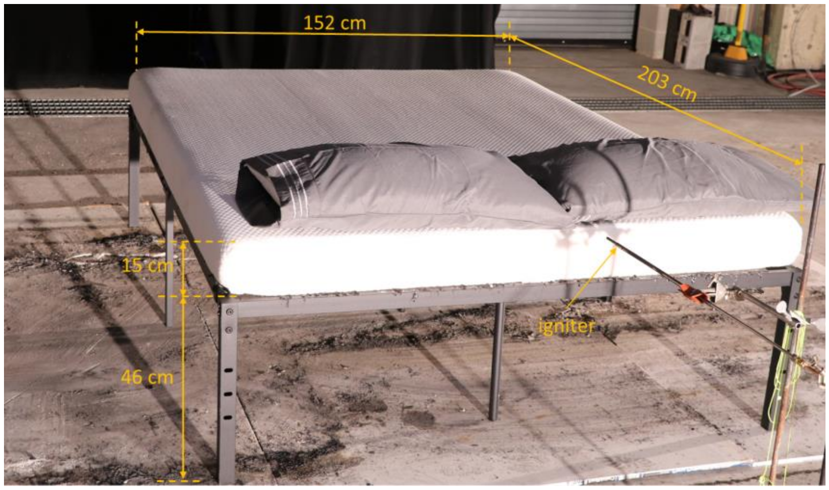


**Figure A31. Test 31 photo with dimensions of Mattress B with two D pillows.**

Figure A31 shows a photo of Test 31 using Mattress B, a 15 cm thick queen size mattress resting on a metal frame 46 cm above the floor. The mattress consisted of 100 % PUF wrapped in a FR sock inside a 100 % polyester batting cover (see diagram in Figure A54). Two D pillows overhung the end of the bed by about 2 cm. The igniter flame was positioned about 2 cm inside the edge of the mattress and 1 cm above it, just below the intersection of the pillows. The experiment was identical to Test 32, except Mattress B, not Mattress C was tested here.


**Figure A32. Test 32 photo with dimensions of Mattress C with two D pillows.**

Figure A32 shows a photo of Test 32 burning Mattress C, a 30 cm thick, queen size mattress, which was resting on a metal frame 46 cm above the floor. The mattress consisted of 100 % PUF wrapped in a FR sock inside a 100 % polyester batting cover (see diagram in Figure A55). Two D pillows overhung the end of the bed by about 2 cm. The igniter flame was positioned about 2 cm inside the edge of the mattress and 1 cm above it, just below the intersection of the pillows. The experiment was identical to Test 31, except Mattress C, not Mattress B was tested here.


**Figure A33. Test 33 photo with dimensions of the bookshelf adjacent to an A pillow.**

Figure A33 shows Test 33 burning a bookshelf and one A pillow. The igniter was positioned under the middle of the pillow, which had been resting on the side of the bookshelf at about 45 degrees. The bookshelf was identical to that used by Di Cristina Torres [2024].

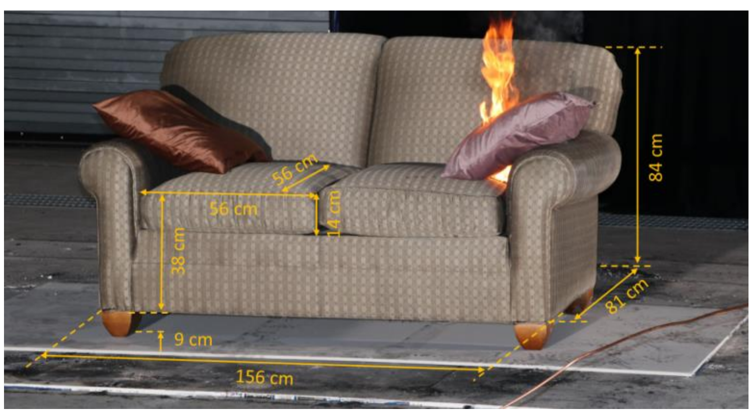


**Figure A34. Test 34 photo with dimensions of Sofa C with two A pillows.**

Figure A34 shows a photo of Test 34 burning Sofa C with two A pillows, each resting on the edge of the seat cushions and armrests at about 45 degrees. The igniter was positioned in the crevice formed between the pillow and the armrest. The sofa frame was solid wood and the back filled with polyester batting. The seat was comprised of metal springs and the seat cushion was composed of a layer of polyurethane foam covered by a polyester batting. The cover fabric was a polyester/cotton blend.

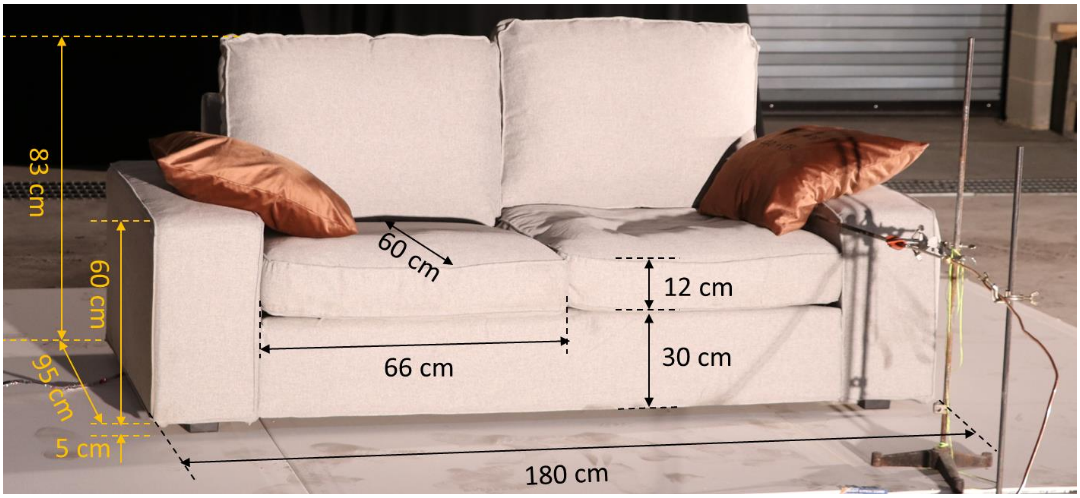


**Figure A 35. Test 35 photo with dimensions of Sofa A with modified seat cushion inserts and two A pillows.**

Figure A35 shows a photo of Test 35 of Sofa A which was identical to Test 29 and Test 40 but with modified seat cushion inserts. Two A pillows rested on the edge of the seat cushions and armrests at about 45 degrees. The igniter was positioned 1 cm below the middle of the right pillow in the crevice between the armrest and pillow. Figure A51 and associated discussion shows a diagram of the modified seat cushion insert. which was composed of a single horizontal layer of low-density polyester batting and two horizontal layers of PUF. Four pieces of PUF lined the lateral walls of the cushion insert base. The cushion inserts were covered by a low-density PE insert cover. The back cushion inserts were composed of polyester fiber. The seat and back cushion inserts were covered by a low-density polyester insert cover and cover fabrics. The sofa back and armrest frames consisted of fiberboard, plywood, solid wood, and particle board.


**Figure A36. Test 36 photo with dimensions of chaise Sofa B with two A pillows on the middle of the sofa.**

Figure A36 shows a photo of Test 36 burning Sofa B with chaise which was identical to Test 30 and Test 41 except for the two A pillows located on the middle of the sofa. The igniter was positioned in the crevice formed by the pillows. The loveseat cushion inserts were composed of a horizontal layer of low-density polyester batting, two horizontal layers of PUF, a spring set, and high-density polyester batting (see Figure A50 and discussion). The back cushion inserts were composed of polyester fiber. The seat and back cushion inserts were covered by a low-density polyester insert cover and cover fabric. The sofa back and armrest frames consisted of fiberboard, plywood, solid wood, and particle board.


**Figure A37. Test 37 photo with dimensions of Mattress B with two D pillows and bedclothes.**

Figure A37 shows a photo of Test 37 burning Mattress B, a 15 cm thick queen size mattress resting on a metal frame 46 cm above the floor. The mattress consisted of 100 % PUF wrapped in a FR sock inside a 100 % polyester batting cover (see diagram in Figure A54). Two D pillows overhung the end of the mattress by about 2 cm. The igniter flame was positioned about 2 cm inside the edge of the mattress and 1 cm above it, just below the intersection of the pillows. The experiment was identical to Test 31, but the mattress was fitted with bedclothes, including a polyester mattress cover, polyester top and bottom sheets, and a comforter with a polyester insert and cover. The same bedclothes were used in Tests 38, 39, and 44.


**Figure A38. Test 38 photo with dimensions of Mattress C with two D pillows and bedclothes.**

Figure A38 shows a photo of Test 38 burning Mattress C, a 30 cm thick queen size mattress resting on a metal frame 46 cm above the floor. The mattress consisted of 100 % PUF wrapped in a FR sock inside a 100 % polyester batting cover (see diagram in Figure A55). Two D pillows overhung the end of the mattress by about 2 cm. The igniter flame was positioned about 2 cm inside the edge of the mattress and 1 cm above it, just below the intersection of the pillows. The experiment was identical to Test 32, but the mattress was fitted with bedclothes, including a polyester mattress cover, polyester top and bottom sheets, and a comforter with a polyester insert and cover. These same bedclothes were used in Tests 37, 39, and 44.


**Figure A39. Test 39 photo with dimensions of Mattress A with two D pillows, bedclothes, and a mattress topper.**

Figure A39 shows a photo of Test 39 burning mattress A, a 15 cm thick queen size innerspring mattress with bedclothes and a mattress topped, resting on a metal frame 46 cm above the floor. The mattress was single-sided with a 12 cm innerspring core. Two layers of PUF (a 2 cm and a 1 cm layer) were situated above the contiguous (unpocketed) metal spring set. The core was covered with a non-woven fire barrier fabric having a thickness of roughly 6 mm on all sides and enclosed by a polyester outer ticking fabric (see the diagram in Figure A53). Two D pillows overhung the end of the mattress by about 2 cm. The igniter flame was positioned about 2 cm inside the edge of the mattress and 1 cm above it, just below the intersection of the pillows. The experiment was identical to Test 26 except the mattress was fitted with bedclothes, including a polyester mattress cover, polyester top and bottom sheets, and a comforter with a polyester insert and cover. The same bedclothes were used in Tests 37, 38, and 44 (with Mattresses B and C). In addition to the bedclothes, a PUF mattress topper was positioned between the mattress and the bedclothes.

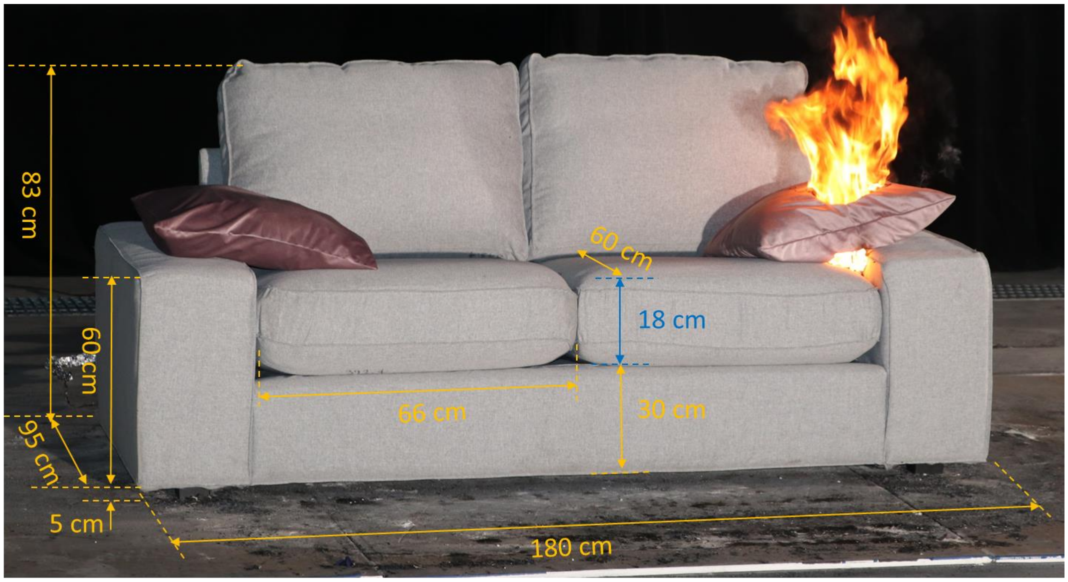


**Figure A40. Test 40 photo with dimensions of Sofa A with two A pillows similar to Tests 29 and 40, but with modified seat cushion inserts that included three layers of PUF.**

Figure A40 shows a photo of Test 40 of Sofa A which was similar to Test 29 and Test 35 but with modified seat cushion inserts. Two A pillows rested on the edge of the seat cushions and armrests at about 45 degrees. The igniter was positioned 1 cm below the middle of the right pillow in the crevice between the armrest and pillow. Figure A52 shows a diagram of the modified seat cushion insert, which was composed of a single horizontal layer of low-density polyester batting and 3 horizontal layers of PUF. Four pieces of PUF lined the lateral walls of the cushion insert base. The cushion inserts were covered by a low-density PE insert cover. The back cushion inserts were composed of polyester fiber. The seat and back cushion inserts were covered by a low-density polyester insert cover and cover fabrics. The sofa back and armrest frames consisted of fiberboard, plywood, solid wood, and particle board.

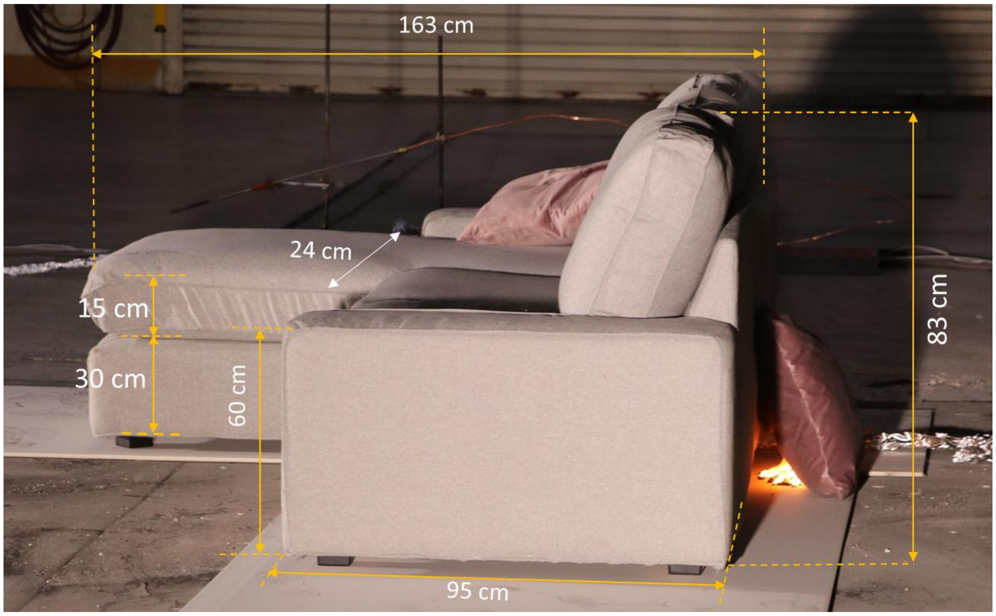


**Figure A41. Test 41 photo with dimensions of chaise Sofa B with two A pillows, one behind the sofa.**

Figure 41 shows a photo of Test 41 burning Sofa B with chaise which was identical to Tests 30 and 36 except one of the A pillows was located on the floor behind the middle of the sofa while the other was positioned over the left armrest. The igniter was positioned in the crevice formed by the pillows. The loveseat cushion inserts were composed of a horizontal layer of low-density polyester batting, two horizontal layers of PUF, a spring set, and high-density polyester batting (see Figure A50 and discussion). The back cushion inserts were composed of polyester fiber. The seat and back cushion inserts were covered by a low-density polyester insert cover and cover fabric. The sofa back and armrest frames consisted of fiberboard, plywood, solid wood, and particle board.

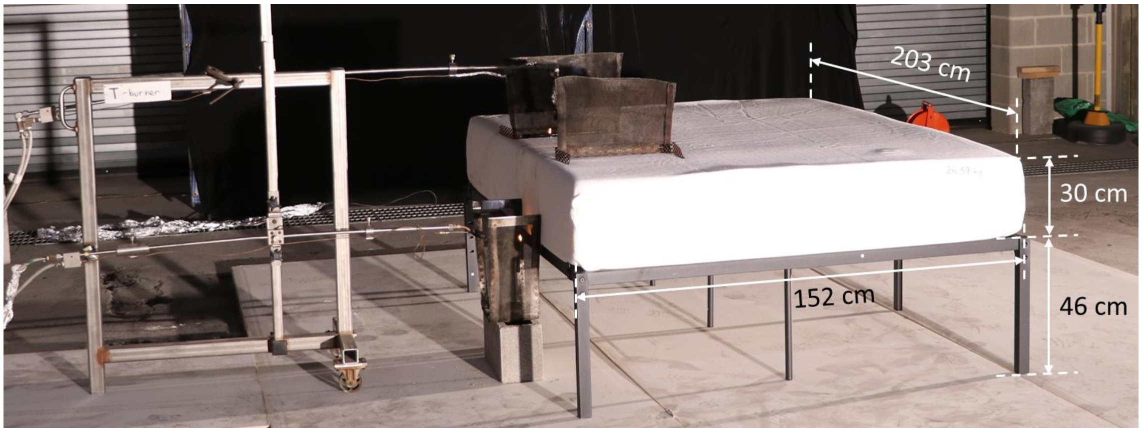


**Figure A42. Test 42 photo with dimensions of Mattress C undergoing the 16 CFR 1633 test protocol.**

Figure A42 shows a photo of Test 42 of mattress C without pillows or bedclothes, resting on a metal frame 46 cm above the floor and undergoing the 16 CFR 1633 test protocol with prescribed top burner and side flames. Mattress C was a 30 cm thick queen size box spring mattress consisting of 100 % PUF wrapped in a FR sock and covered by a 100 % polyester batting cover (see diagram in Figure A55**Figure A55**). The experiment was identical to Test 43.

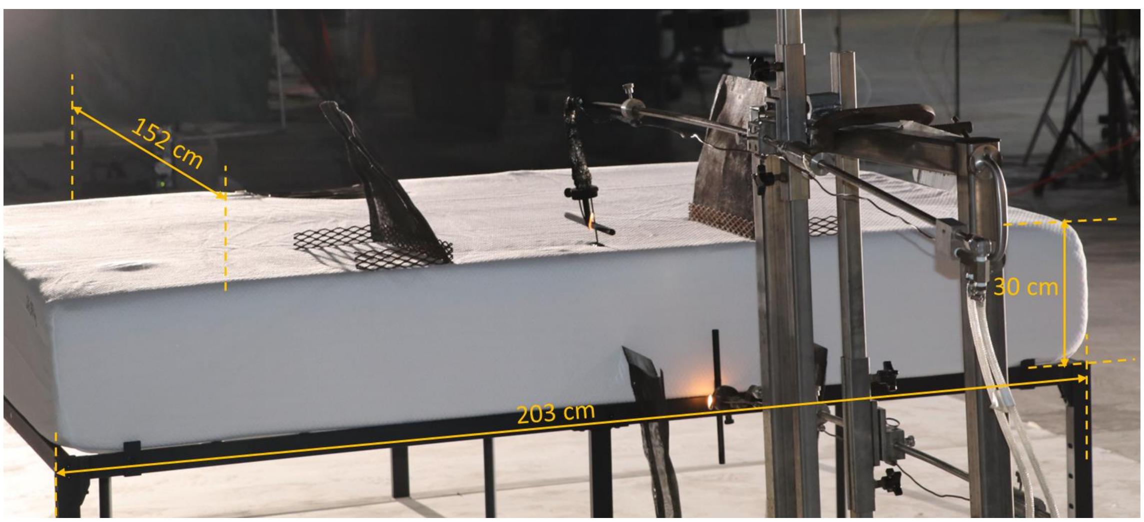


**Figure A43. Test 43 photo with dimensions of Mattress C undergoing the 16 CFR 1633 test protocol.**

Figure A43 shows a photo of Test 43 of mattress C without pillows or bedclothes, resting on a metal frame 46 cm above the floor and undergoing the 16 CFR 1633 test protocol with prescribed top burner and side flames. Mattress C was a 30 cm thick queen size box spring mattress consisting of 100 % PUF wrapped in a FR sock and covered by a 100 % polyester batting (see diagram in Figure A55). The experiment was identical to Test 42.

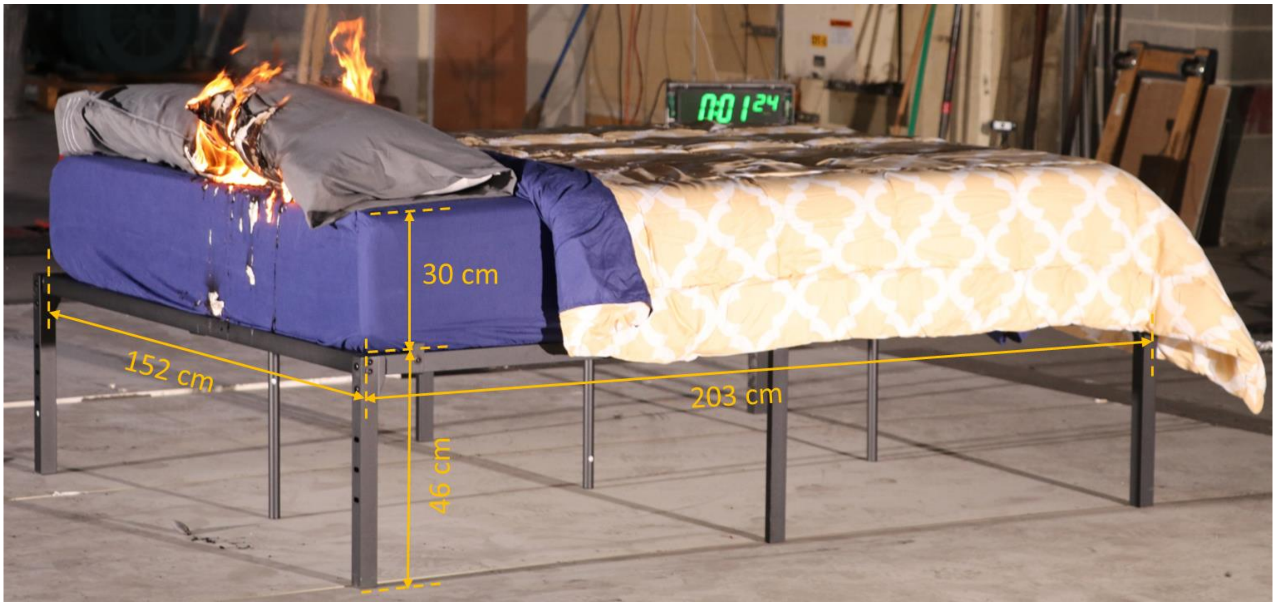


**Figure A44. Test 44 photo with dimensions of Mattress C with two pillows and bedclothes and the mattress' FR sock removed.**

Figure A44 shows a photo of Test 44 burning Mattress C, a 30 cm thick queen size mattress resting on a metal frame 46 cm above the floor. The mattress consisted of 100 % PUF covered by a 100 % polyester batting cover, but with the FR sock removed. Two D pillows overhung the end of the mattress by about 2 cm. The igniter flame was positioned about 2 cm inside the edge of the mattress and 1 cm above it, just below the intersection of the pillows. The experiment was like Test 38 except the FR sock was removed from the mattress. The mattress was fitted with bedclothes, including a polyester mattress cover, polyester top and bottom sheets, and a comforter with a polyester insert and cover. The same bedclothes were used in Tests 37, 38, and 39.

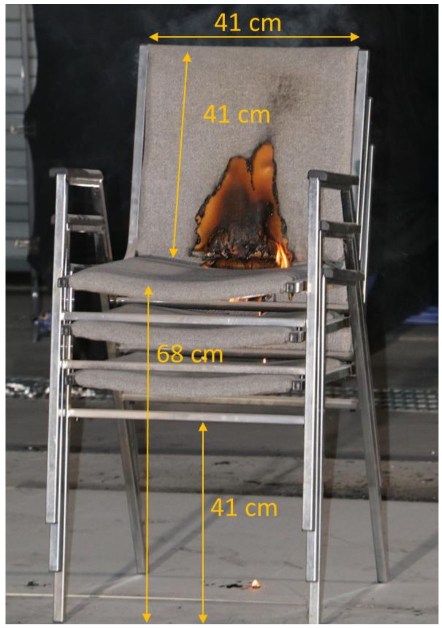


**Figure A45. Test 45 photo with dimensions of three stacked I chairs.**

Figure A45 shows a photo of Test 45 burning three stacked I chairs, each composed of a metal frame, particle board seat and back, PUF seat and back cushions, and cover fabric after ignition at the middle of the bottom of the back cushion of the uppermost chair.

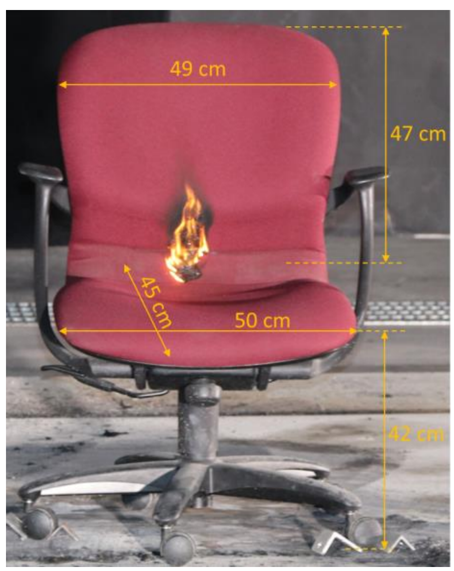


**Figure A46. Test 46 photo with dimensions of Chair J.**

Figure A46 shows a photo of Test 46 of wheeled office Chair J with arms, composed of a contoured hard plastic frame and backing, PUF seat and back cushions and cover fabric, after ignition at the middle of the bottom of the back cushion.

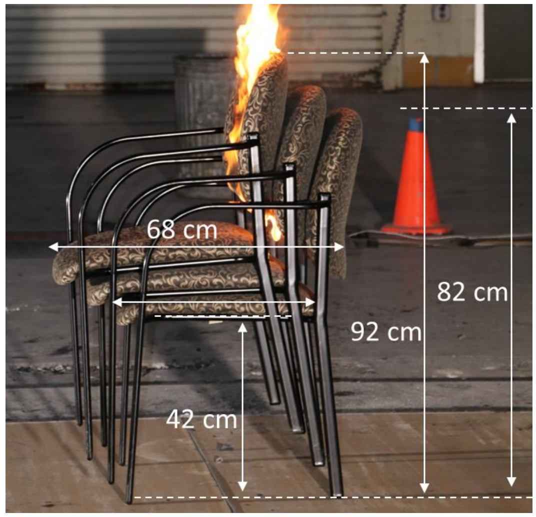


**Figure A47. Test 47 photo with dimensions of three stacked D chairs.**

Figure A47 shows a photo of Test 47 burning three stacked D chairs, each chair was composed of a metal frame, wood seat and back layers, contoured foam cushions and cover fabrics, ignited at the middle, bottom of the back cushion of the uppermost chair. This chair was also used in Test 20.


**Figure A48. Test 48 photo with dimensions of wheeled office Chair K.**

Figure A48 shows a photo of Test 48 burning wheeled office Chair K with arms, composed of a hard plastic frame, a PUF cushion and webbed backing after ignition at the middle, bottom of the seat back.

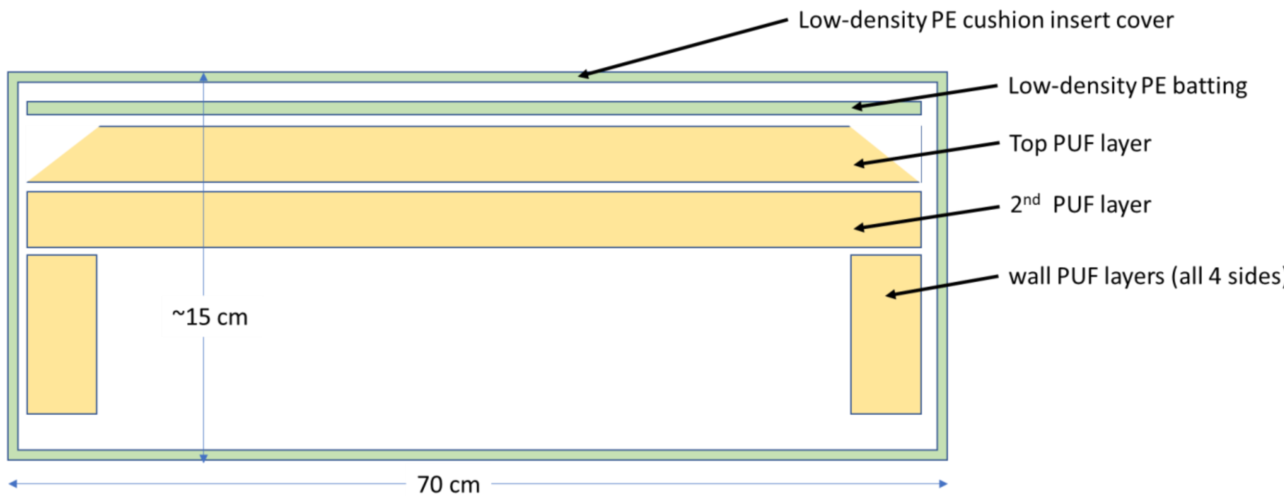


**Figure A49. Cutaway drawing of the modified seat cushion inserts with 2 layers of polyurethane foam without the cushion spring set used in Test 29.**

Figure A49 shows a drawing (not to scale) of the modified seat cushion used in Test 29, which was composed of a horizontal layer of low-density polyester (PE) batting and two horizontal layers of polyurethane foam (PUF), above four pieces of PUF lining the walls of the cushion base. The cushion inserts were surrounded by a low-density PE insert cover. The two original seat cushion inserts were modified by removing the seat cushion spring set and the high-density PE bottom batting layer.

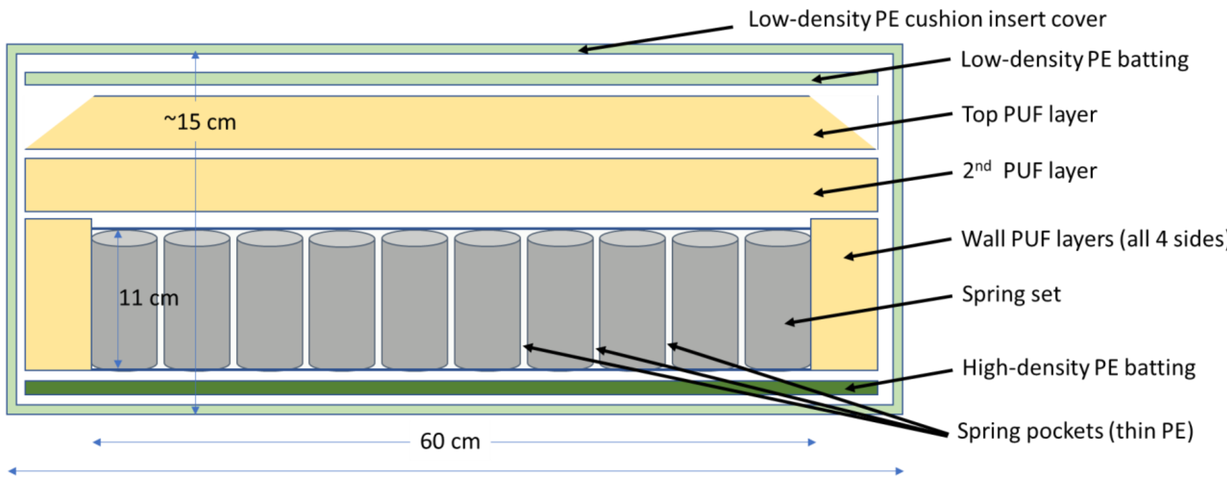


**Figure A50. Cutaway drawing of the seat cushion inserts with 2 layers of PUF used in Tests 30, 36, and 41.**

Figure A50 shows a drawing (not to scale) of the seat cushion used in Tests 30, 36, and 41, which was composed of a horizontal layer of low-density polyester (PE) batting, two horizontal layers of polyurethane foam (PUF), a spring set and four pieces of PUF lining the walls of the cushion base, and a high-density PE bottom batting layer. The cushion inserts were surrounded by a low-density PE insert cover.

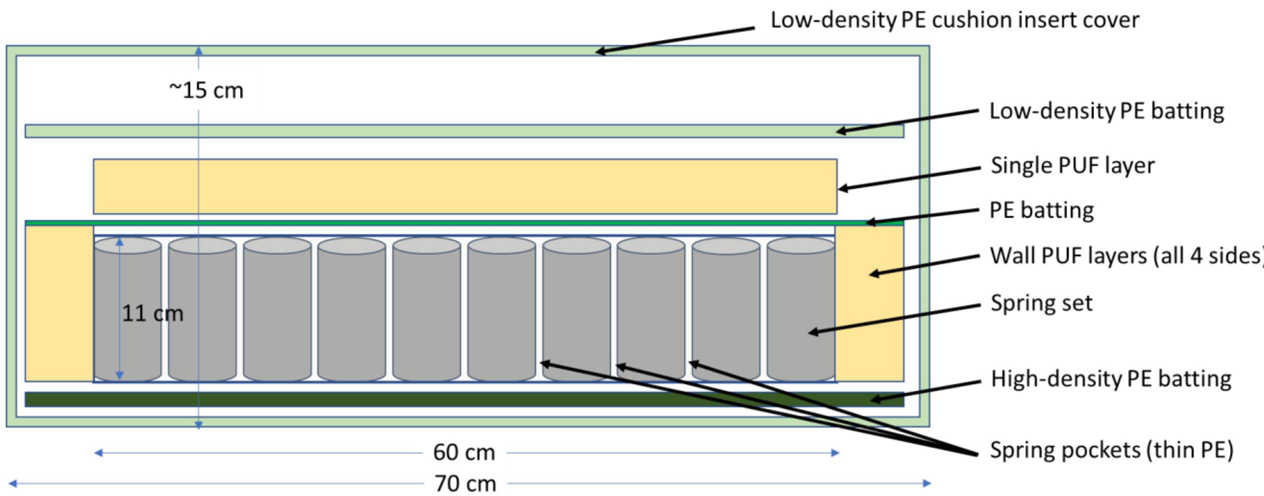


**Figure A51. Cutaway drawing of the modified seat cushion inserts with 1 layer of polyurethane foam used in Test 35.**

Figure A51 shows a drawing (not to scale) of the seat cushion used in Test 35, which was composed of a thin horizontal layer of low-density polyester (PE) batting and 1 horizontal layer of polyurethane foam (PUF), above a seat cushion spring set, 4 pieces of PUF lining the walls of the cushion base, and a high-density PE batting. The cushion insert was surrounded by a low-density PE insert cover. The two original seat cushion inserts were modified by removing one horizontal PUF layer.

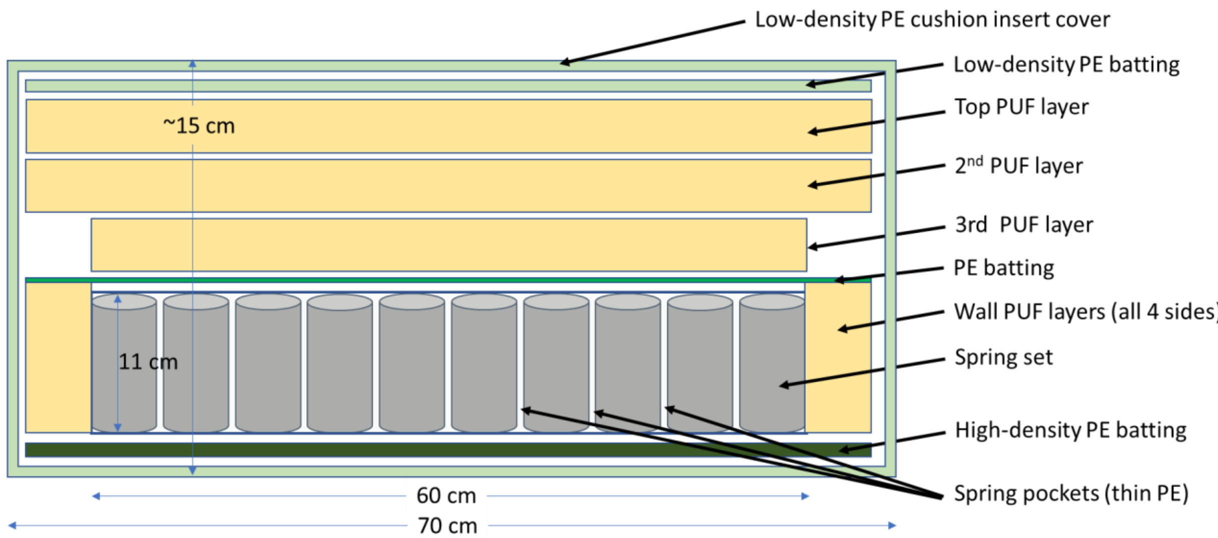


**Figure A52. Cutaway drawing of the modified seat cushion inserts with 3 horizontal layers of polyurethane foam (PUF) used in Test 40.**

Figure A52 shows a drawing (not to scale) of the seat cushion used in Test 40, which was composed of a thin horizontal layer of low-density polyester (PE) batting and 3 horizontal layers of polyurethane foam (PUF), above a seat cushion spring set, 4 pieces of PUF lining the walls of the cushion base, and a high-density PE batting. The cushion insert was surrounded by a low-density PE insert cover. The two original seat cushion inserts were modified by adding the third horizontal PUF layer.

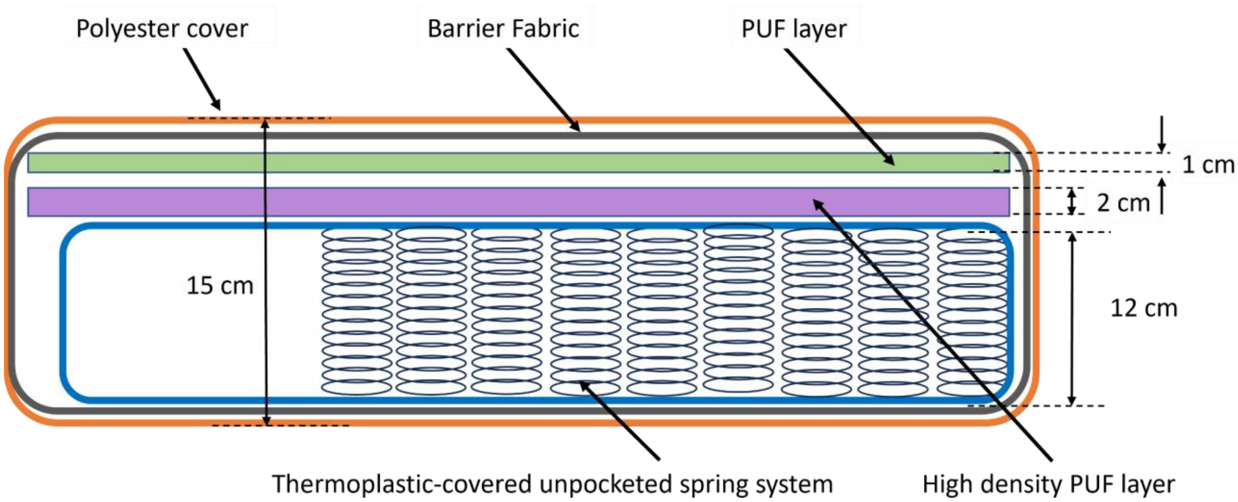


**Figure A53. Cutaway drawing of Mattress A.**

Figure A53 shows a drawing (not to scale) of the 15 cm queen size Mattress A used in Test 26 and Test 39, which was composed of an unpocketed metal coil spring system with two layers of PUF (a 2 cm and a 1 cm layer) surrounded on all sides by an inner non-woven fire barrier fabric and an outer polyester cover.

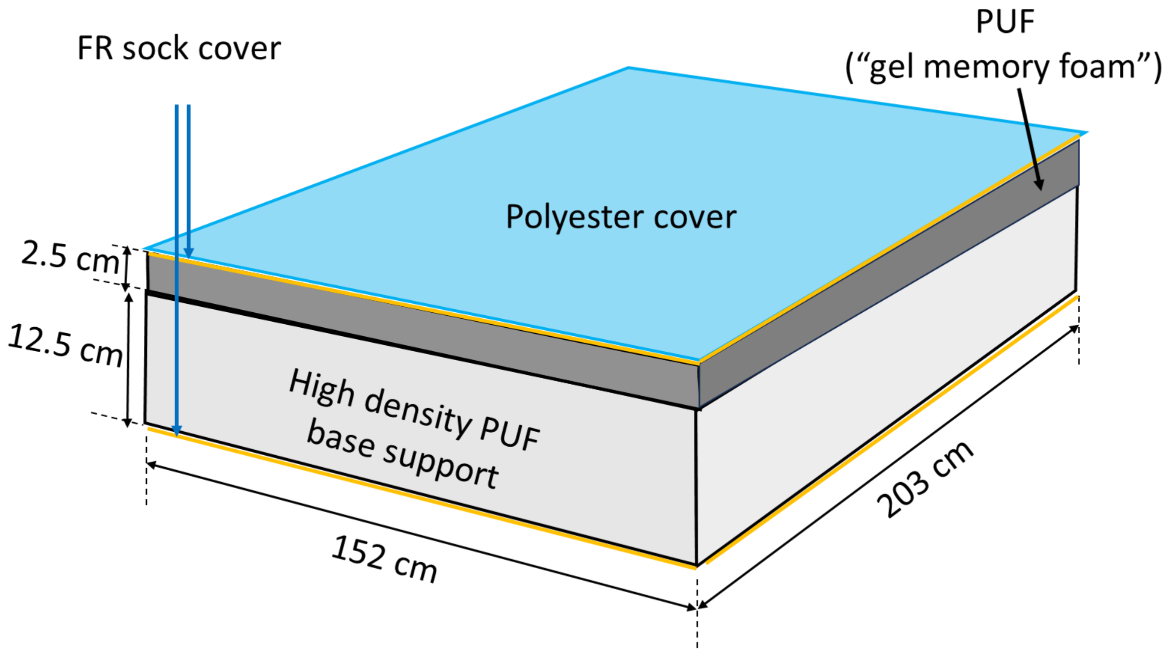


**Figure A54. Cutaway drawing of Mattress B.**

Figure A54 shows a drawing (not to scale) of the 15 cm queen size Mattress B used in Test 31 and Test 37, which was composed of 100 % polyurethane foam covered by a FR sock inside a 100 % polyester cover.

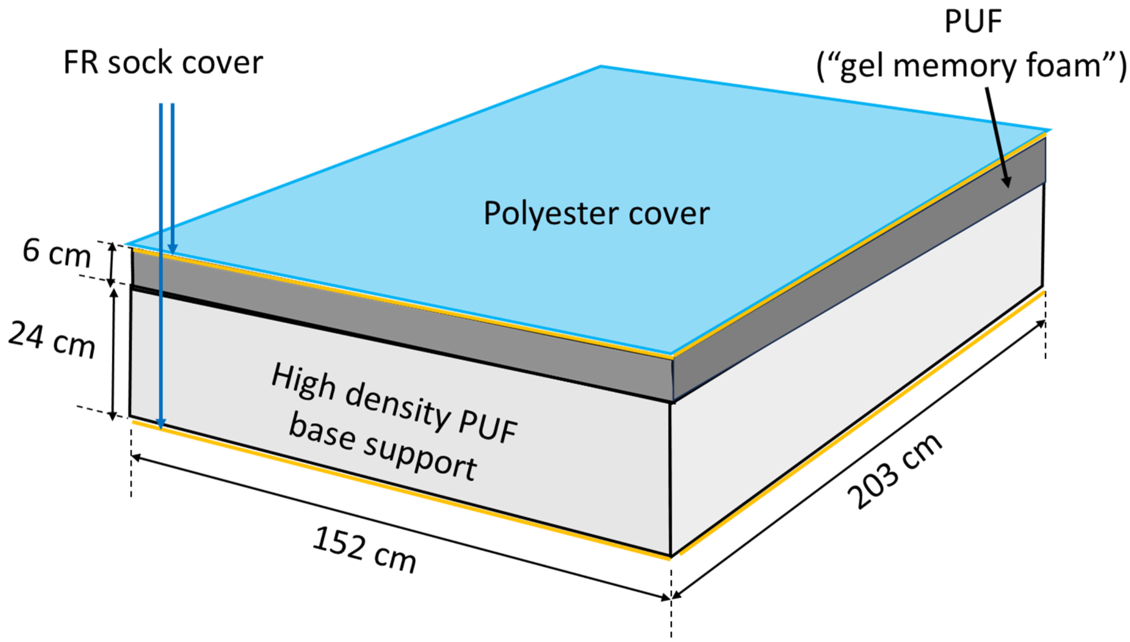


**Figure A55. Cutaway drawing of Mattress C.**

Figure A55 shows a drawing of the 30 cm queen size Mattress C used in Tests 32, 28, 42, 43, and 44, which was composed of 100 % polyurethane foam covered by a FR sock inside a 100 % polyester cover. In Test 44, the FR sock was removed.

## Appendix B. Heat Flux

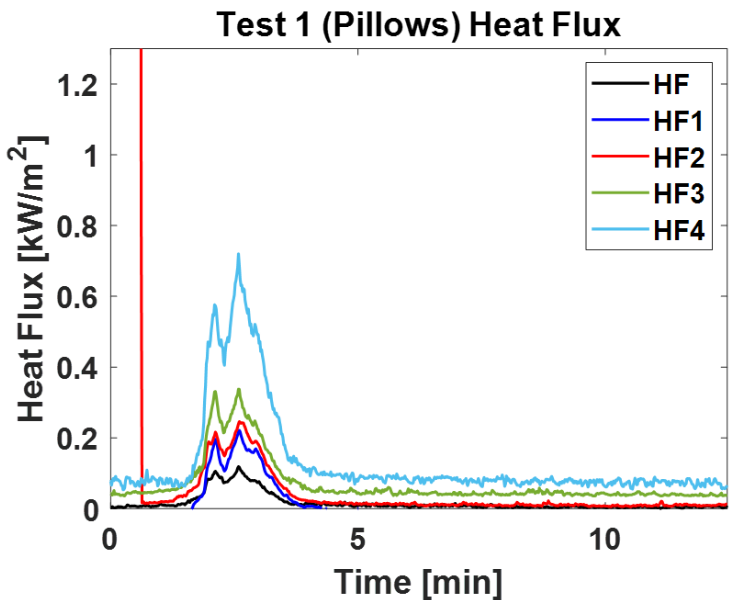


**Figure B 1: Radiative heat flux measurements during Test 1, a polyester foam pillow with a polyester cover.**

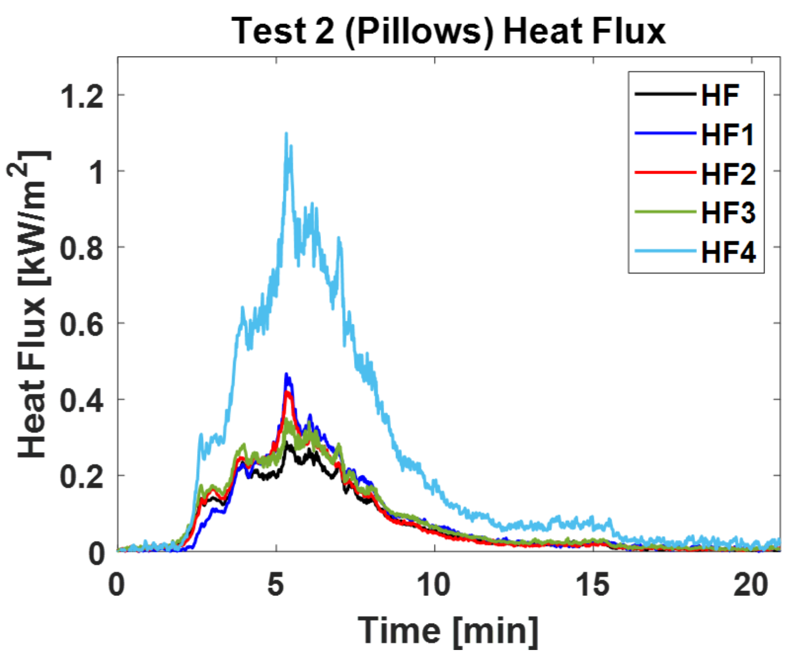


**Figure B 2: Radiative heat flux measurements during Test 2, a PUF pillow with polyester cover.**

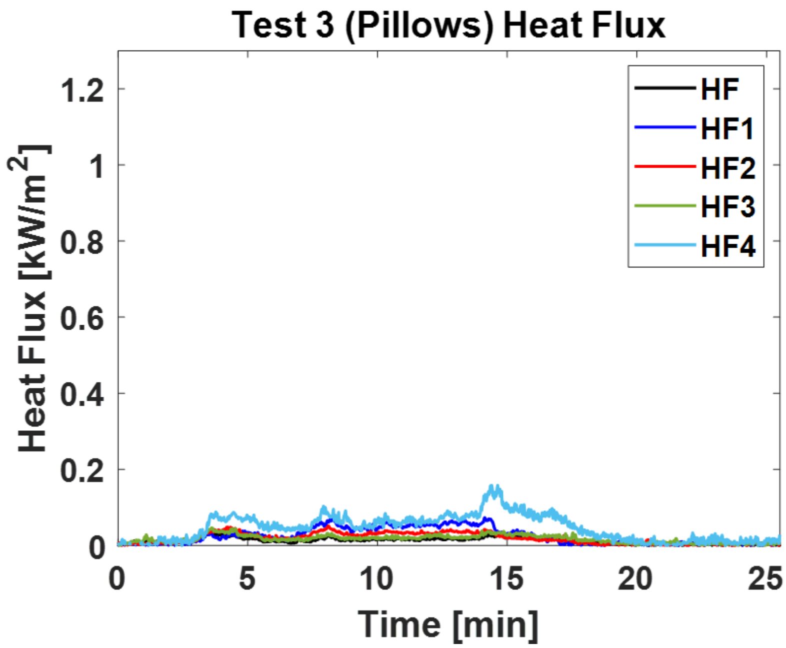


**Figure B 3: Radiative heat flux measurements during Test 3, a feather pillow with a polyester cover.**

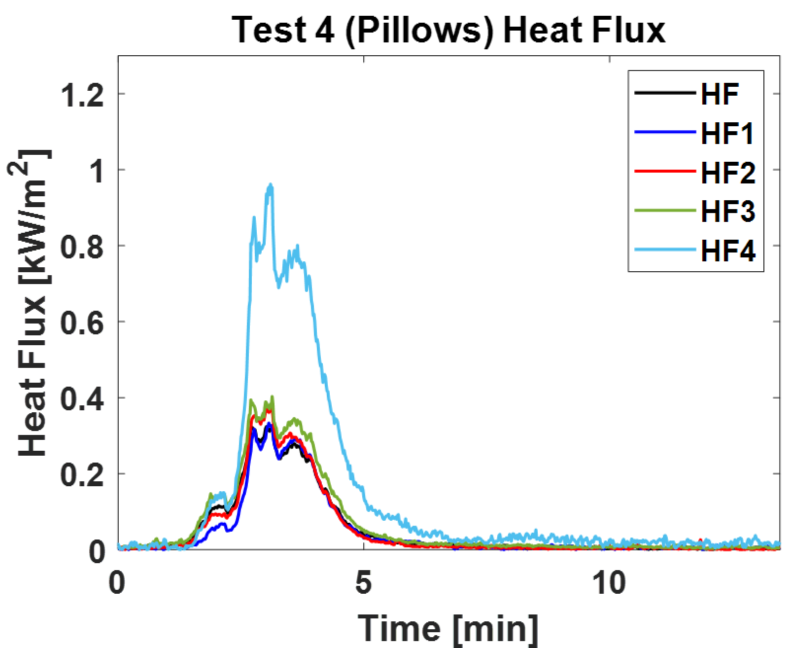


**Figure B 4: Radiative heat flux measurements during Test 4, a polypropylene foam insert pillow with a polypropylene cover.**

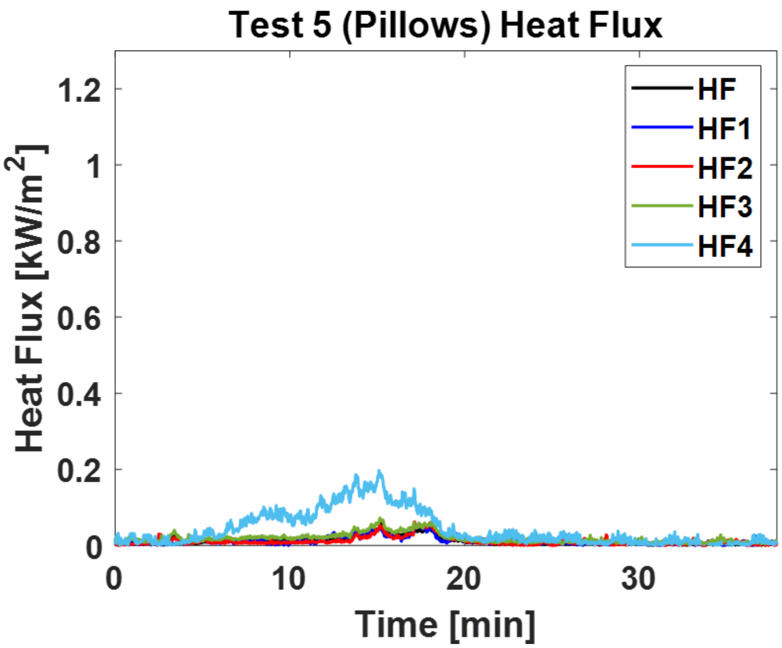


**Figure B 5: Radiative heat flux measurements during Test 5, a feather pillow with a polyester cover.**

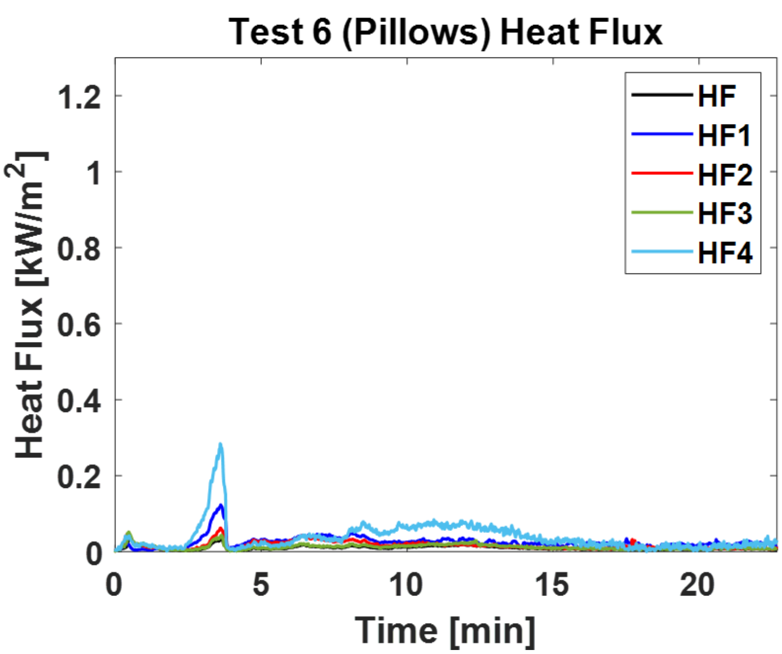


**Figure B 6: Radiative heat flux measurements during Test 6, a pillow with polyester foam insert and polyester cover.**

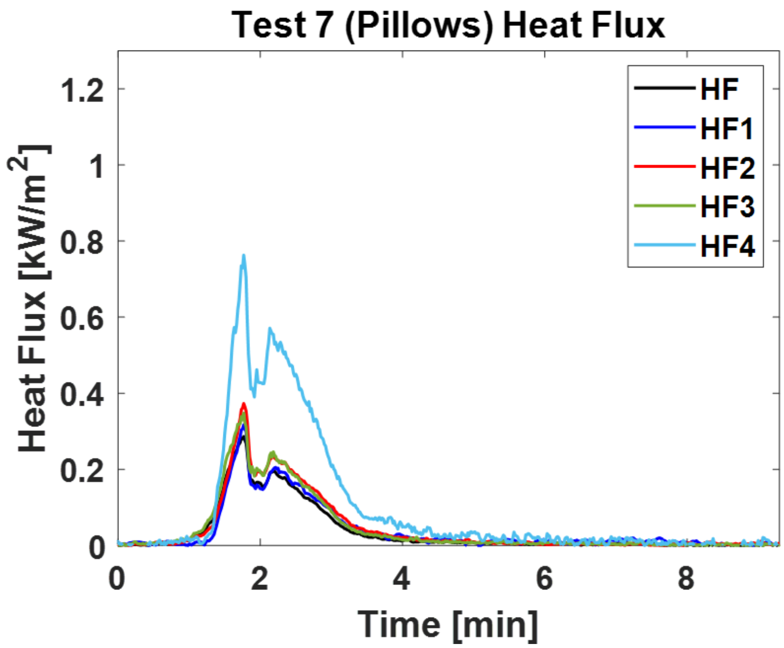


**Figure B 7: Radiative heat flux measurements during Test 7, a pillow with polyester foam insert and polyester cover.**

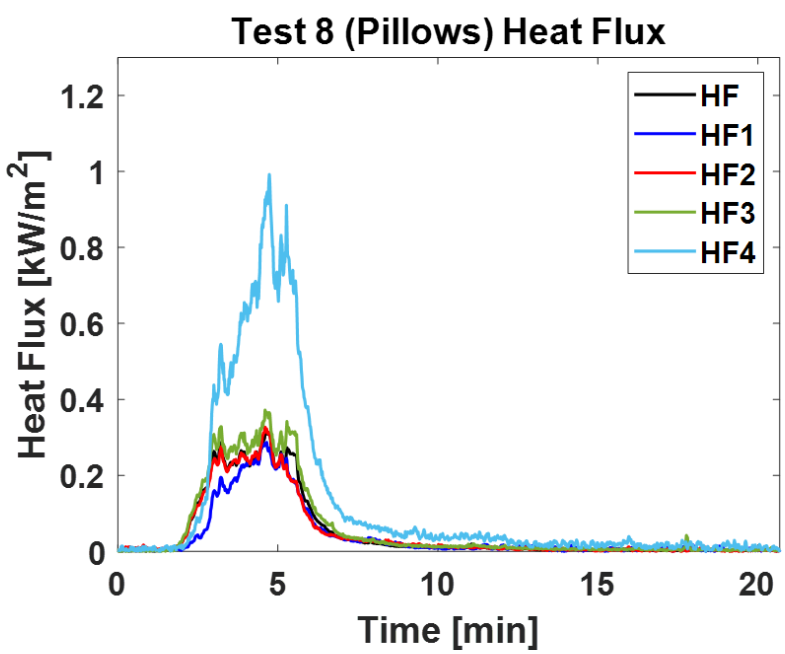


**Figure B 8: Radiative heat flux measurements during Test 8, two pillows with polypropylene foam inserts and polypropylene covers.**

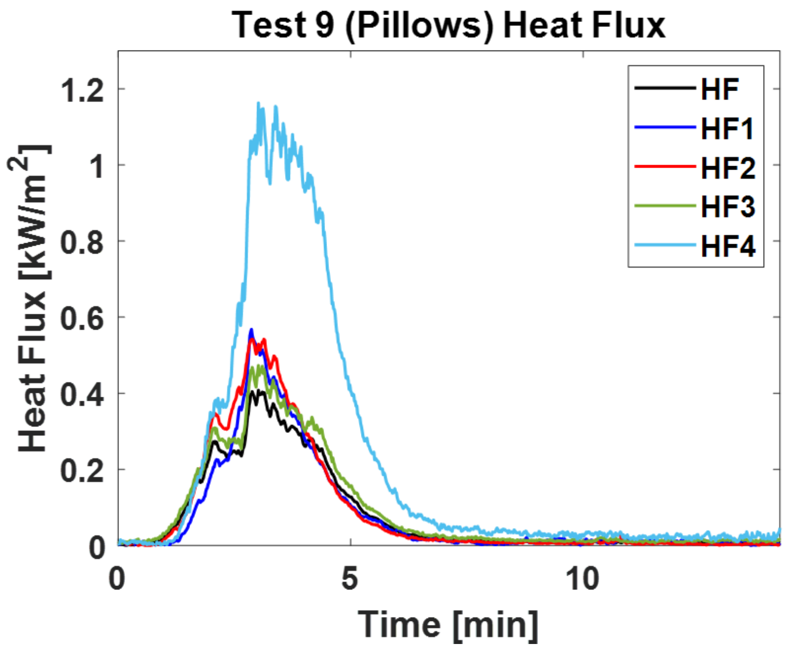


**Figure B 9: Radiative heat flux measurements during Test 9, four pillows with polyester foam inserts and polyester covers.**

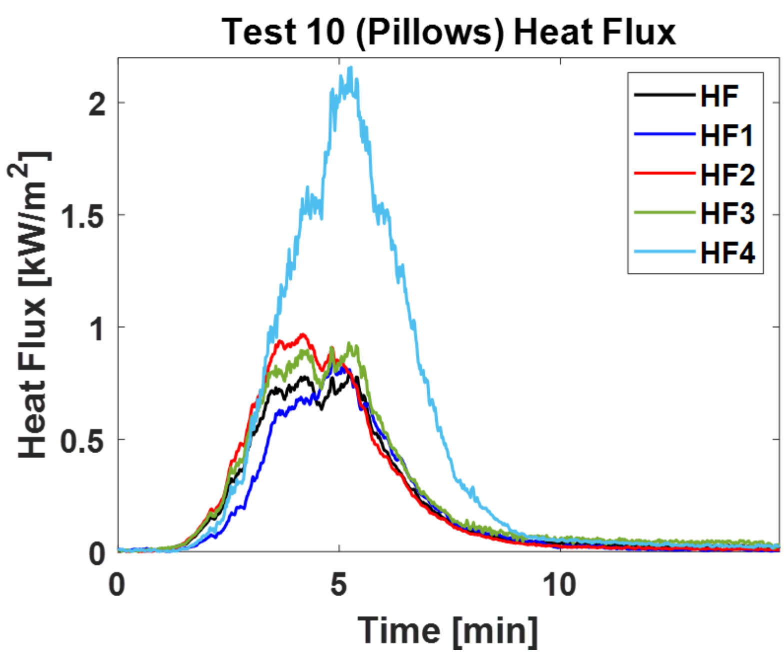


**Figure B 10: Radiative heat flux measurements during Test 10, four pillows with polypropylene foam inserts and polypropylene covers.**

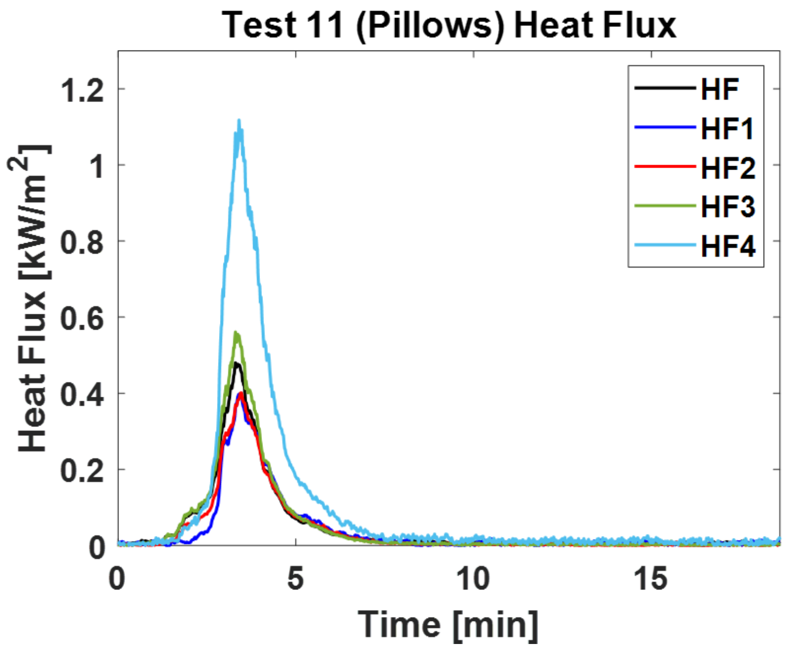


**Figure B 11: Radiative heat flux measurements during Test 11, a pillow with polypropylene foam insert and polypropylene cover.**

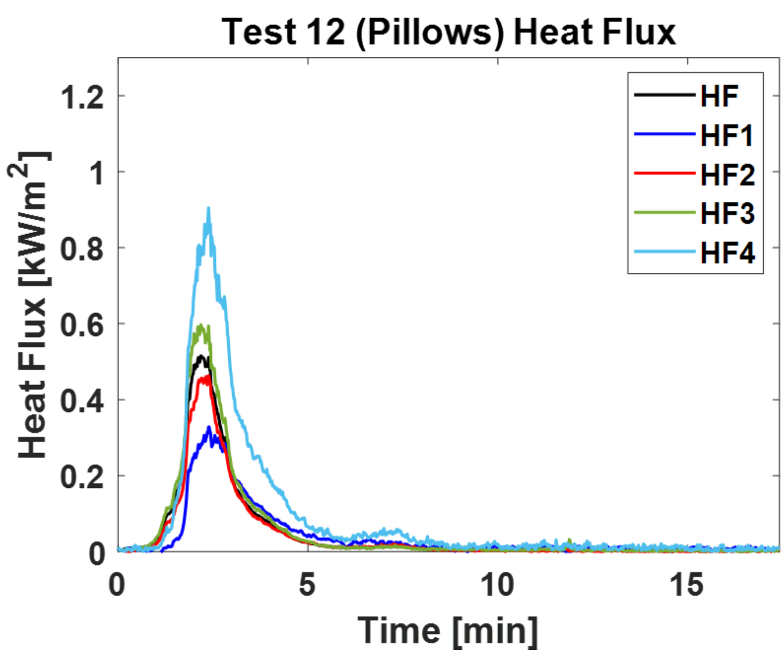


**Figure B 12: Radiative heat flux measurements during Test 12, a pillow with polypropylene foam insert and polypropylene cover.**

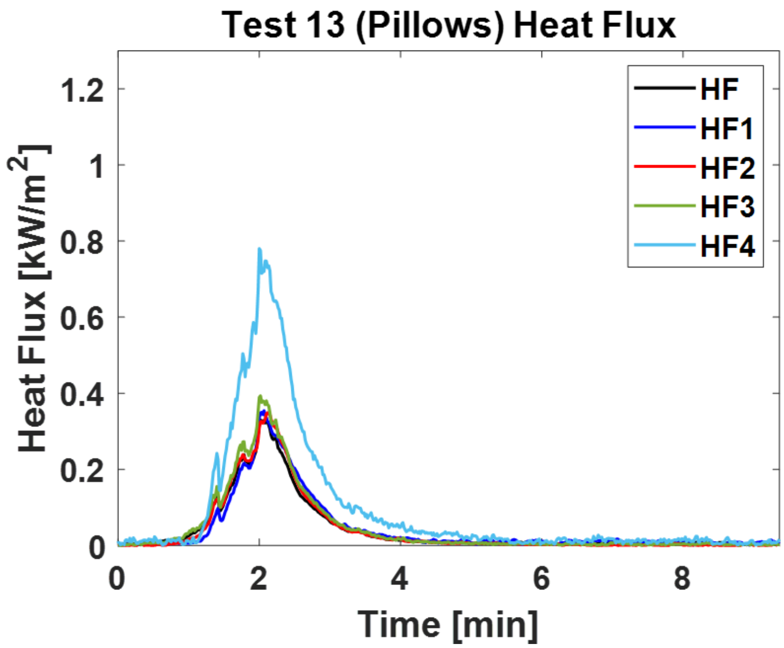


**Figure B 13: Radiative heat flux measurements during Test 13, a pillow with polyester foam insert and polyester cover.**

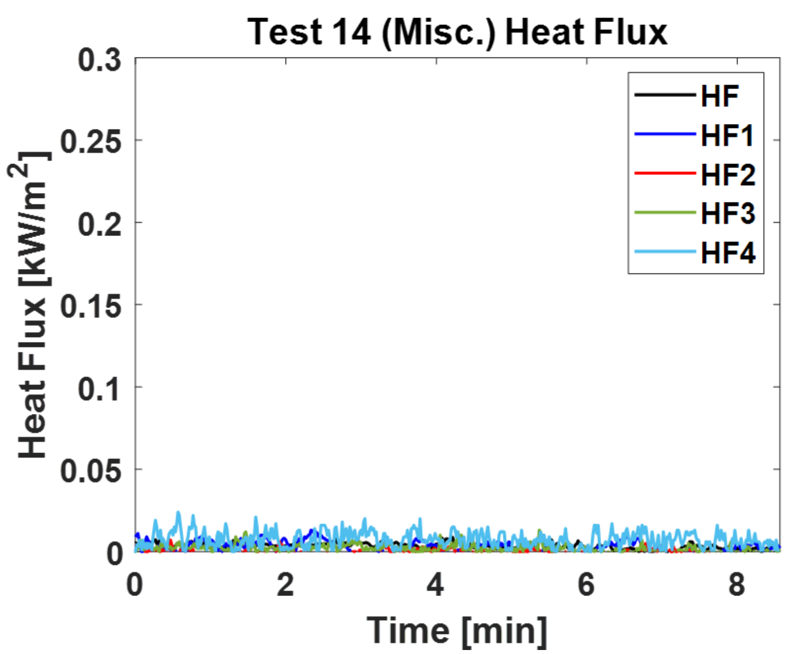


**Figure B 14: Radiative heat flux measurements during Test 14, a laptop.**

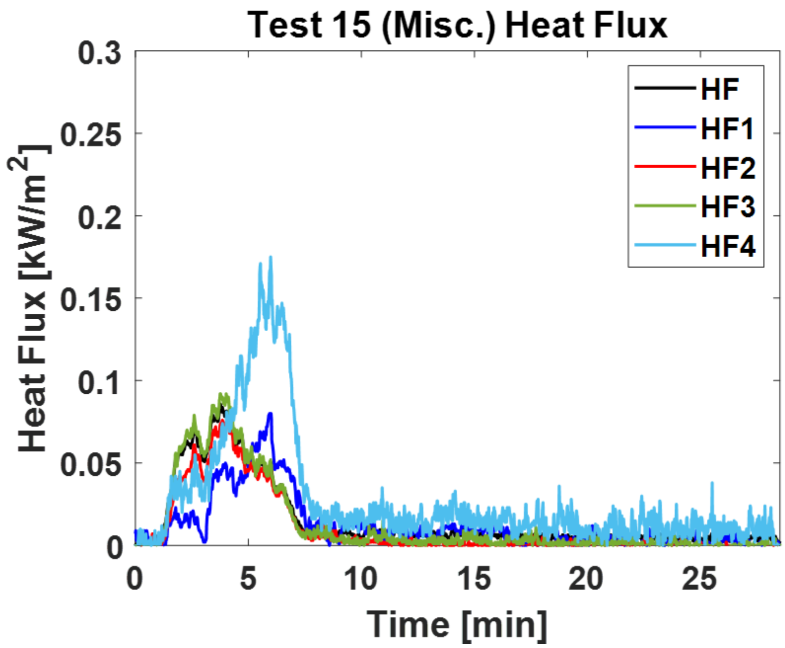


**Figure B 15: Radiative heat flux measurements during Test 15, a laptop on a pillow (polyester foam insert and polyester cover).**

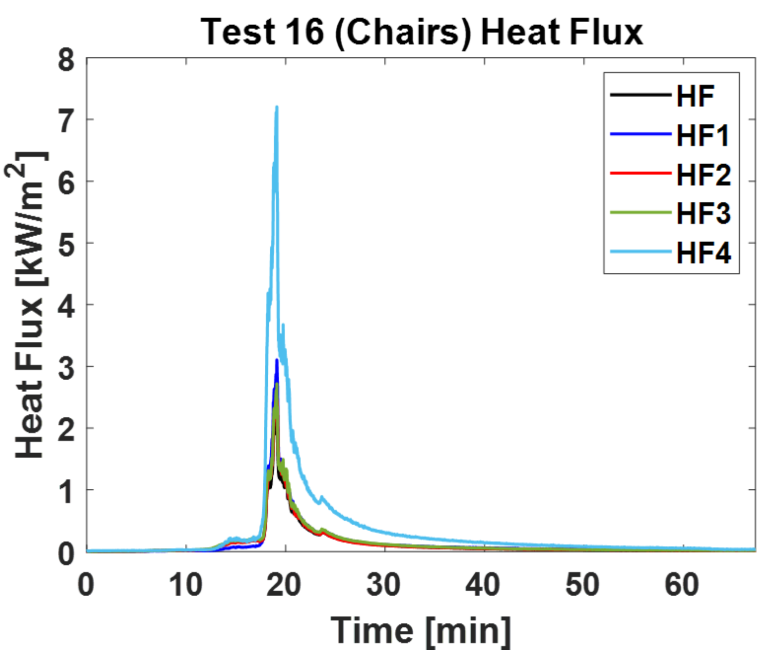


**Figure B 16: Radiative heat flux measurements during Test 16, a chair with PUF padding.**

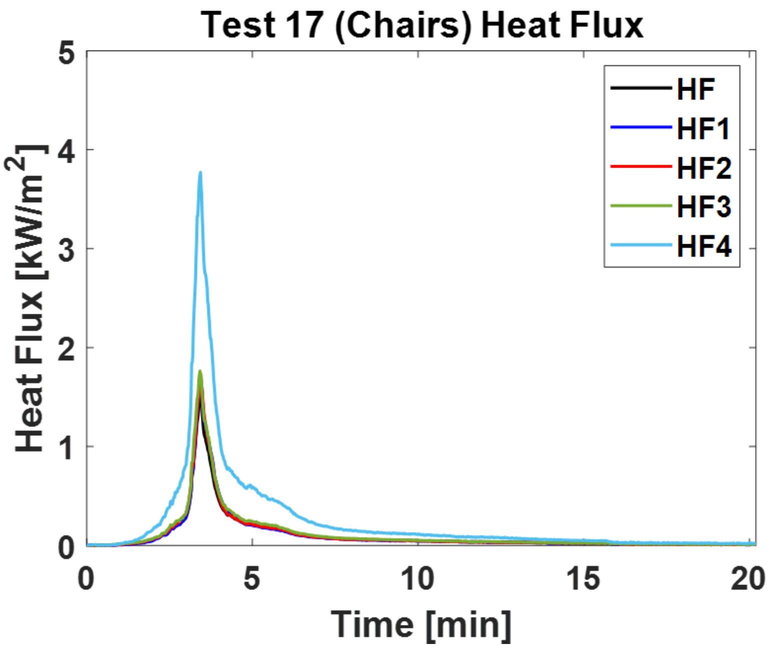


**Figure B 17: Radiative heat flux measurements during Test 17, a chair with PUF padding.**

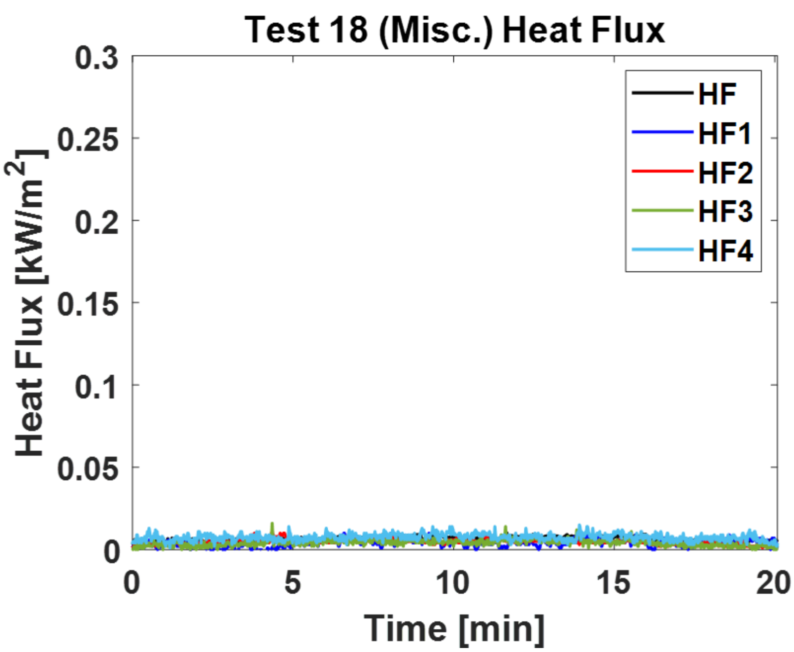


**Figure B 18: Radiative heat flux measurements during Test 18, a side table composed of particleboard.**

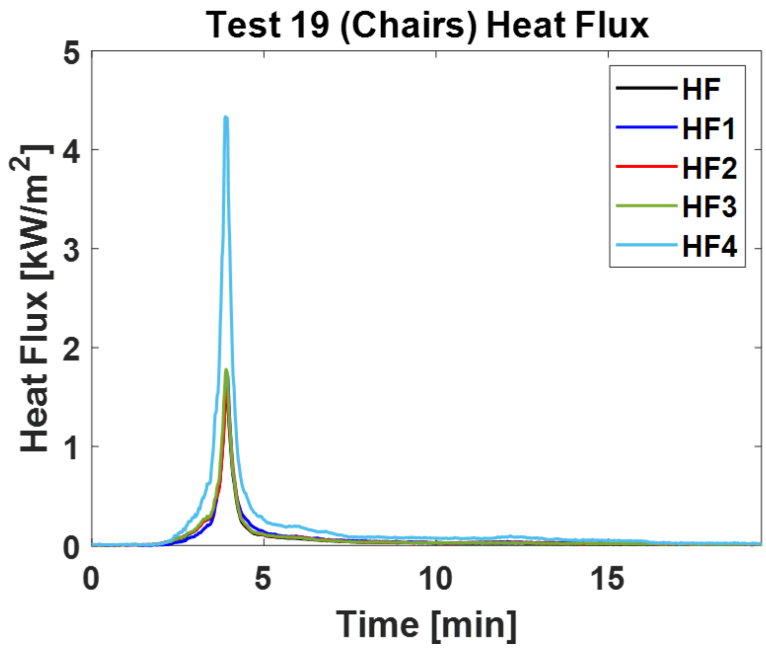


**Figure B 19: Radiative heat flux measurements during Test 19, a chair with PUF padding.**

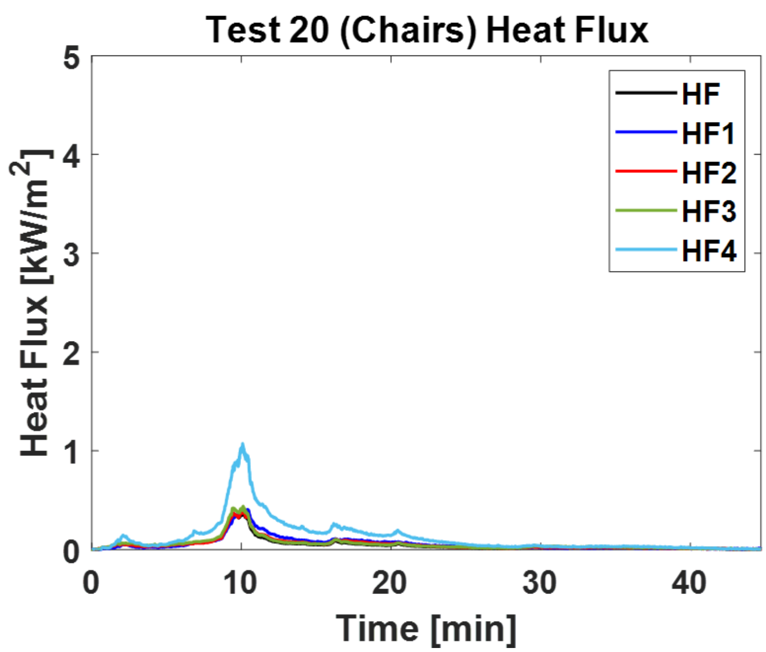


**Figure B 20: Radiative heat flux measurements during Test 20, a chair with PUF padding. and a wooden frame.**

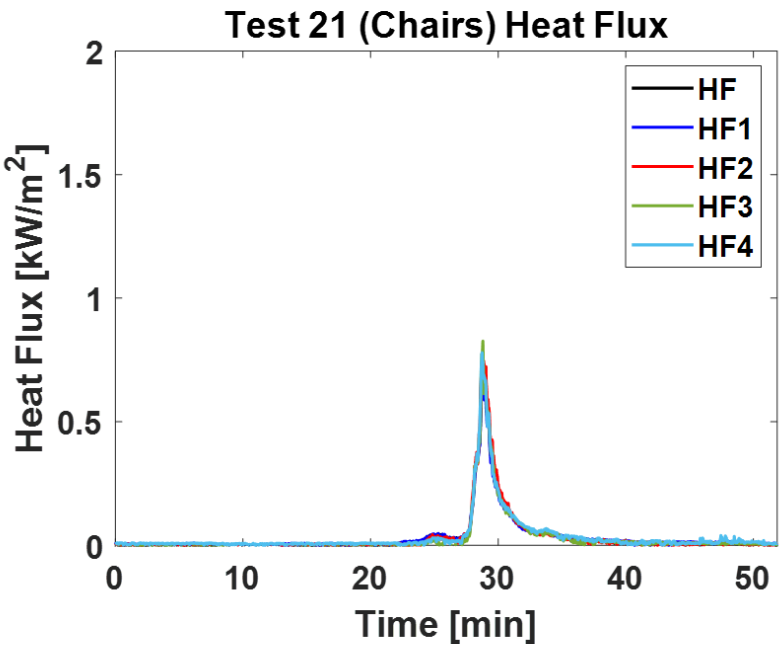


**Figure B 21: Radiative heat flux measurements during Test 21, a chair with PUF padding.**

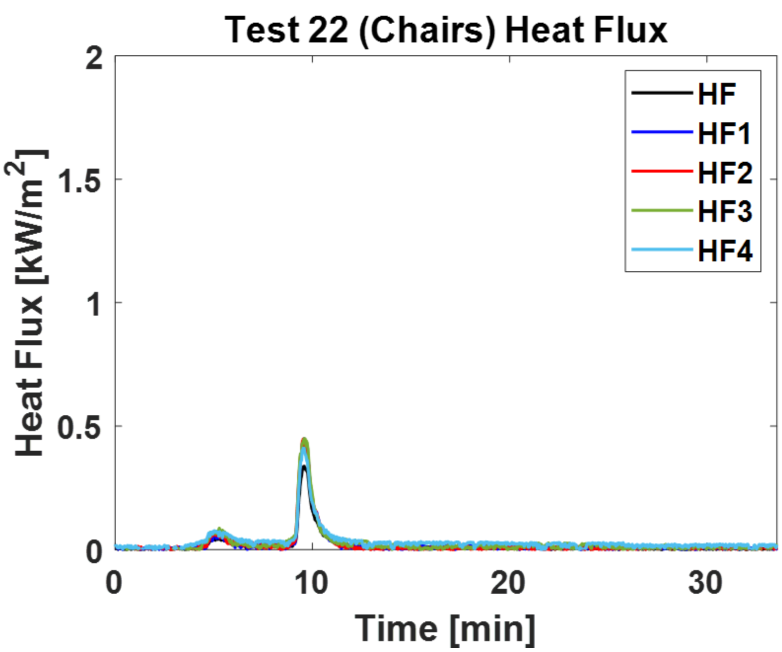


**Figure B 22: Radiative heat flux measurements during Test 22, a chair with PUF padding.**

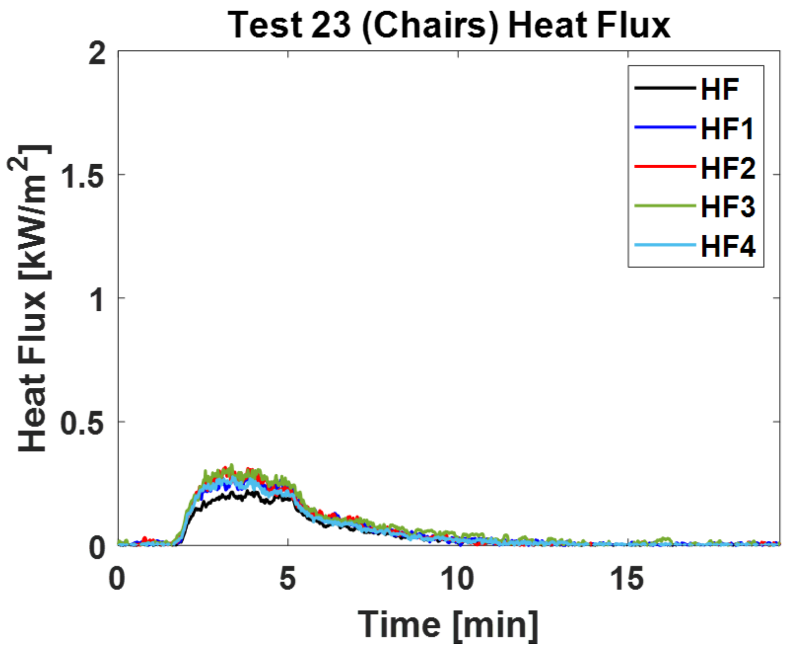


**Figure B 23: Radiative heat flux measurements during Test 23, a chair with expanded polystyrene beads (bean bag chair).**

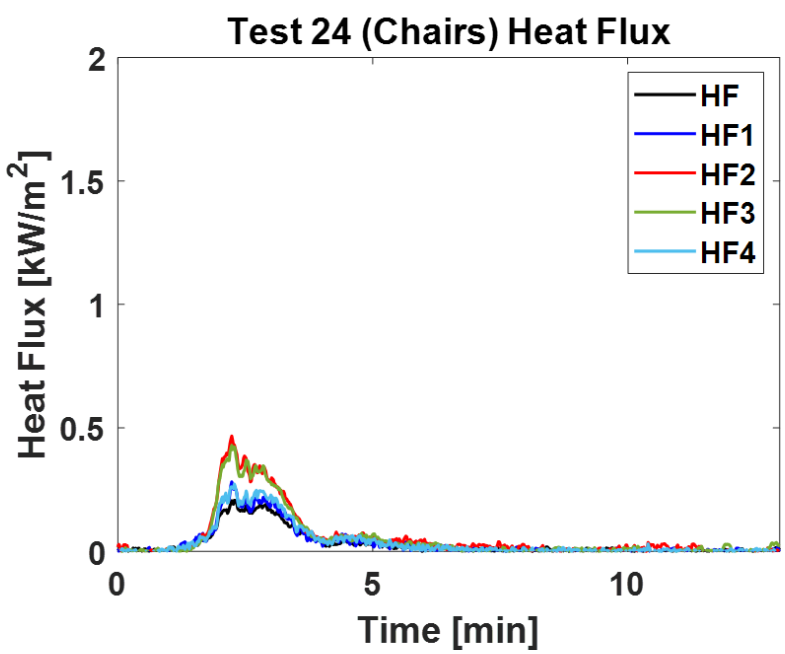


**Figure B 24: Radiative heat flux measurements during Test 24, a chair with PUF padding.**

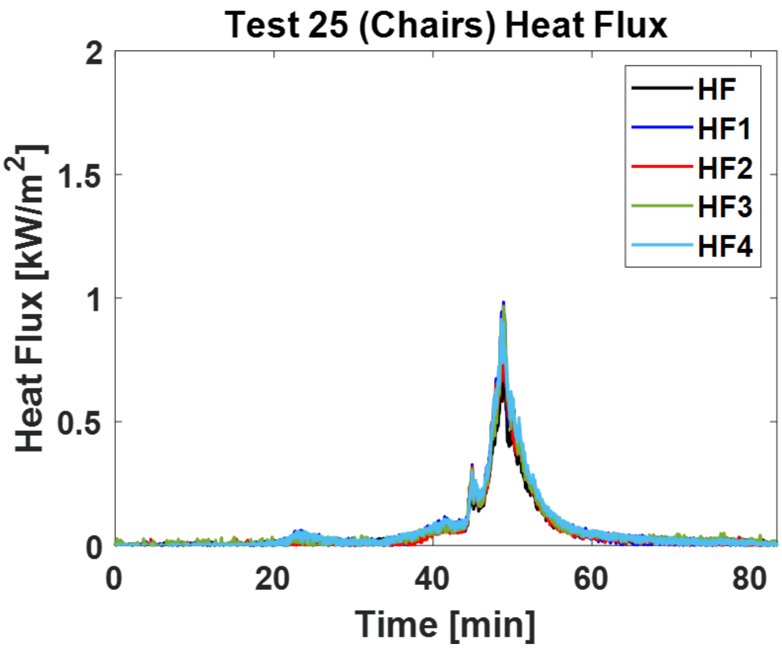


**Figure B 25: Radiative heat flux measurements during Test 25, a chair with PUF padding.**

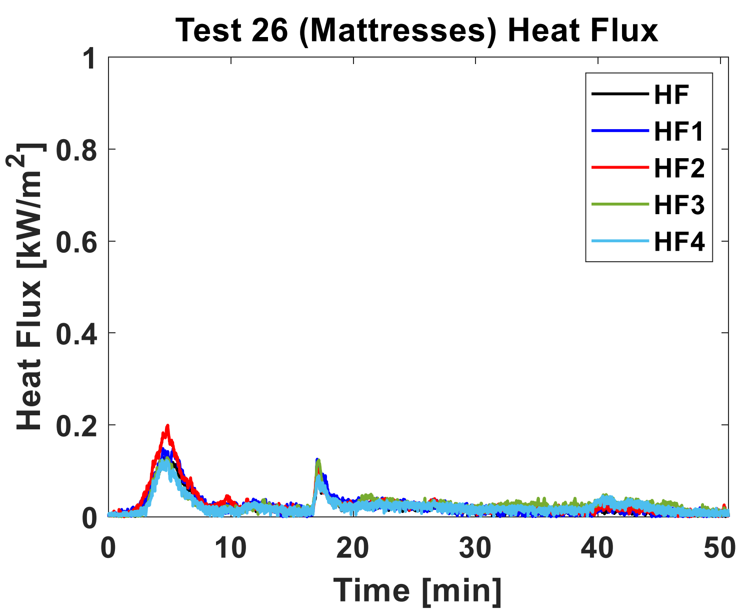


**Figure B 26: Radiative heat flux measurements during Test 26, a 15 cm (6'') thick mattress (inner spring) with 2 pillows.**

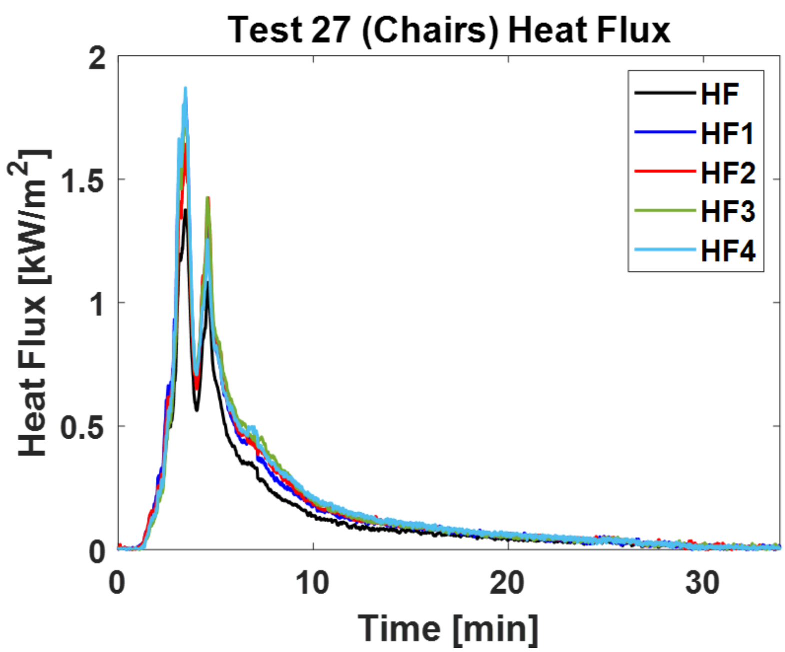


**Figure B 27: Radiative heat flux measurements during Test 27, a large armchair composed of a wood frame, PUF cushions, metal springs, thin fiberglass cloth with ignition at the bottom of the back cushion.**

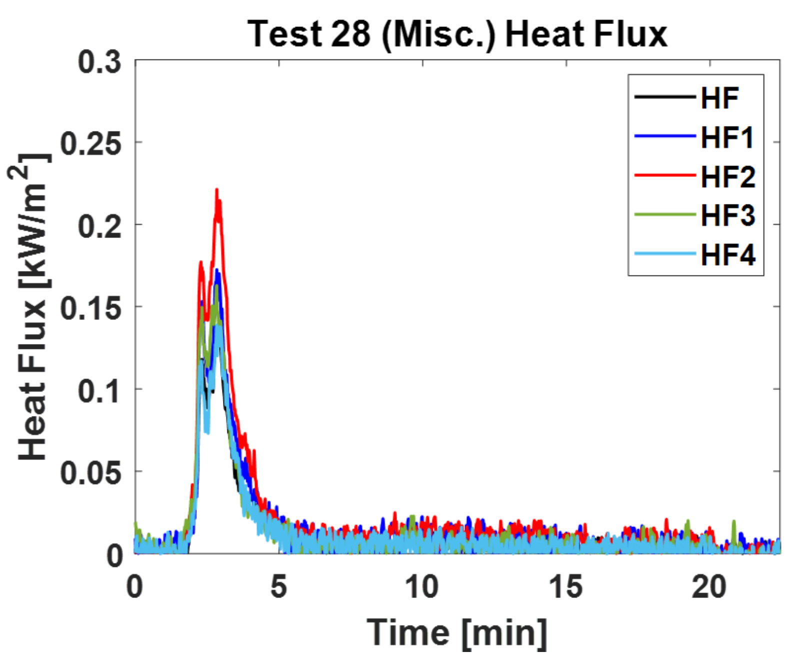


**Figure B 28: Radiative heat flux measurements during Test 28, a polypropylene carpet with two polyester foam pillows (identical to those used in Test 1).**

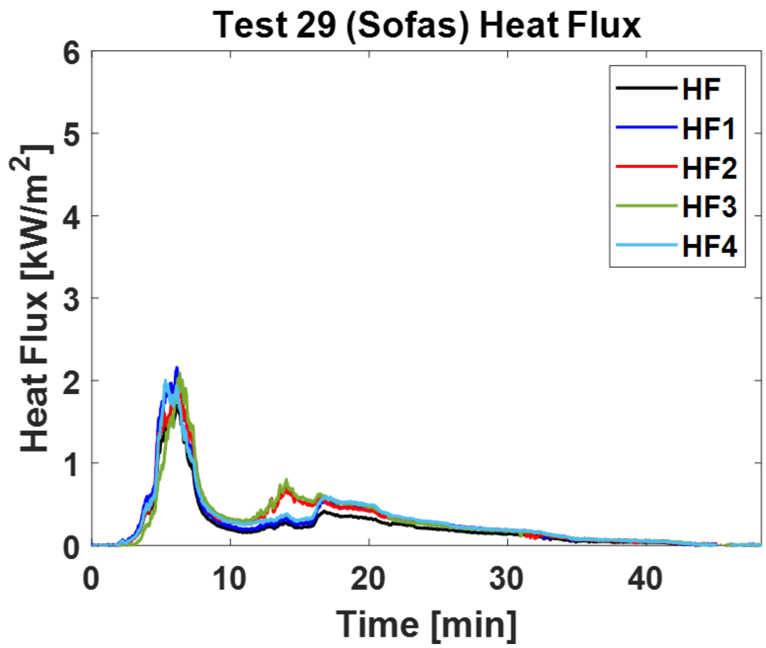


**Figure B 29: Radiative heat flux measurements during Test 29, sofa A with modified seat cushion inserts. Pillows rested on each of the arm rests.**

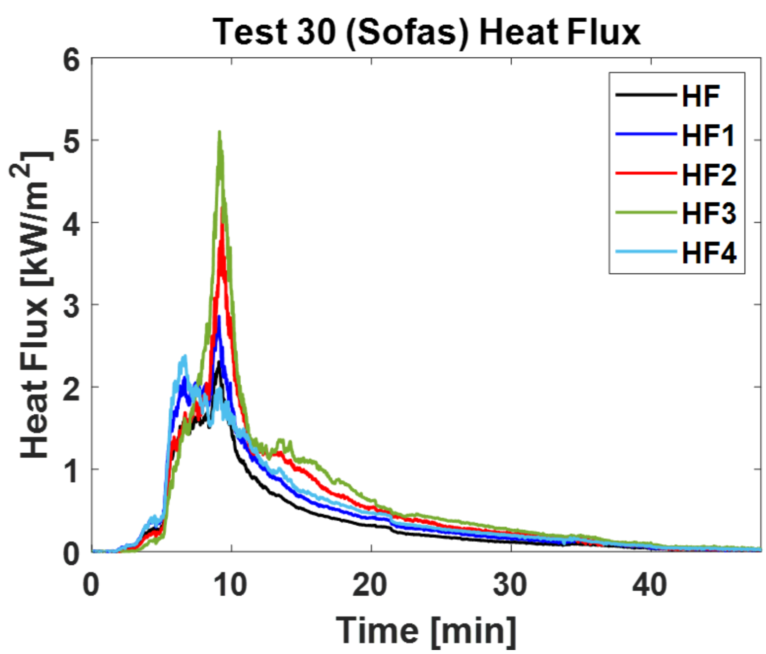


**Figure B 30: Radiative heat flux measurements during Test 30, sofa B. Pillows rested on each of the arm rests.**

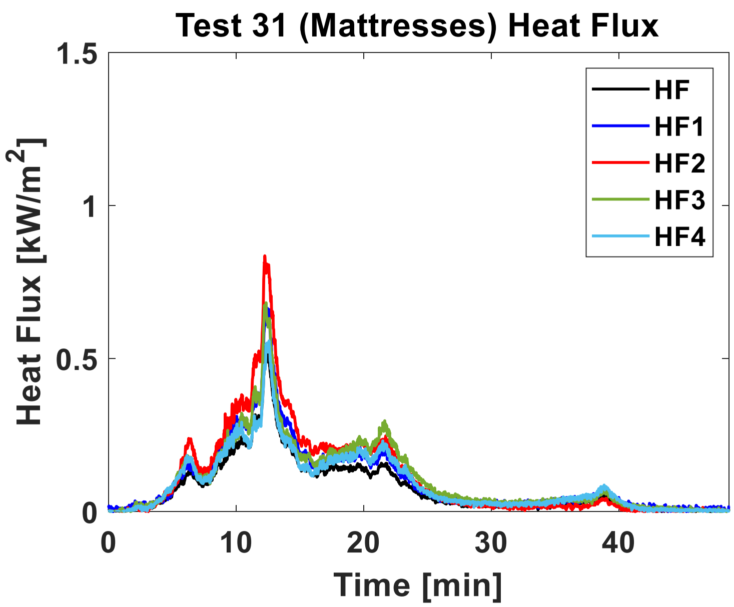


**Figure B 31: Radiative heat flux measurements during Test 31, a 15 cm (6'') thick queen size PUF mattress (Type B). Two pillows were placed on one end of the bed.**

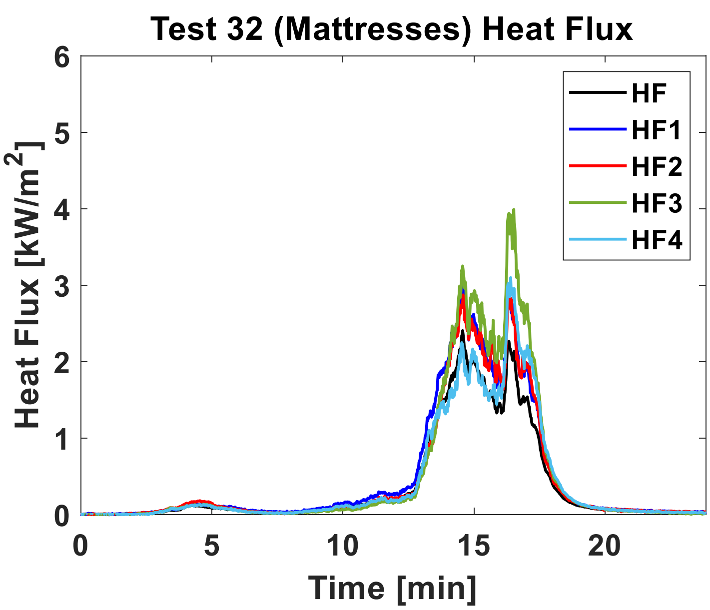


**Figure B 32: Radiative heat flux measurements during Test 32, a 30 cm (12'') thick queen size PUF mattress (Type C). Two pillows were placed on one end of the bed.**

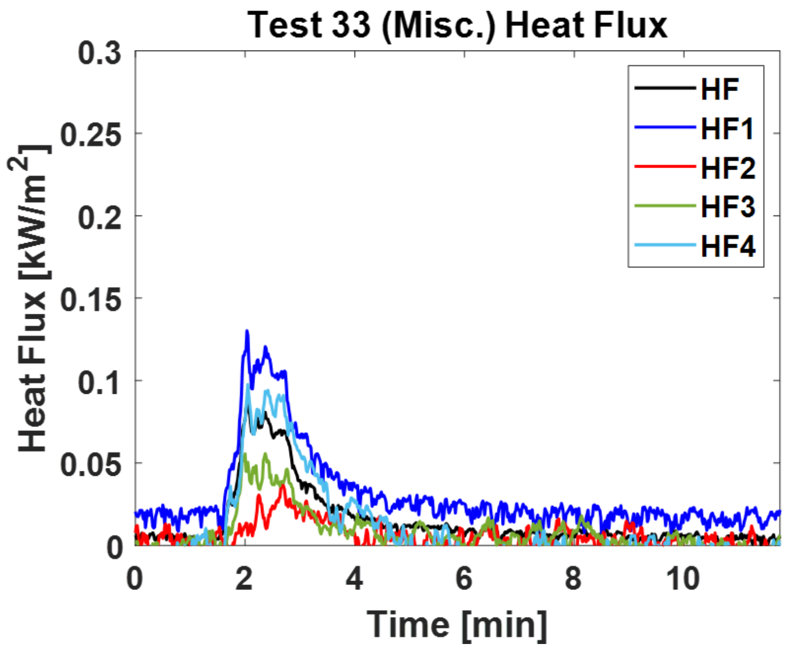


**Figure B 33: Radiative heat flux measurements during Test 33, a bookshelf with a pillow at the base.**

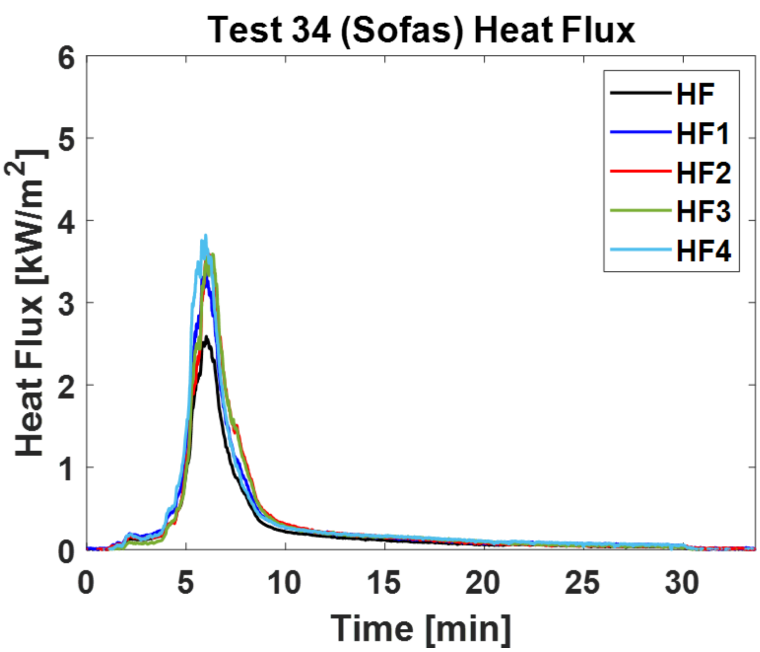


**Figure B 34: Radiative heat flux measurements during Test 34, Sofa C. Pillows rested on each of the arm rests.**

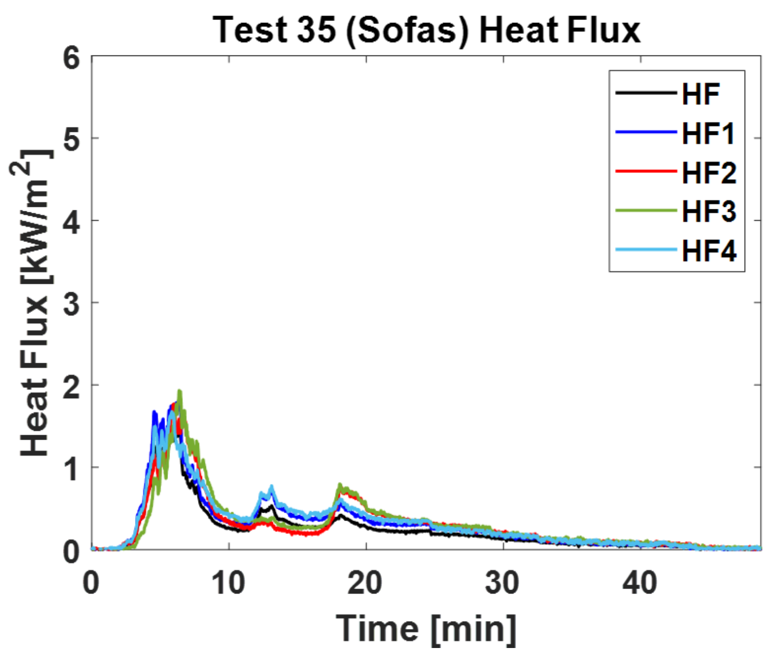


**Figure B 35: Radiative heat flux measurements during Test 35, Sofa A but with modified seat cushion inserts. Pillows rested on each of the arm rests.**

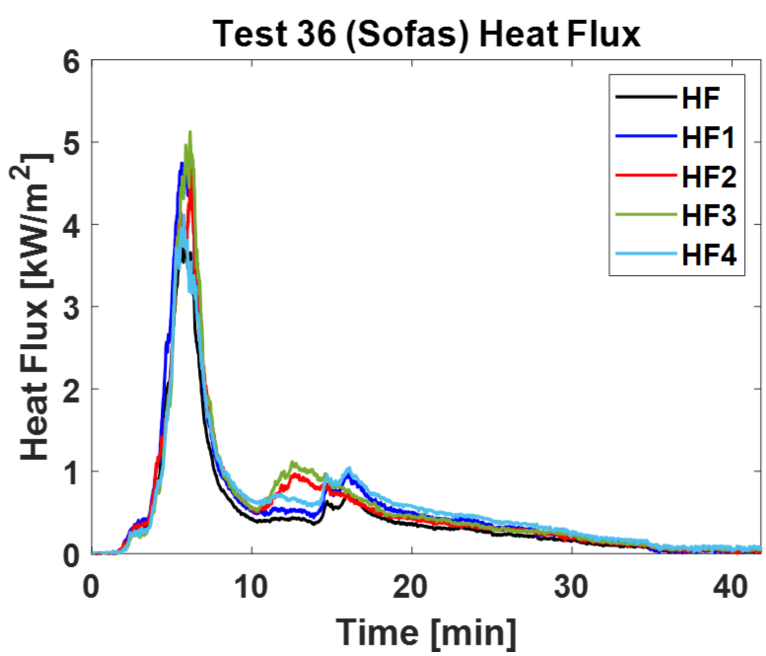


**Figure B 36: Radiative heat flux measurements during Test 36, Sofa B. Two Pillows rested on middle of the sofa adjacent to the back cushion.**

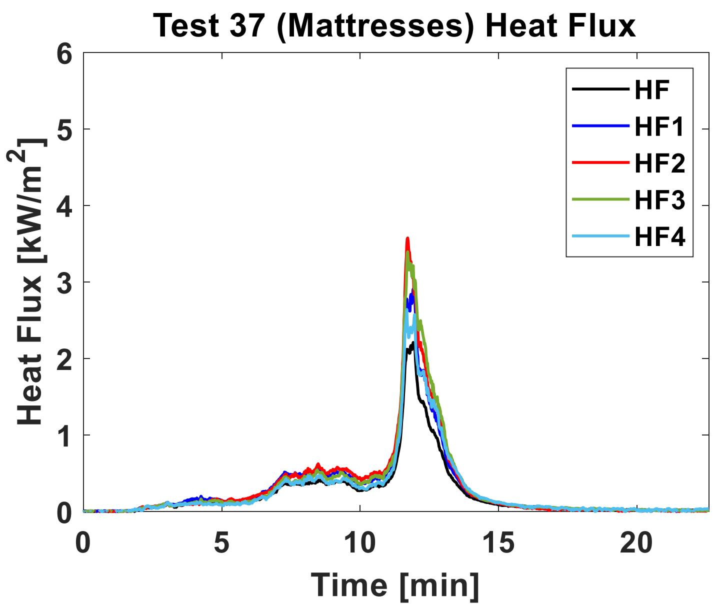


**Figure B 37: Radiative heat flux measurements during Test 37, a 15 cm (6'') thick queen size PUF mattress (Type B). The experiment was identical to Test 31 but the mattress was fitted with bedclothes including a polyester mattress cover, polyester top and bottom sheets, and a comforter with a polyester insert and cover. Two pillows were placed on one end of the bed.**

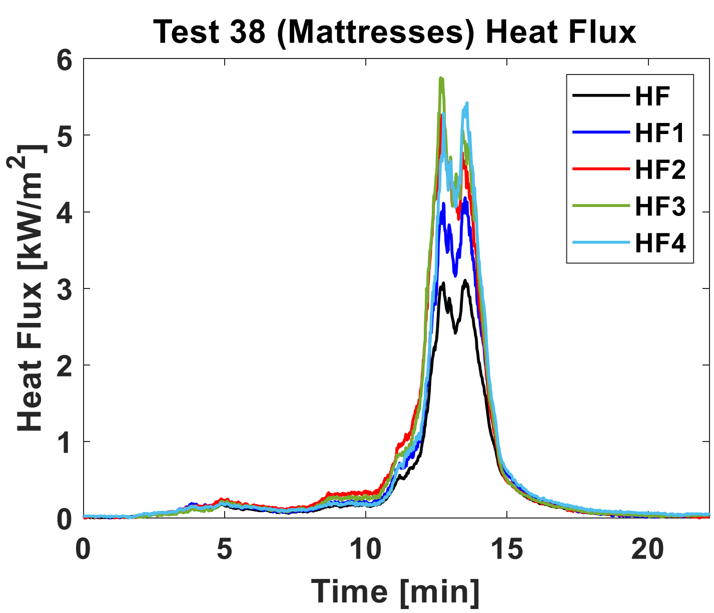


**Figure B 38: Radiative heat flux measurements during Test 38, a 30 cm (12'') thick queen size PUF mattress (Type C). The experiment was identical to Test 31, but the mattress was fitted with bedclothes.**

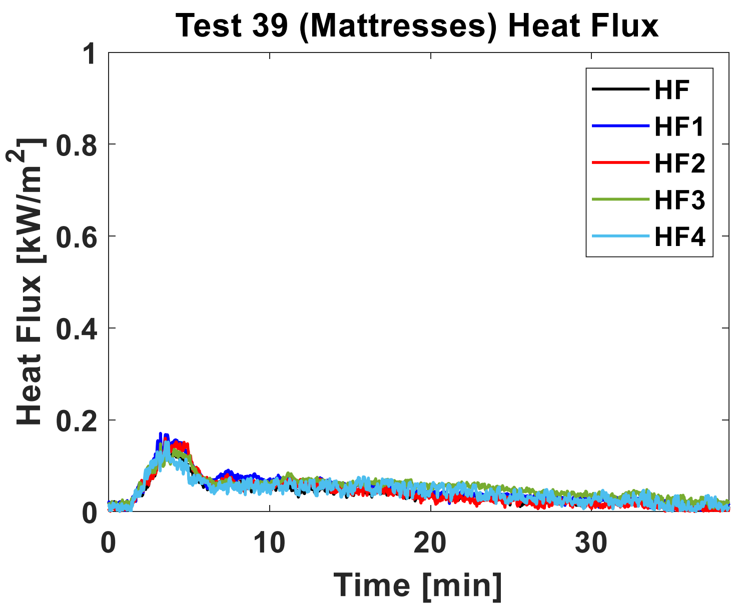


**Figure B 39: Radiative heat flux measurements during Test 39, a 15 cm (6'') thick queen size inner spring mattress (Type A). The experiment was identical to Test 26, but the mattress was fitted with bedclothes.**

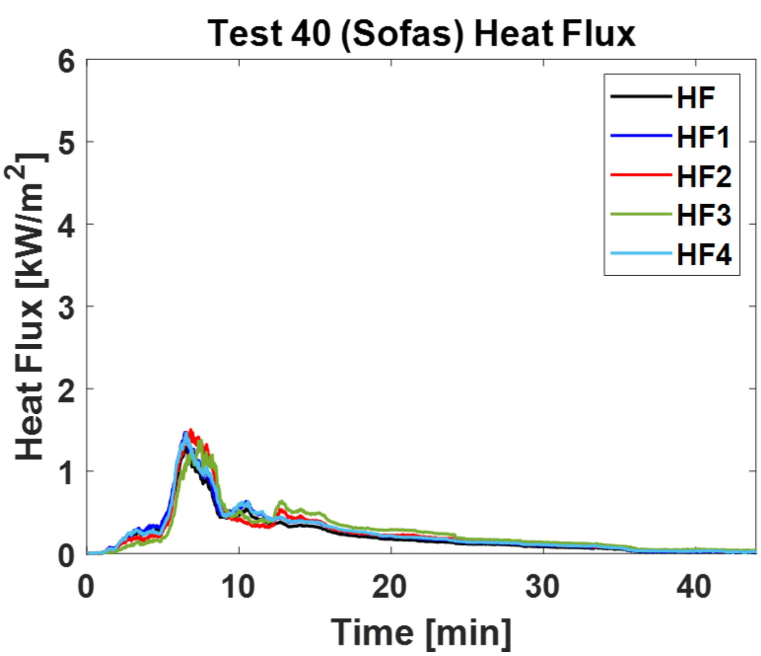


**Figure B 40: Radiative heat flux measurements during Test 40, Sofa A but with modified seat cushion inserts. Pillows rested on each of the arm rests.**

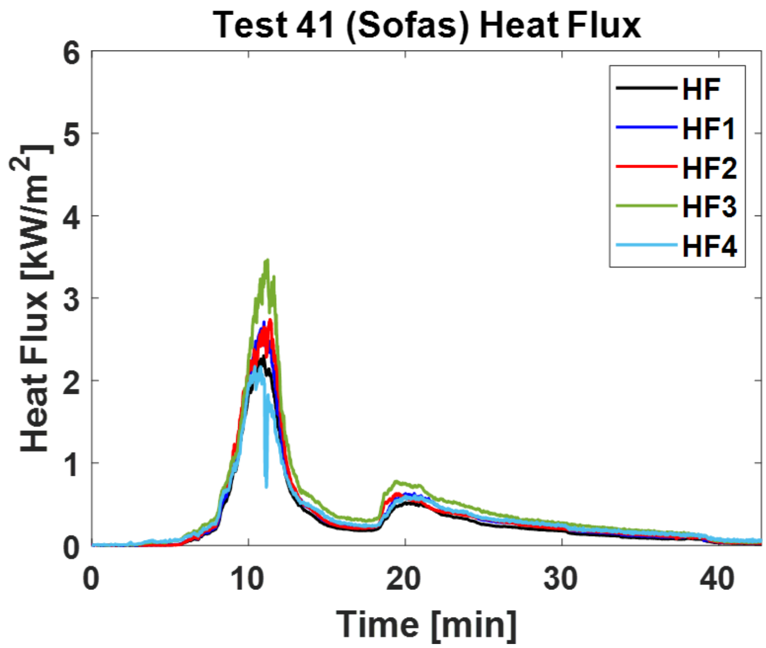


**Figure B 41: Radiative heat flux measurements during Test 41, Sofa B. One pillow rested on the left armrest and one behind the middle of the sofa on the floor.**

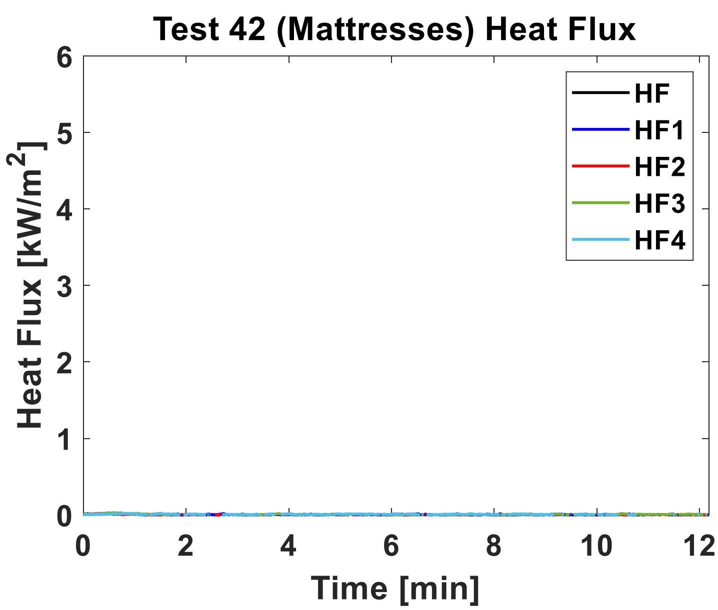


**Figure B 42: Radiative heat flux measurements during Test 42, a 30 cm (12'') thick queen size PUF mattress (Type C) undergoing the 16 CFR 1633 test protocol with top burner and side flame.**

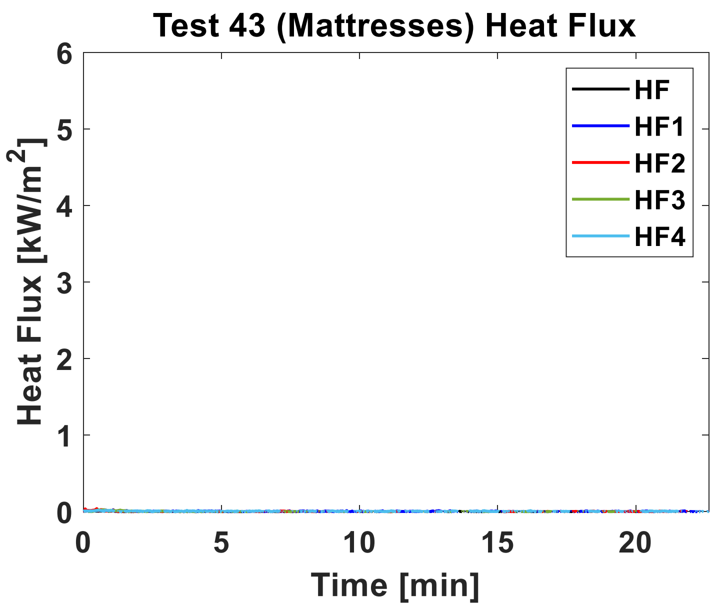


**Figure B 43: Radiative heat flux measurements during Test 43, a 30 cm (12'') thick queen size PUF mattress (Type C) undergoing the 16 CFR 1633 test protocol with top burner and side flame.**

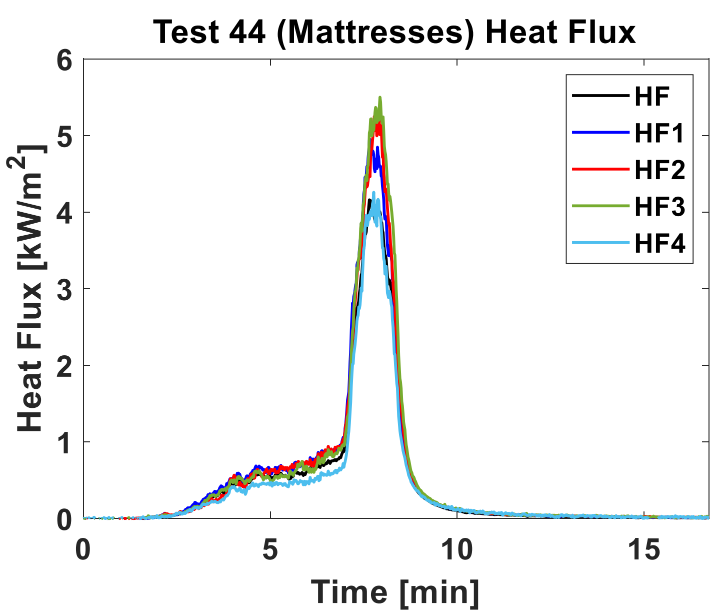


**Figure B 44: Radiative heat flux measurements during Test 44, a 30 cm (12'') thick queen size PUF mattress (Type C) with bedclothes with mattress' FR sock was removed.**

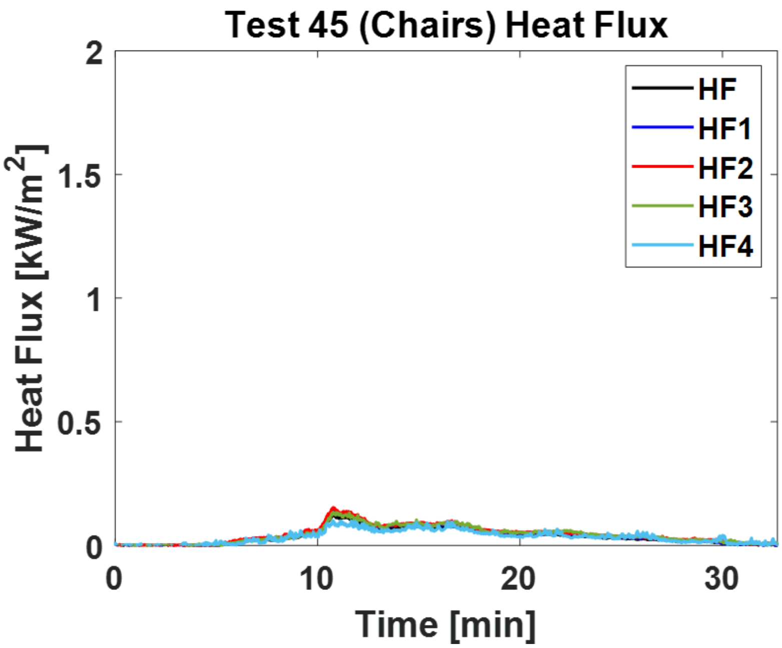


**Figure B 45: Radiative heat flux measurements during Test 45, a stack of chairs with PUF padding.**

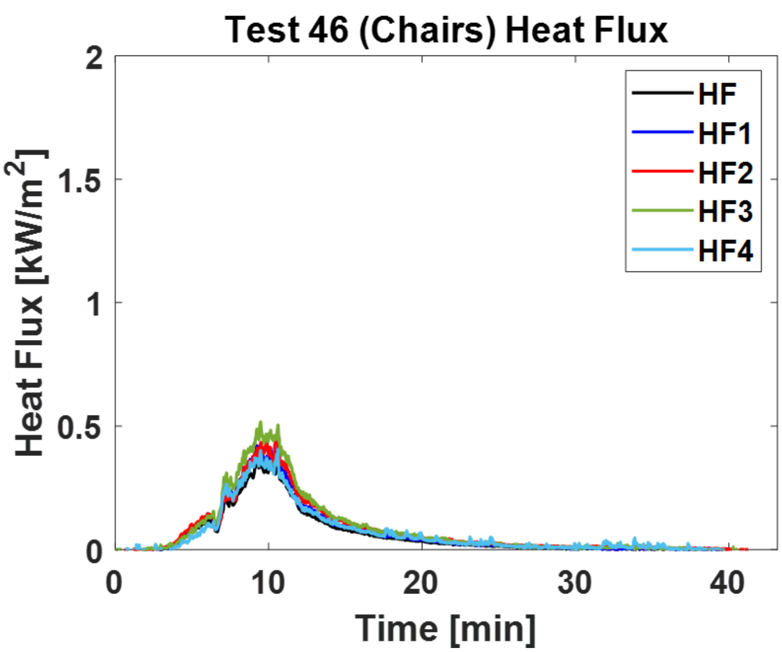


**Figure B 46: Radiative heat flux measurements during Test 46, an office chair with PUF padding.**

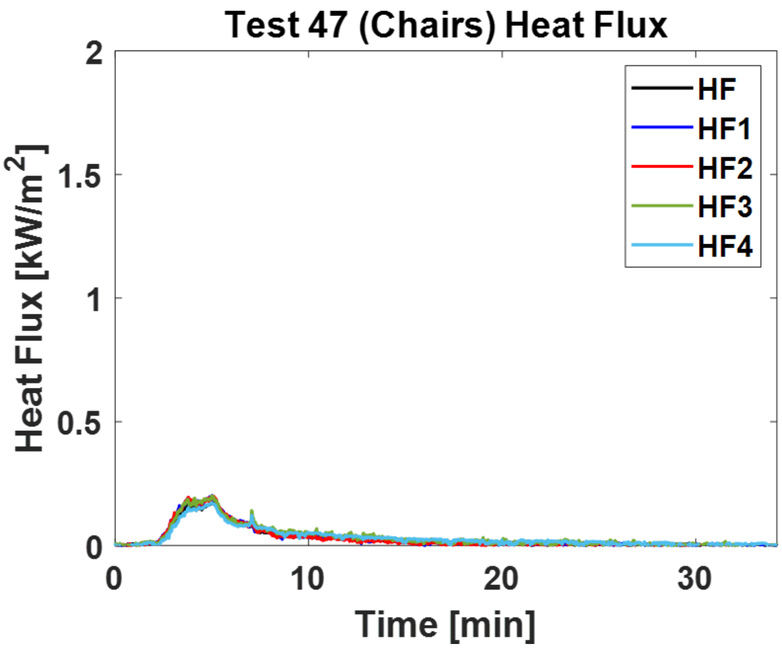


**Figure B 47: Radiative heat flux measurements during Test 47, a stack of three chairs with PUF padding.**

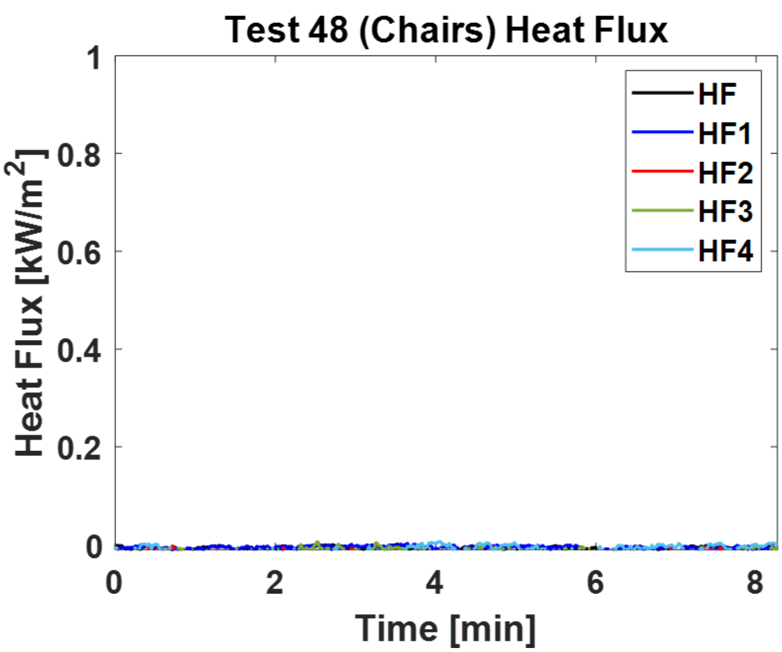


**Figure B 48: Radiative heat flux measurements during Test 48, an office chair with PUF padding.**

## Appendix C. Mass loss

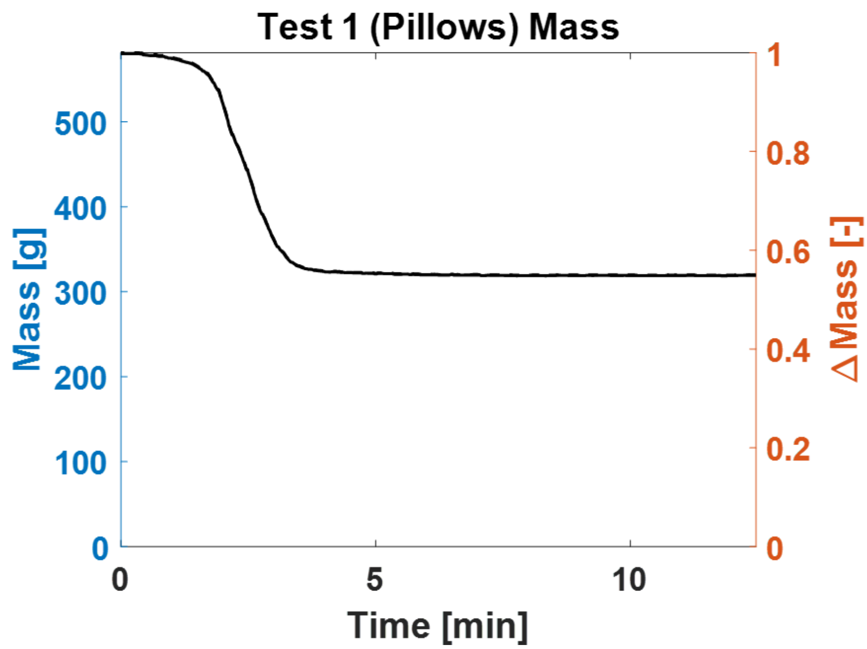


**Figure C 1. Measurement of the transient mass (left) and its fractional change (right) during Test 1, a polyester foam pillow with a polyester cover.**

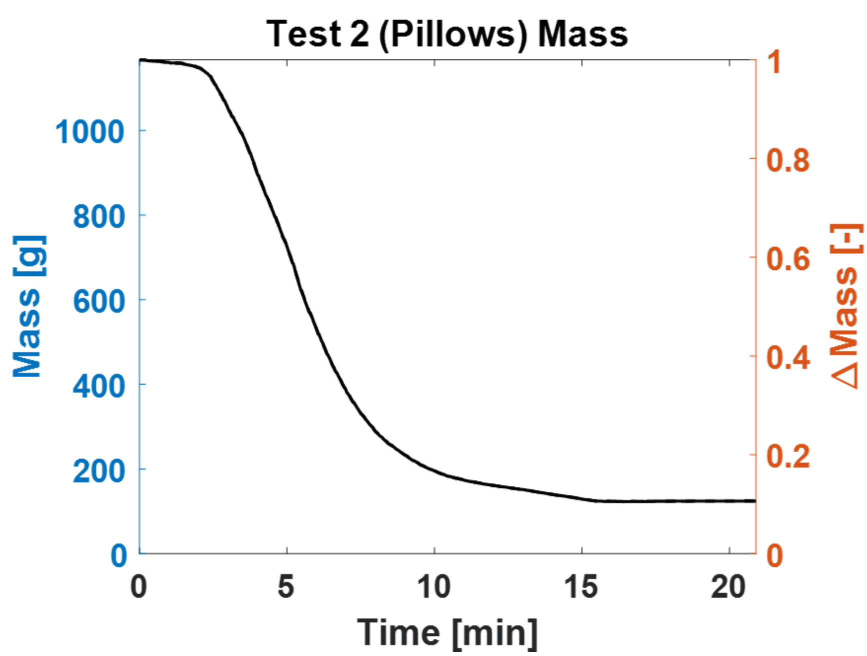


**Figure C 2: Measurement of the transient mass (left) and its fractional change (right) during Test 2, a PUF pillow with polyester cover.**

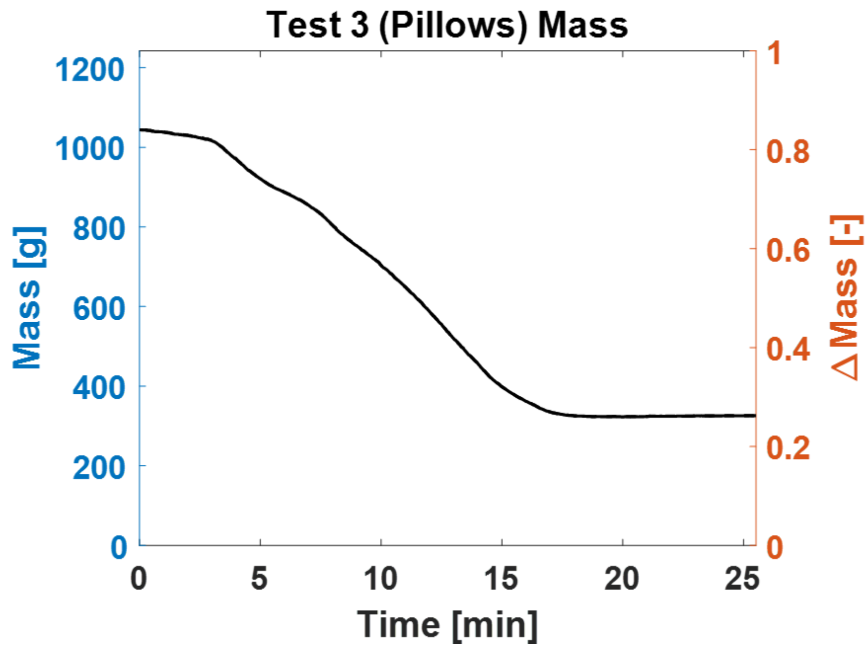


**Figure C 3: Measurement of the transient mass (left) and its fractional change (right) during Test 3, a feather pillow with a polyester cover.**

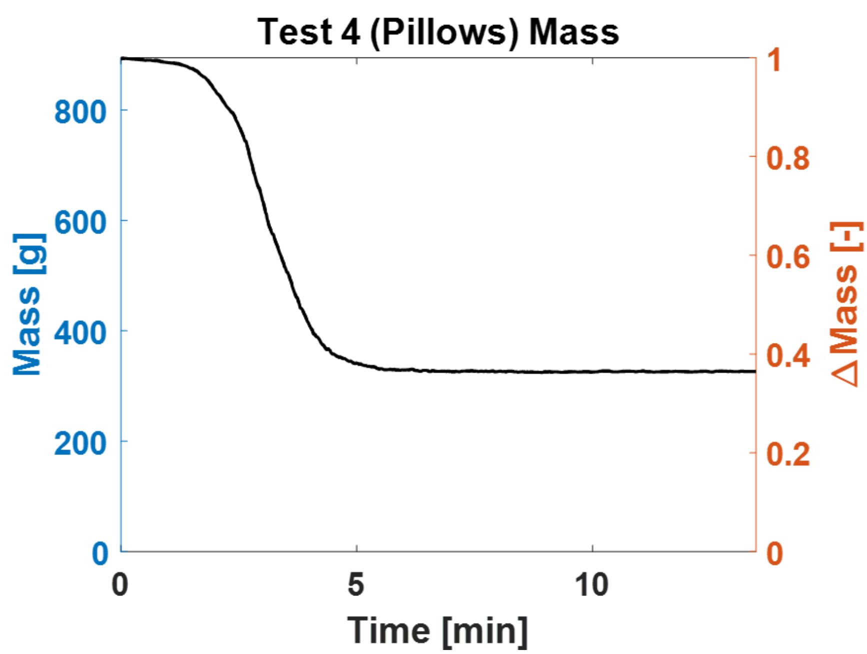


**Figure C 4: Measurement of the transient mass (left) and its fractional change (right) during Test 4, a polypropylene foam insert pillow with a polypropylene cover.**

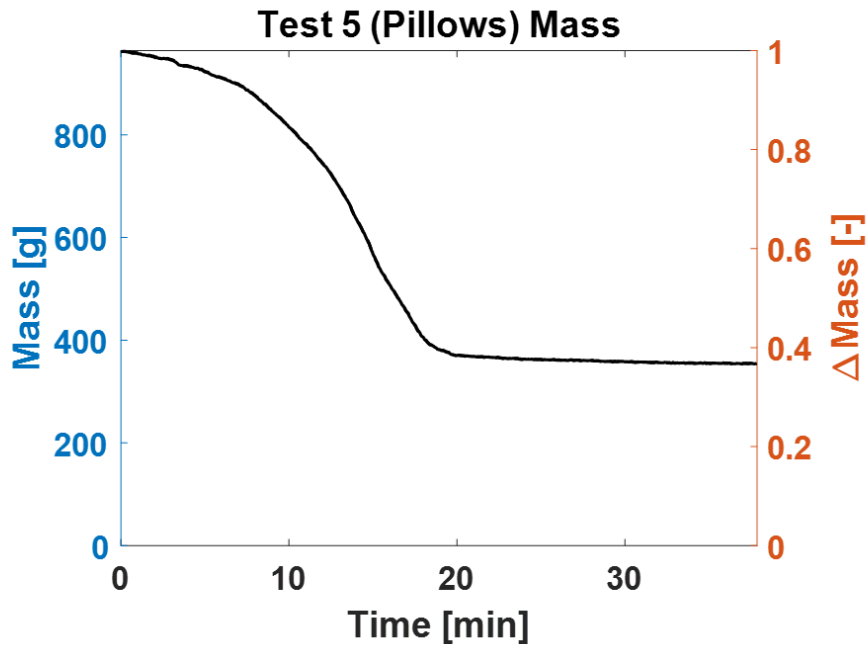


**Figure C 5: Measurement of the transient mass (left) and its fractional change (right) during Test 5, a feather pillow with a polyester cover.**

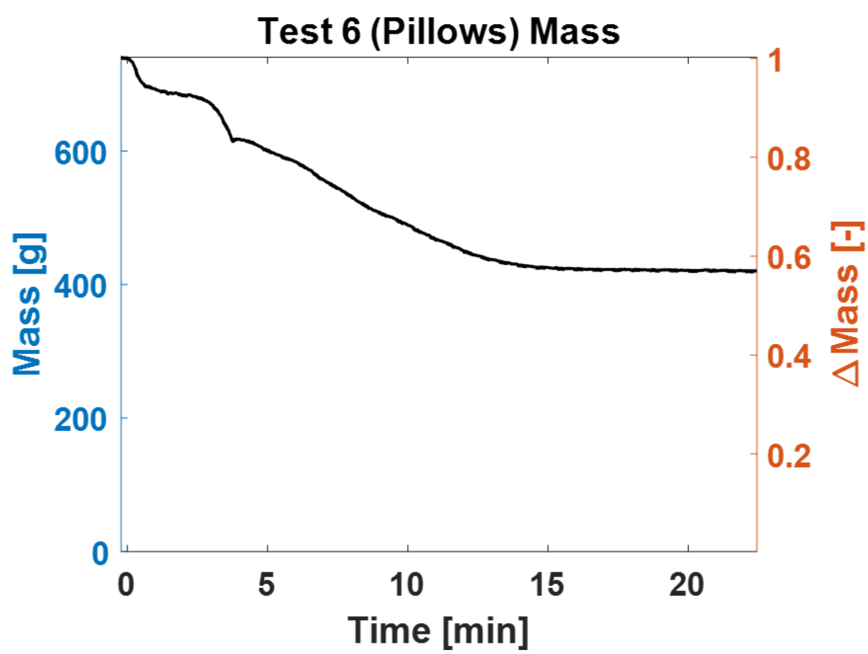


**Figure C 6: Measurement of the transient mass (left) and its fractional change (right) during Test 6, a pillow with polyester foam insert and polyester cover.**

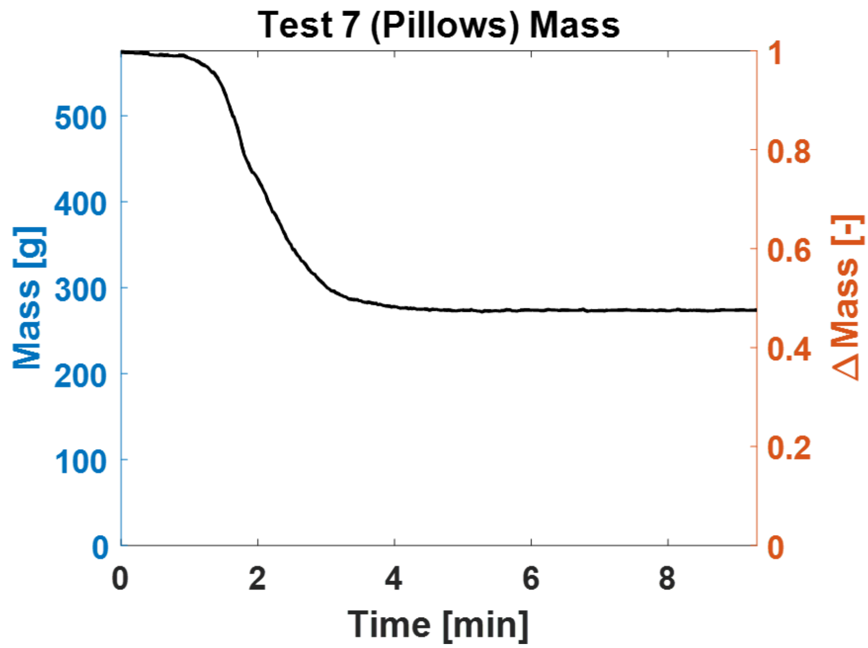


**Figure C 7: Measurement of the transient mass (left) and its fractional change (right) during Test 7, a pillow with polyester foam insert and polyester cover.**

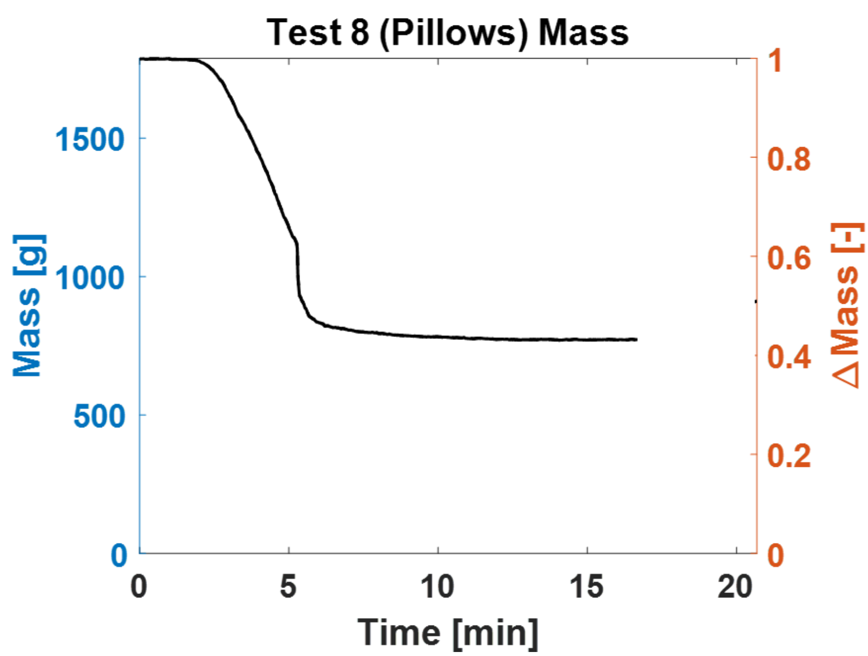


**Figure C 8: Measurement of the transient mass (left) and its fractional change (right) during Test 8, two pillows with polypropylene foam insert and polypropylene cover.**

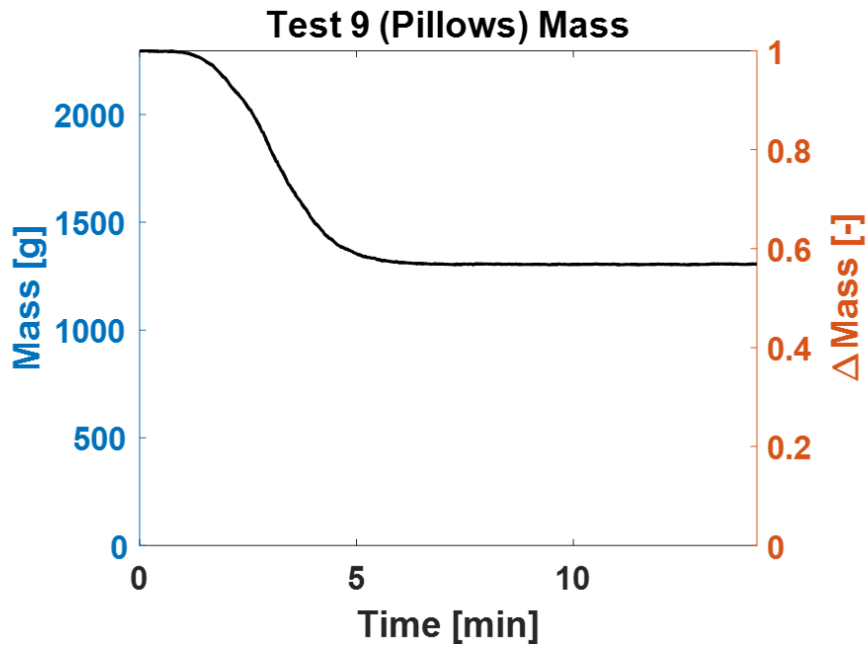


**Figure C 9: Measurement of the transient mass (left) and its fractional change (right) during Test 9, four pillows with polyester foam insert and polyester cover.**

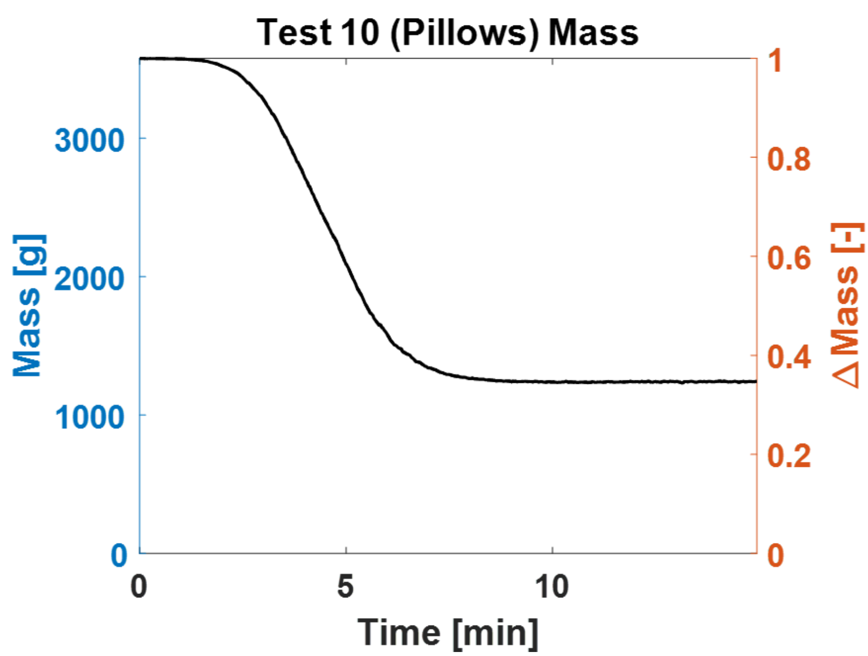


**Figure C 10: Measurement of the transient mass (left) and its fractional change (right) during Test 10, four pillow with polypropylene foam insert and polypropylene cover.**

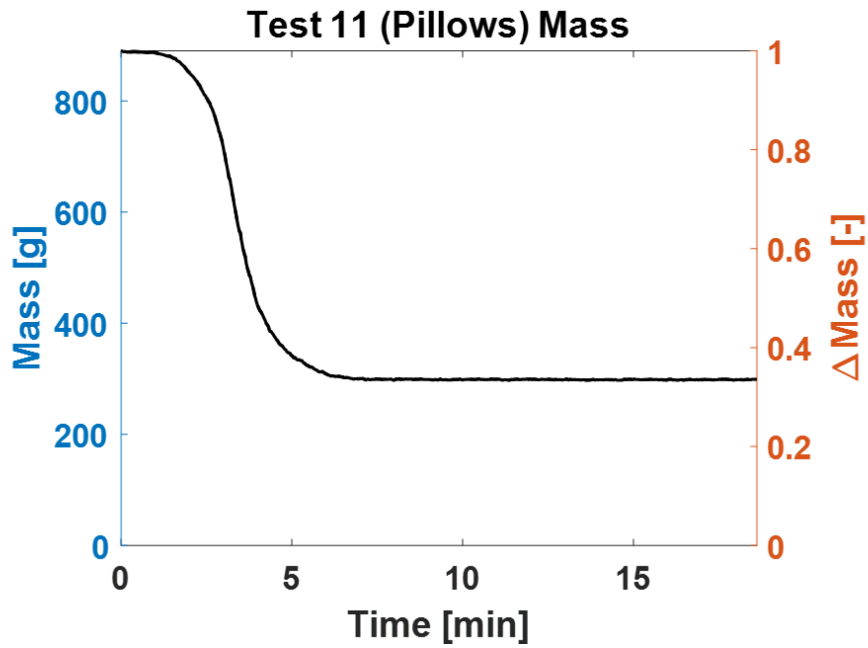


**Figure C 11: Measurement of the transient mass (left) and its fractional change (right) during Test 11, a pillow with polypropylene foam insert and polypropylene cover.**

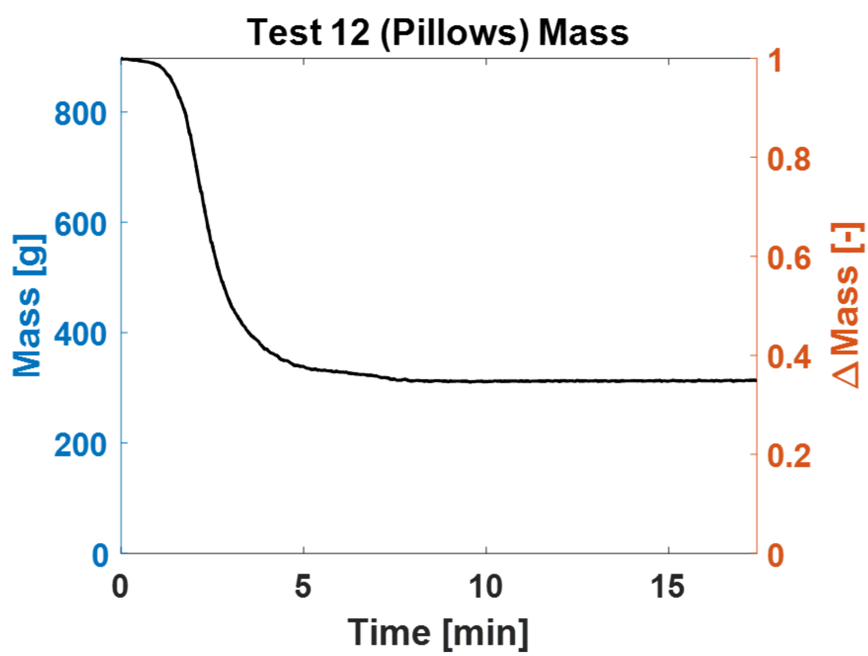


**Figure C 12: Measurement of the transient mass (left) and its fractional change (right) during Test 12, a pillow with polypropylene foam insert and polypropylene cover.**

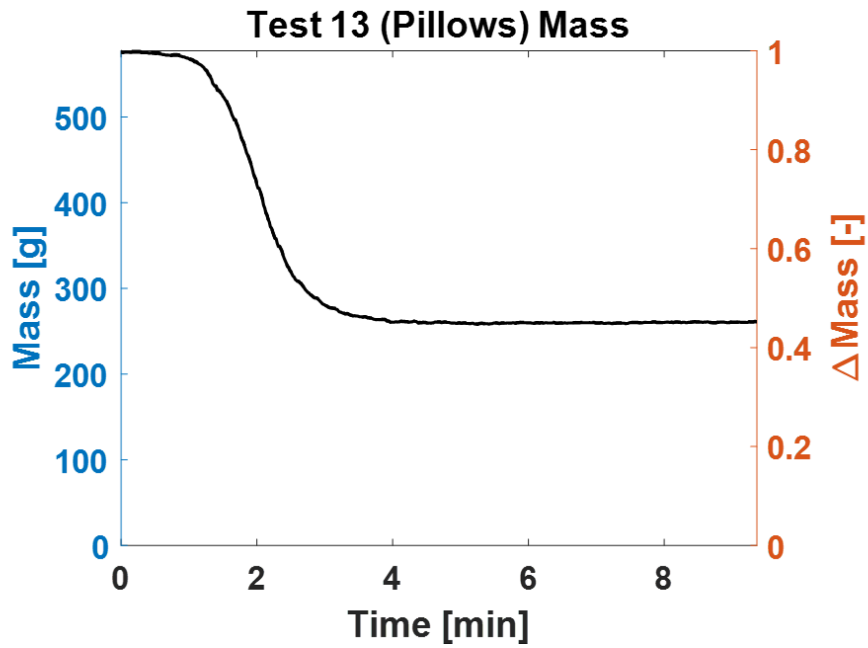


**Figure C 13: Measurement of the transient mass (left) and its fractional change (right) during Test 13, a pillow with polyester foam insert and polyester cover.**

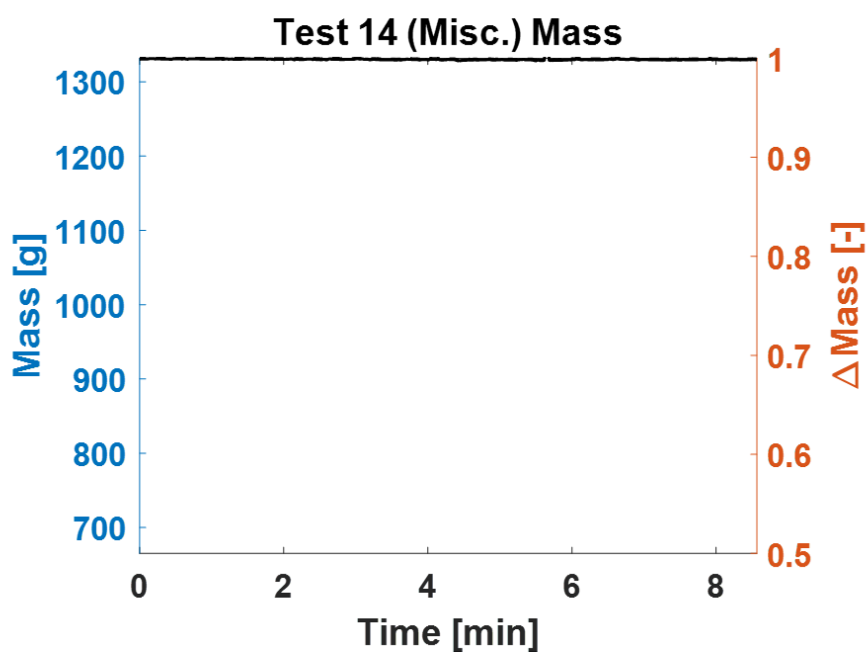


**Figure C 14: Measurement of the transient mass (left) and its fractional change (right) during Test 14, a laptop.**

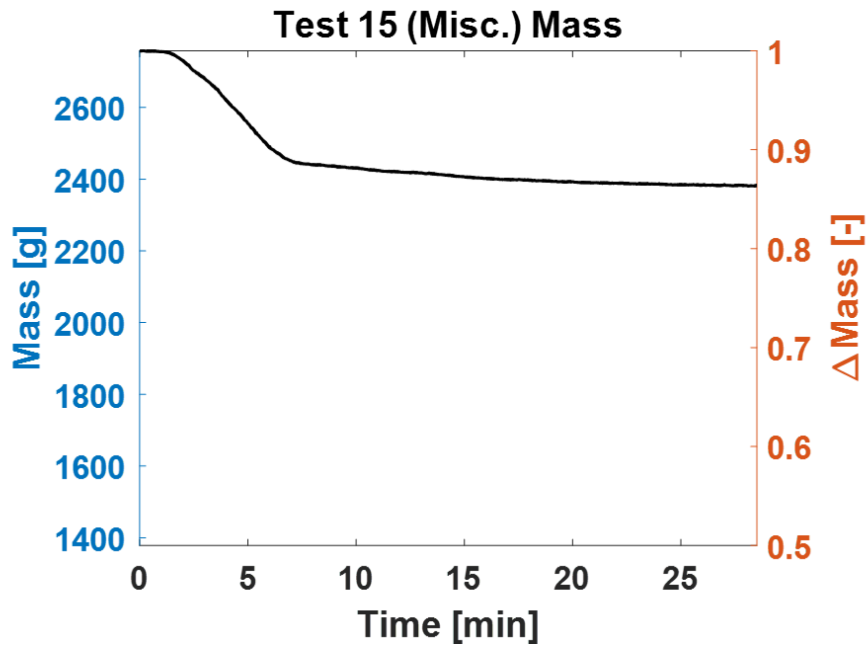


**Figure C 15: Measurement of the transient mass (left) and its fractional change (right) during Test 15, a laptop on a pillow (polyester foam insert and polyester cover).**

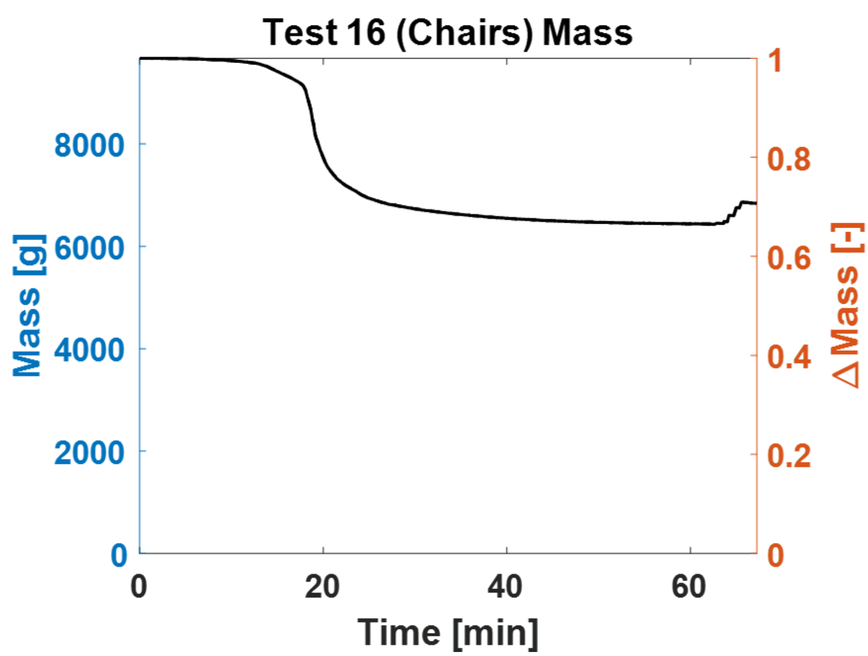


**Figure C 16: Measurement of the transient mass (left) and its fractional change (right) during Test 16, a chair with PUF padding.**

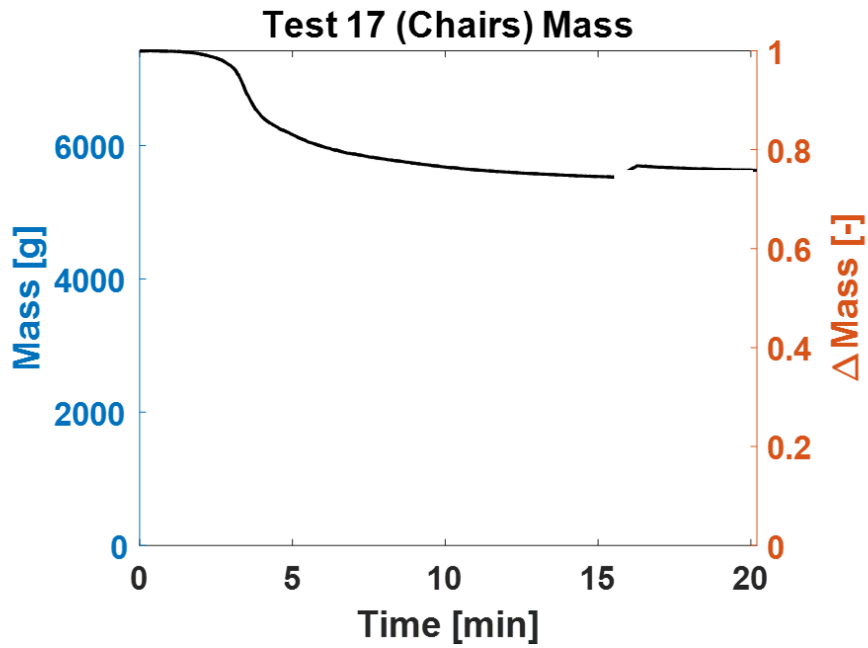


**Figure C 17: Measurement of the transient mass (left) and its fractional change (right) during Test 17, a chair with PUF padding.**

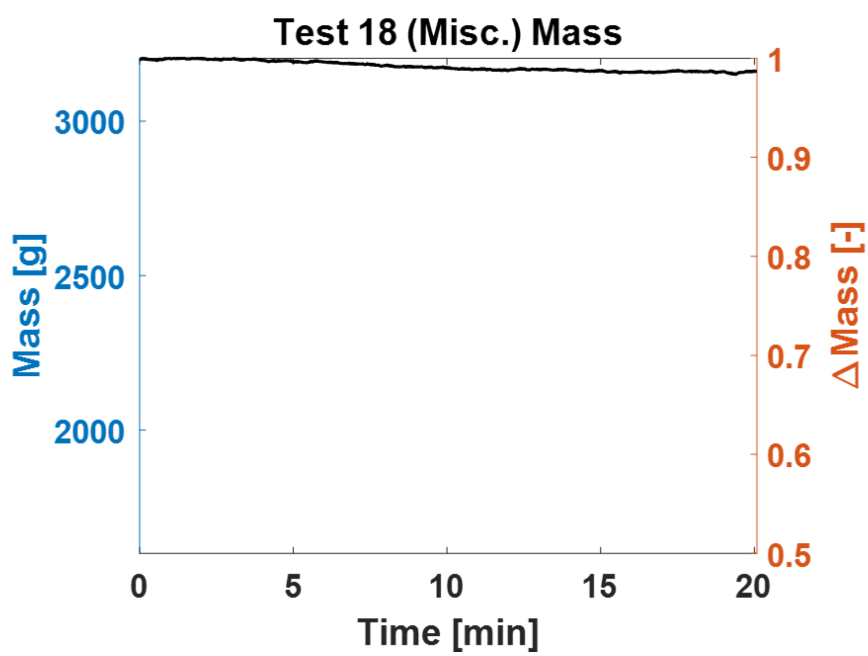


**Figure C 18: Measurement of the transient mass (left) and its fractional change (right) during Test 18, a side table composed of particleboard.**

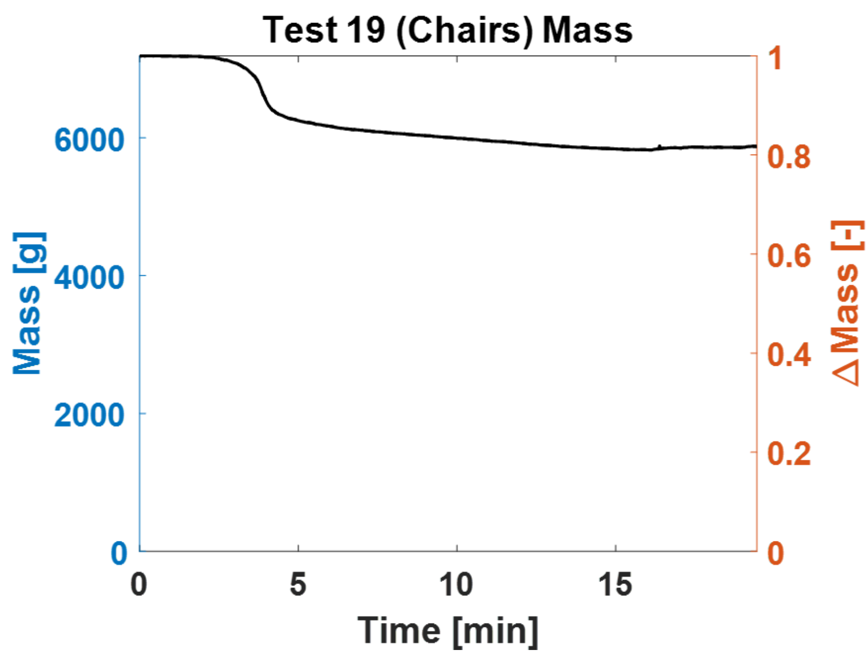


**Figure C 19: Measurement of the transient mass (left) and its fractional change (right) during Test 19, a chair with PUF padding.**

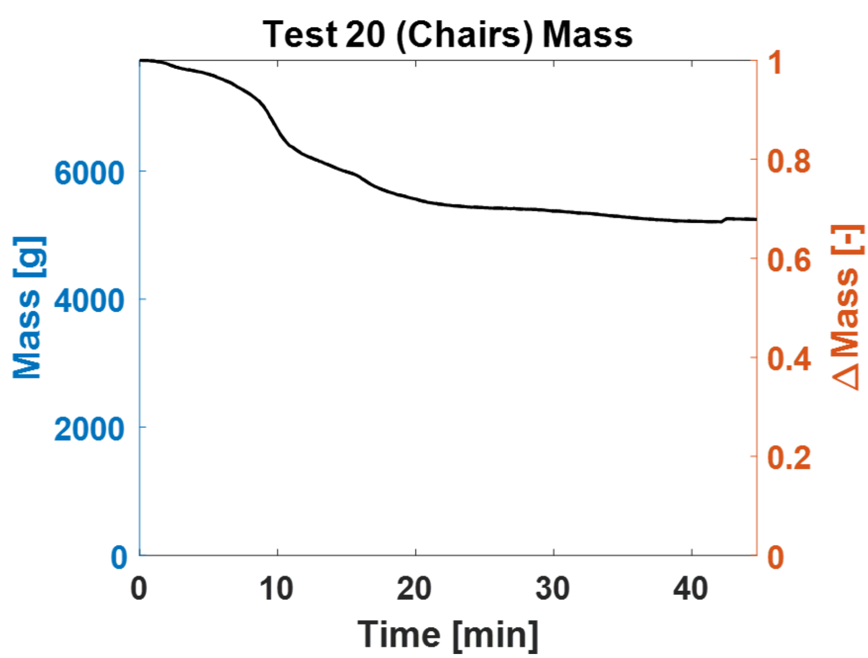


**Figure C 20: Mass Measurement of the transient mass (left) and its fractional change (right) during Test 20, a chair with PUF padding. and a wooden frame.**

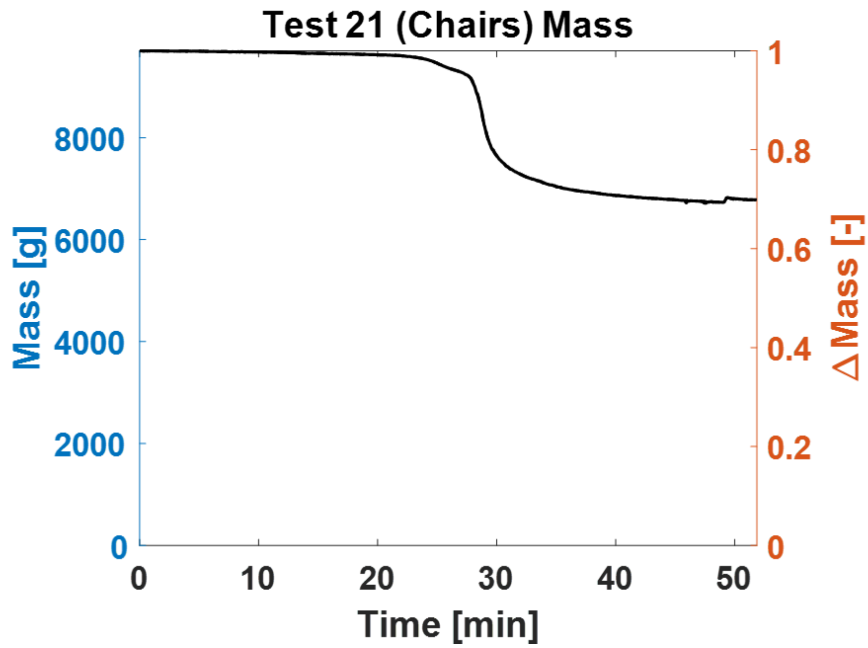


**Figure C 21: Measurement of the transient mass (left) and its fractional change (right) during Test 21, a chair with PUF padding.**

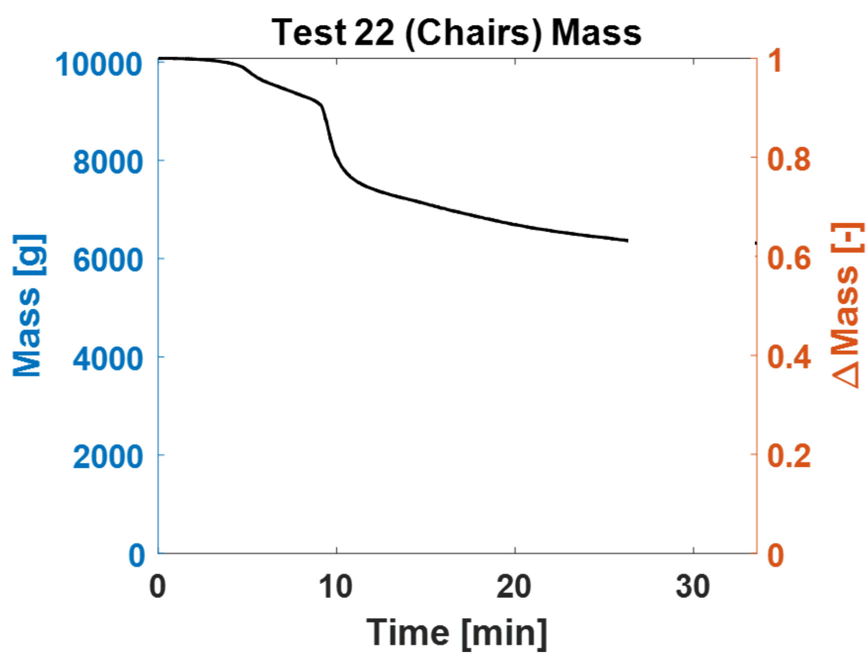


**Figure C 22: Measurement of the transient mass (left) and its fractional change (right) during Test 22, a chair with PUF padding.**

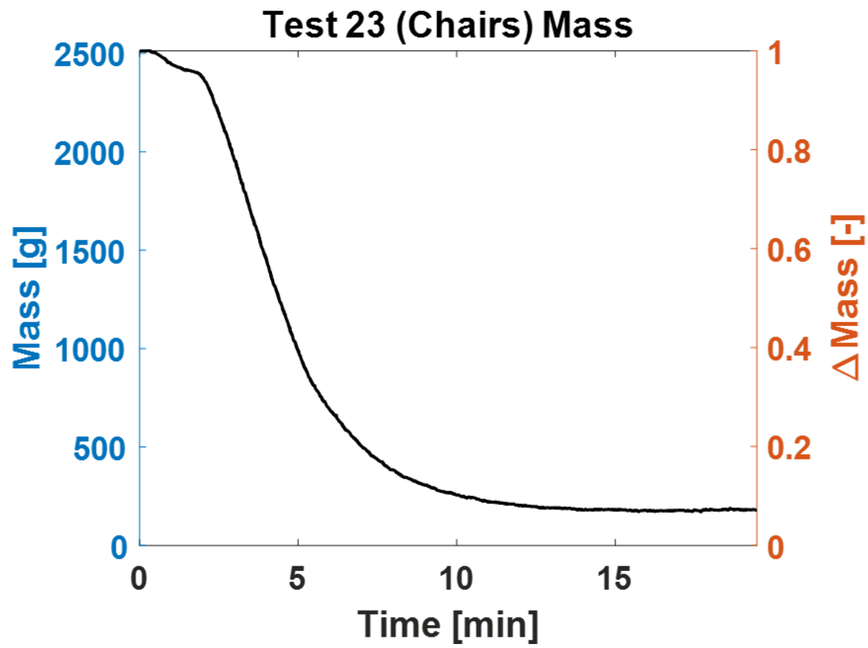


**Figure C 23: Measurement of the transient mass (left) and its fractional change (right) during Test 23, a chair with expanded polystyrene beads (bean bag chair).**

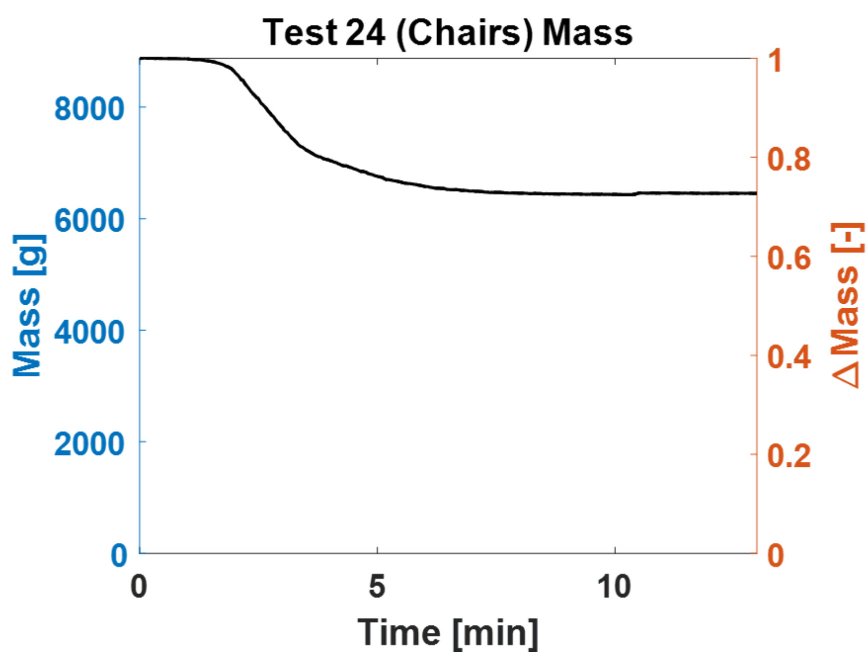


**Figure C 24: Measurement of the transient mass (left) and its fractional change (right) during Test 24, a chair with PUF padding.**

## Appendix D. Heat Release Rate

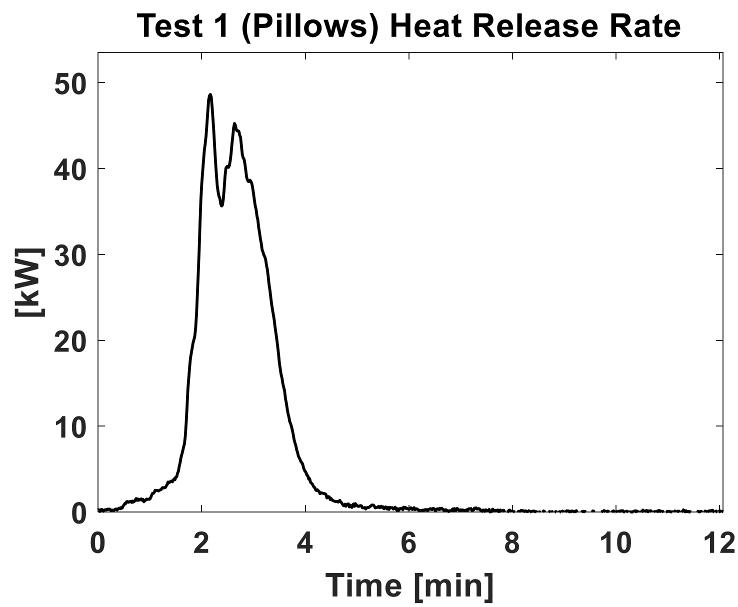


**Figure D 1: Heat Release Rate measurements during Test 1, a polyester foam pillow with a polyester cover.**

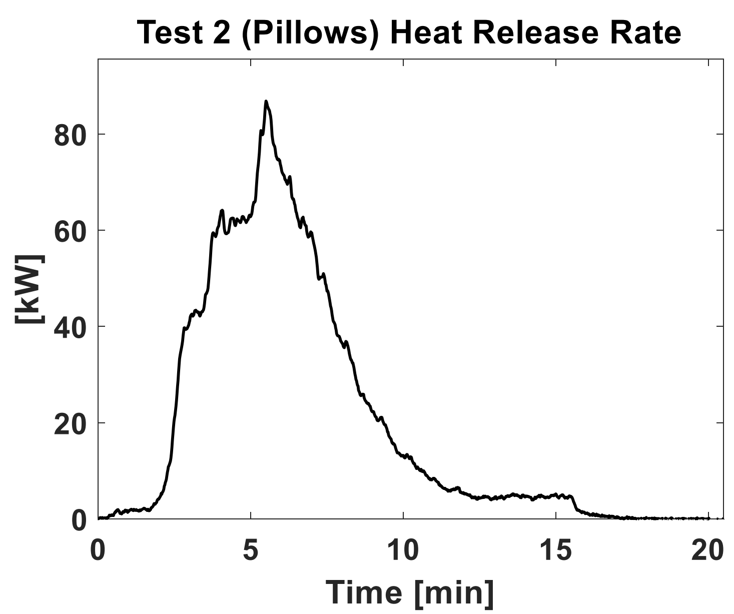


**Figure D 2: Heat Release Rate measurements during Test 2, a polyurethane foam pillow with polyester cover.**

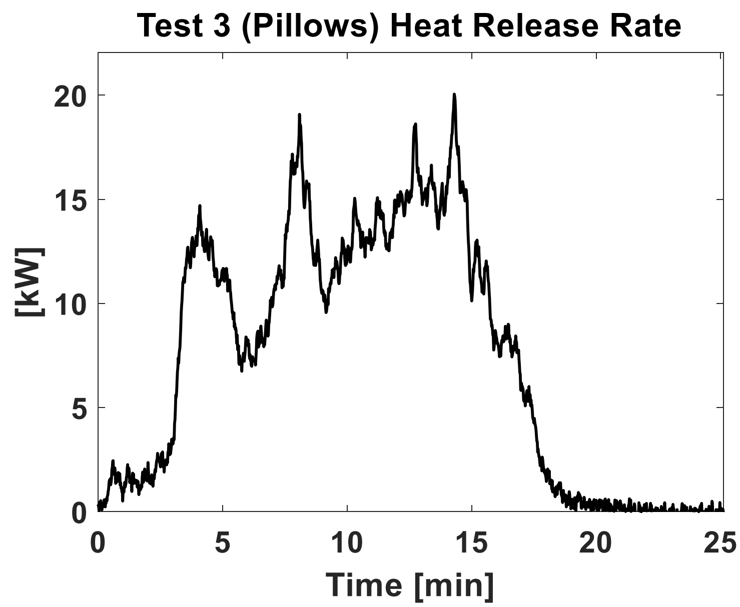


**Figure D 3: Heat Release Rate measurements during Test 3, a feather pillow with a polyester cover.**

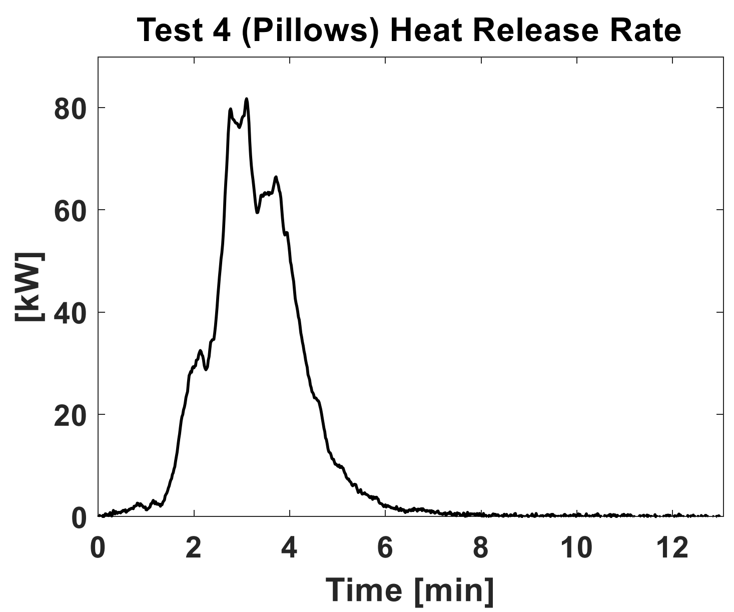


**Figure D 4: Heat Release Rate measurements during Test 4, a polypropylene foam insert pillow with a polypropylene cover.**

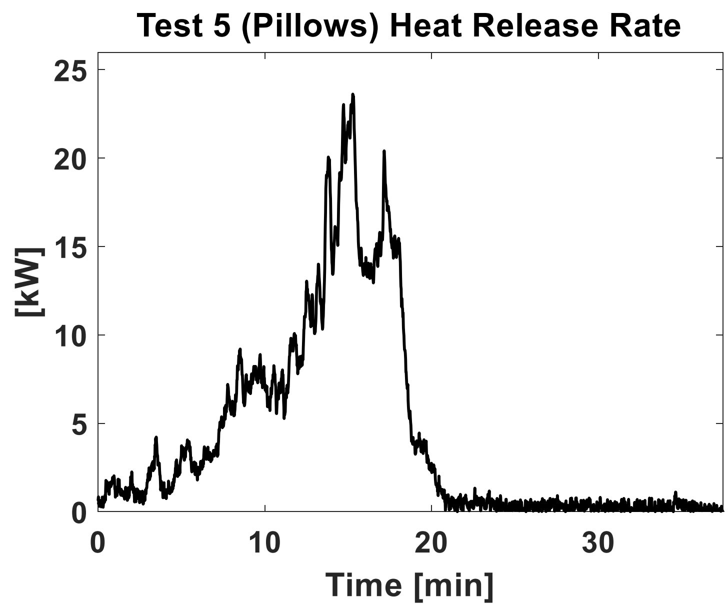


**Figure D 5: Heat Release Rate measurements during Test 5, a feather pillow with a polyester cover.**

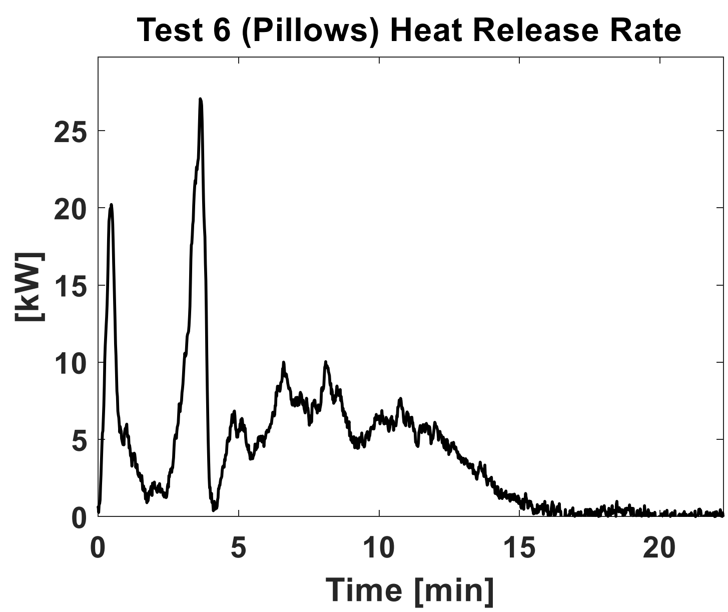


**Figure D 6: Heat Release Rate measurements during Test 6, a pillow with polyester foam insert and polyester cover.**

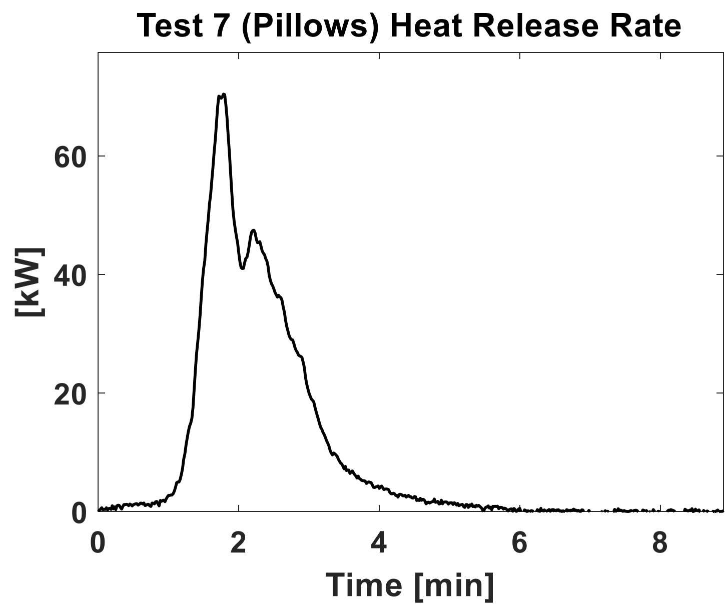


**Figure D 7: Heat Release Rate measurements during Test 7, a pillow with polyester foam insert and polyester cover.**

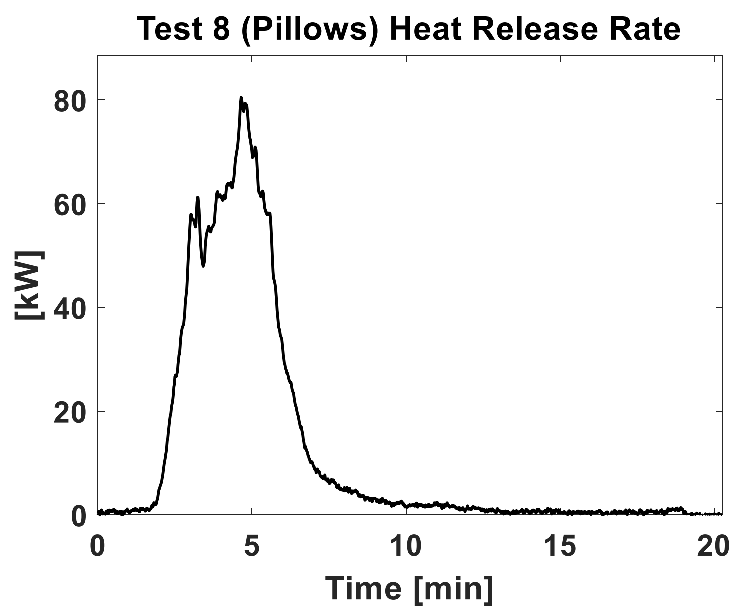


**Figure D 8: Heat Release Rate measurements during Test 8, two pillows with polypropylene foam inserts and polypropylene covers.**

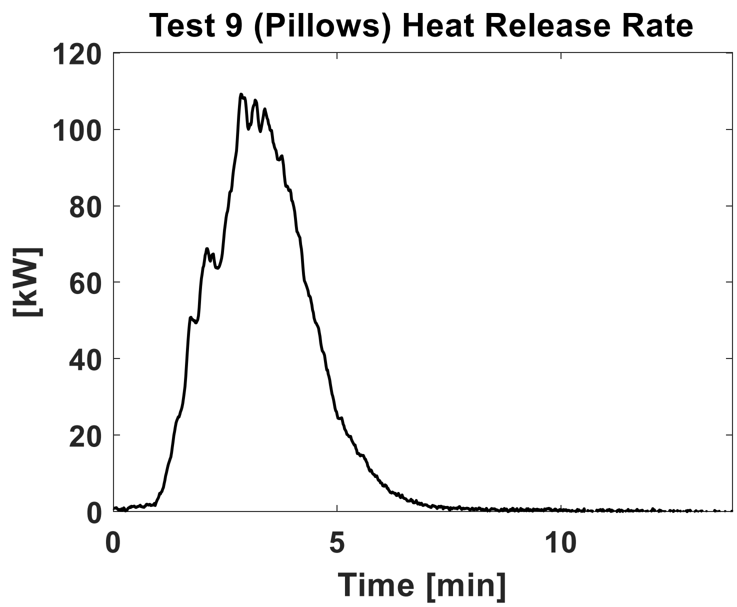


**Figure D 9: Heat Release Rate measurements during Test 9, four pillows with polyester foam inserts and polyester covers.**

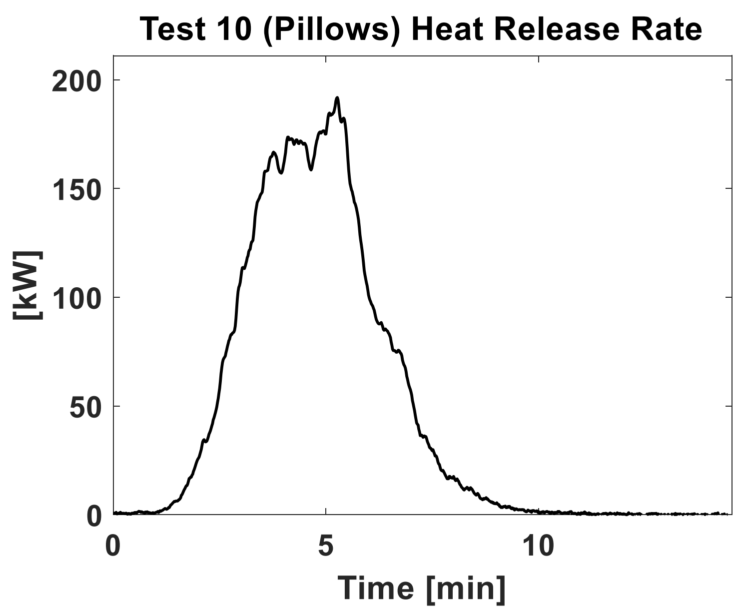


**Figure D 10: Heat Release Rate measurements during Test 10, four pillows with polypropylene foam inserts and polypropylene covers.**

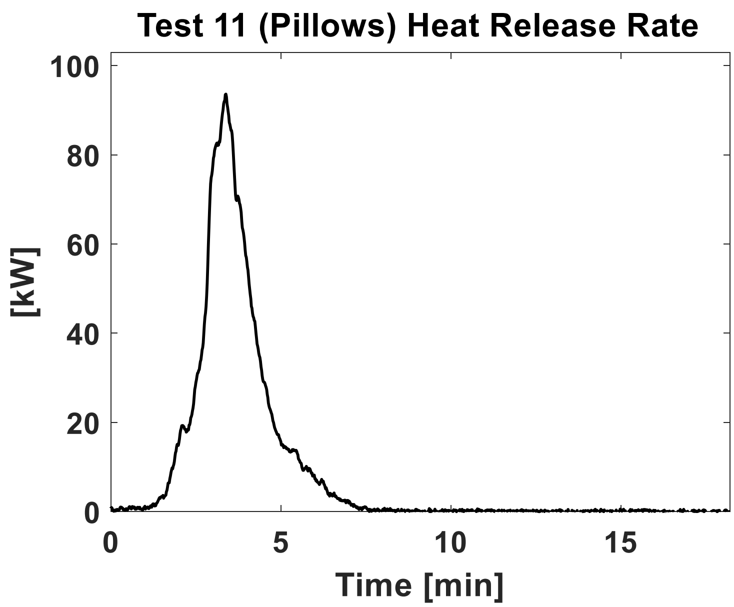


**Figure D 11: Heat Release Rate measurements during Test 11, a pillow with polypropylene foam insert and polypropylene cover.**

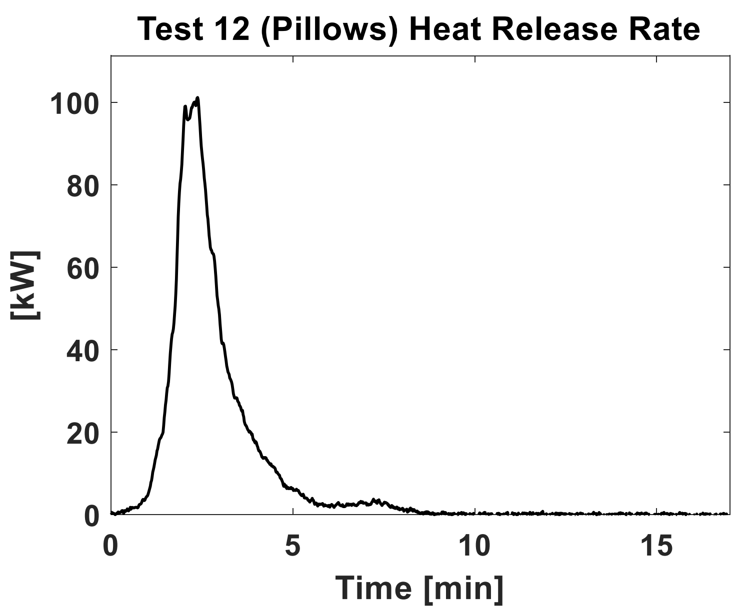


**Figure D 12: Heat Release Rate measurements during Test 12, a pillow with polypropylene foam insert and polypropylene cover.**

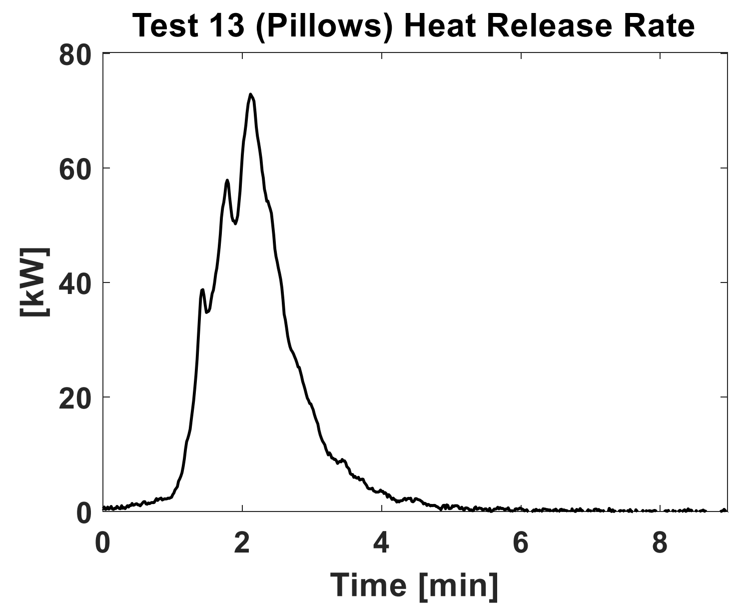


**Figure D 13: Heat Release Rate during Test 13, a pillow with polyester foam insert and polyester cover.**

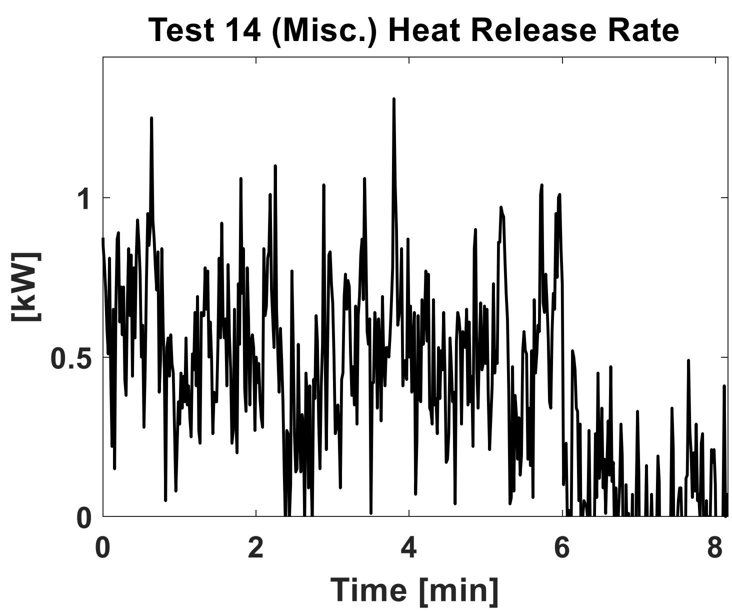


**Figure D 14: Heat Release Rate measurements during Test 14, a laptop.**

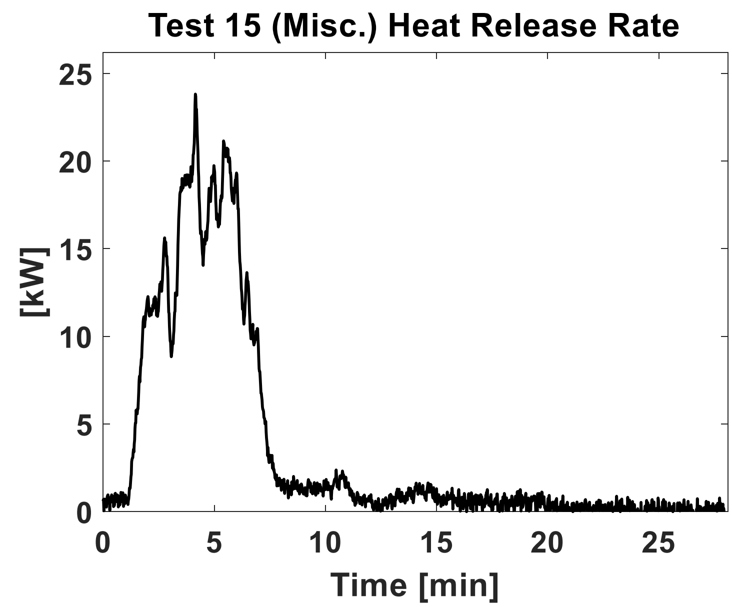


**Figure D 15: Heat Release Rate measurements during Test 15, a laptop on a pillow (polyester foam insert and polyester cover).**

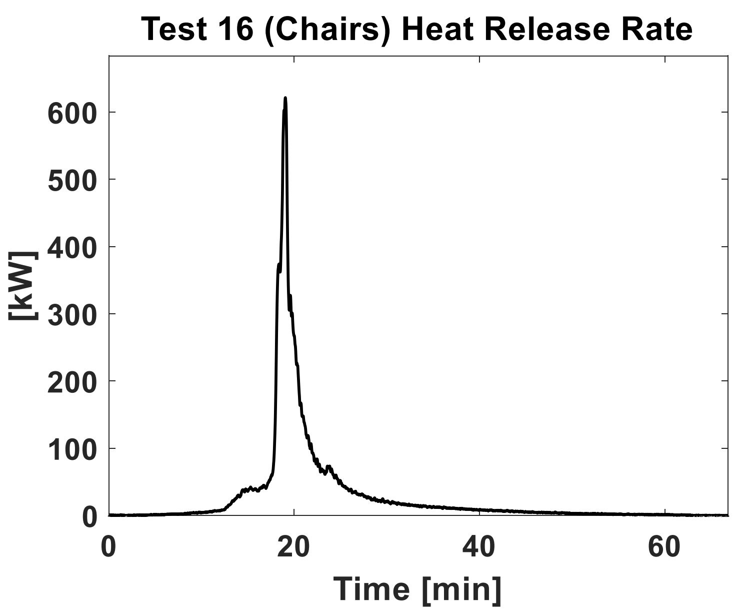


**Figure D 16: Heat Release Rate measurements during Test 16, a chair with polyurethane foam padding.**

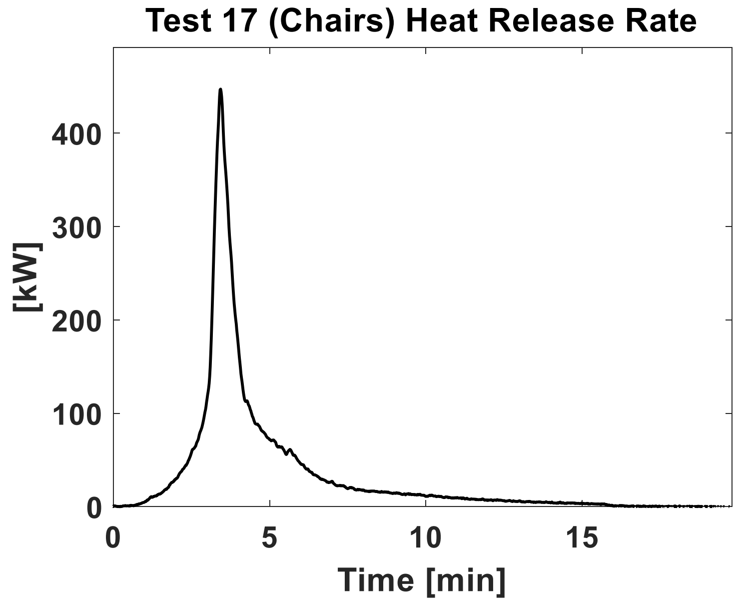


**Figure D 17: Heat Release Rate measurements during Test 17, a chair with polyurethane foam padding.**

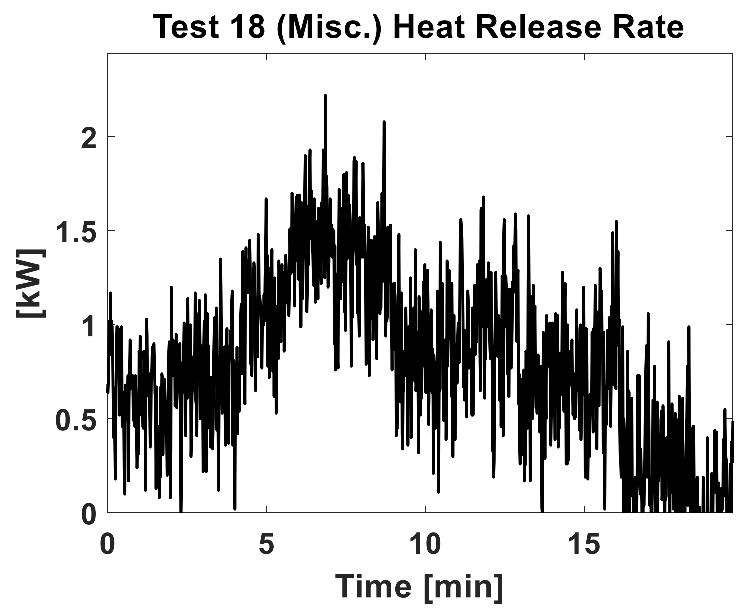


**Figure D 18: Heat Release Rate measurements during Test 18, a side table composed of particleboard.**

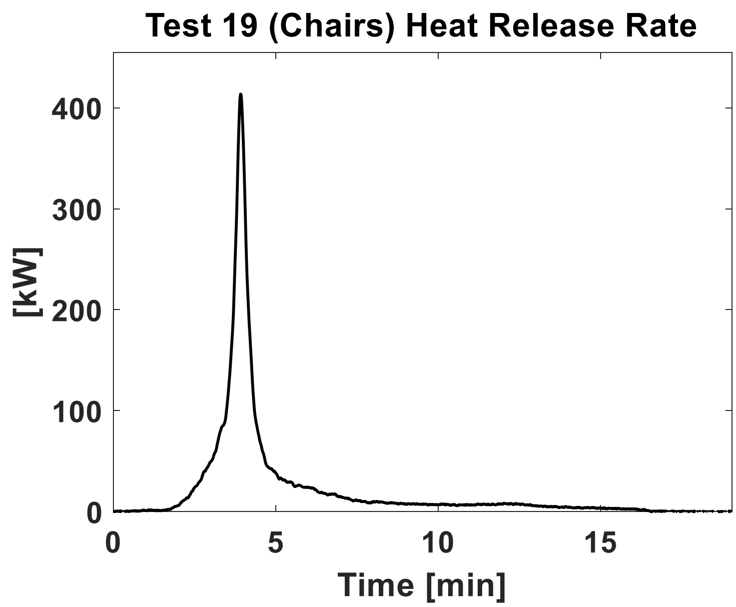


**Figure D 19: Heat Release Rate measurements during Test 19, a chair with polyurethane foam padding.**

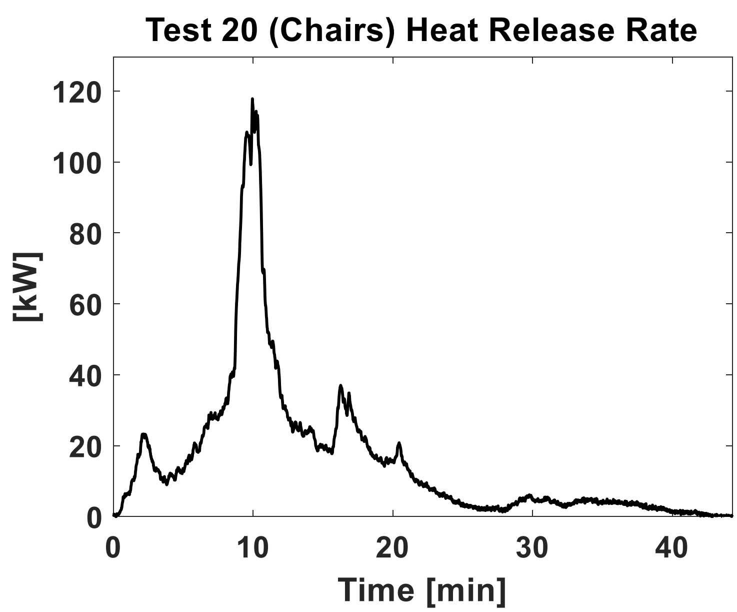


**Figure D 20: Heat Release Rate measurements during Test 20, a chair with polyurethane foam padding. and a wooden frame.**

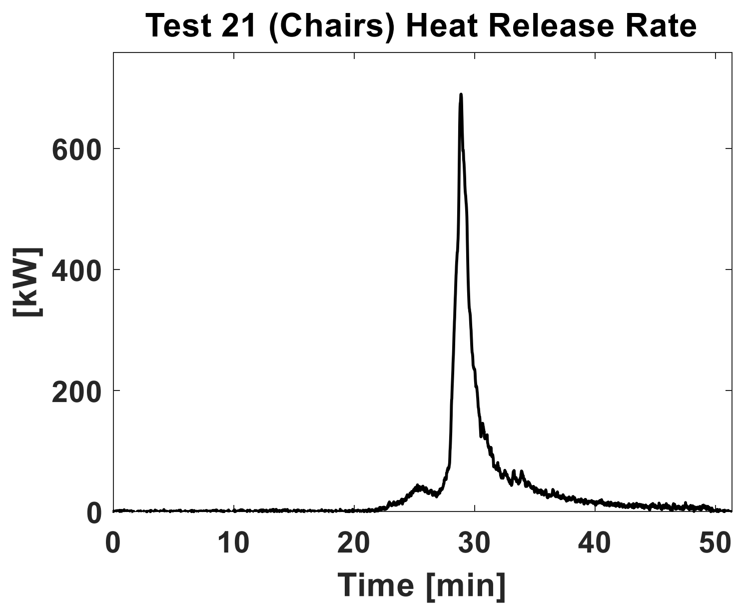


**Figure D 21: Heat Release Rate measurements during Test 21, a chair with polyurethane foam padding.**

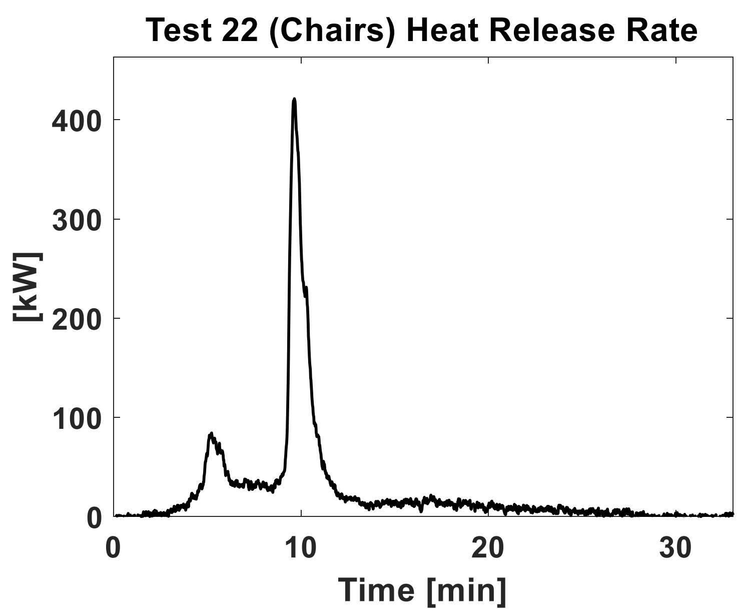


**Figure D 22: Heat Release Rate measurements during Test 22, a chair with polyurethane foam padding.**

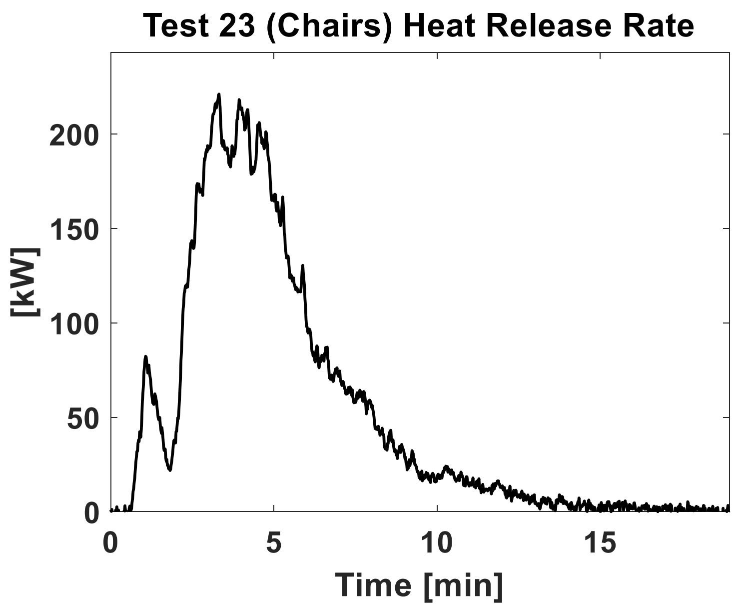


**Figure D 23: Heat Release Rate measurements during Test 23, a chair with expanded polystyrene beads (bean bag chair).**

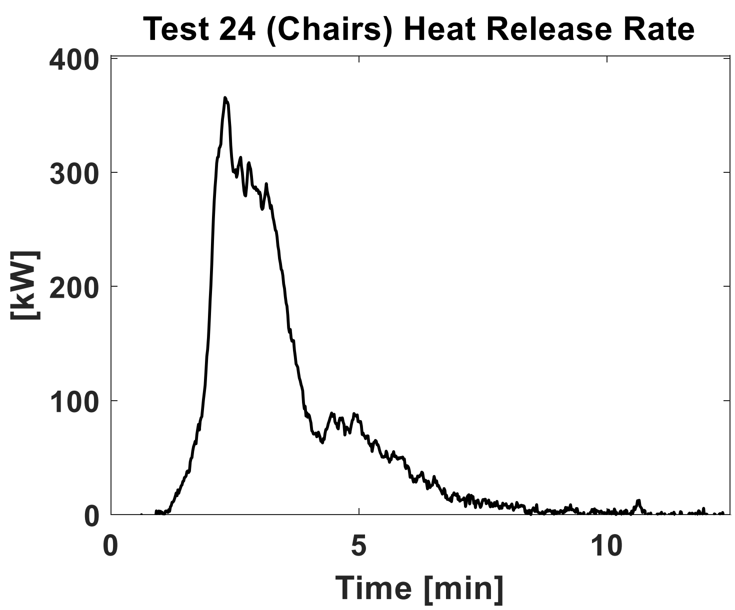


**Figure D 24: Heat Release Rate measurements during Test 24, a chair with polyurethane foam padding.**

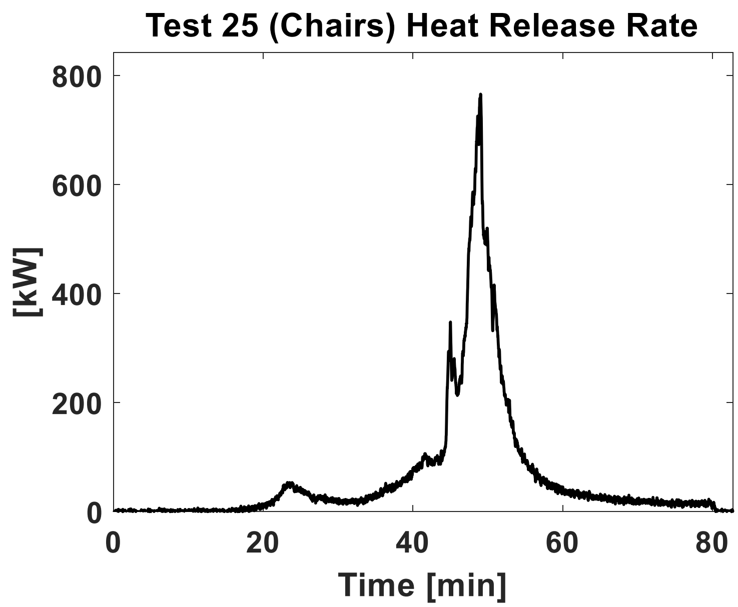


**Figure D 25: Heat Release Rate measurements during Test 25, a chair with polyurethane foam padding.**

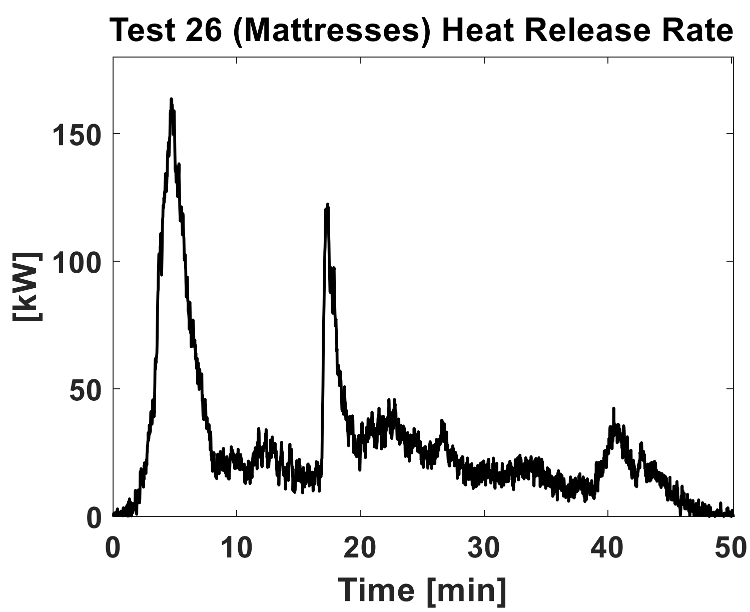


**Figure D 26: Heat Release Rate measurements during Test 26, a 15 cm (6'') thick mattress (inner spring) with 2 pillows.**

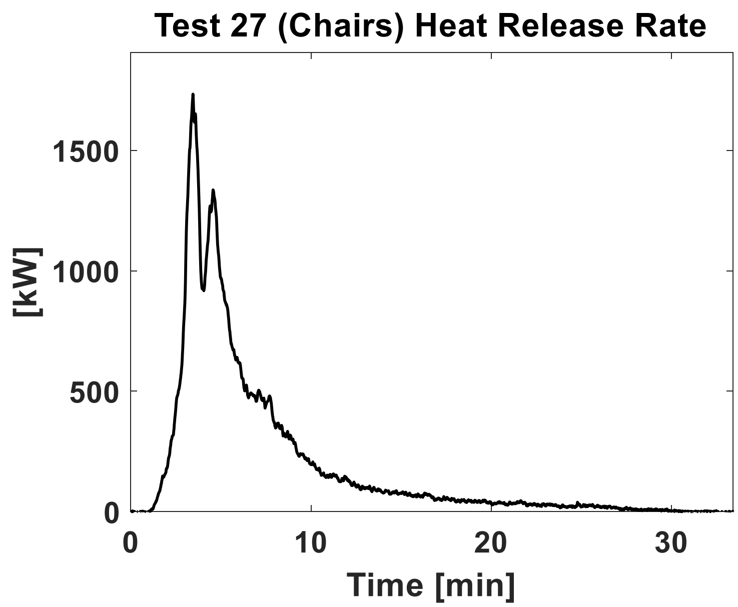


**Figure D 27: Heat Release Rate measurements during Test 27, a large armchair composed of a wood frame, polyurethane foam cushions, metal springs, thin fiberglass cloth with ignition at the bottom of the back cushion.**

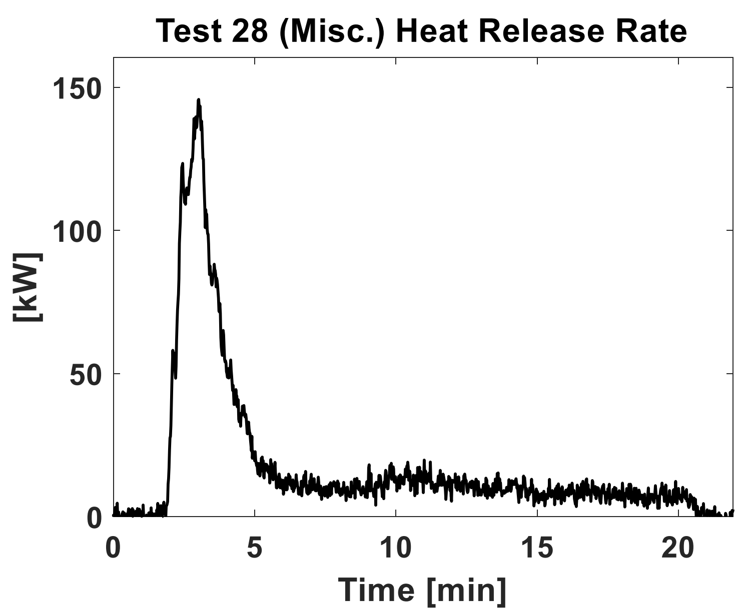


**Figure D 28: Heat Release Rate measurements during Test 28, a polypropylene carpet with two polyester foam pillows (identical to those used in Test 1).**

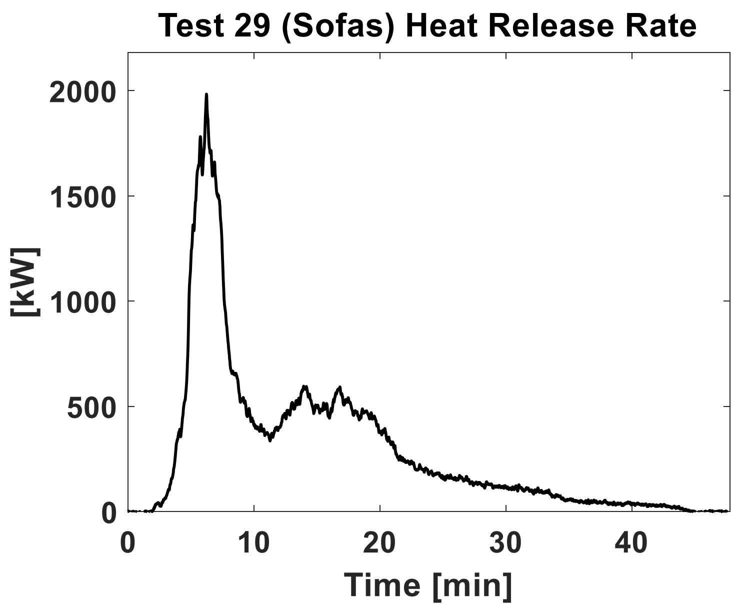


**Figure D 29: Heat Release Rate measurements during Test 29, Sofa A with modified seat cushion inserts. Pillows rested on each of the arm rests.**

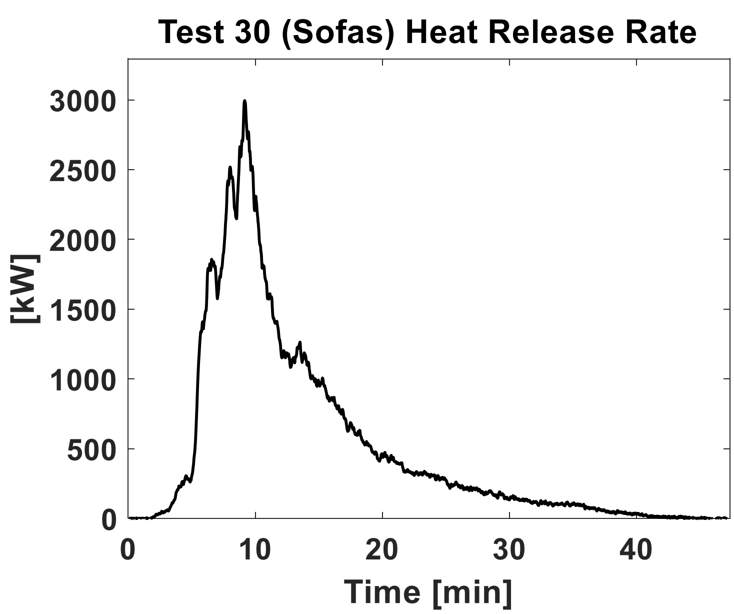


**Figure D 30: Heat Release Rate measurements during Test 30, Sofa B. Pillows rested on each of the arm rests.**

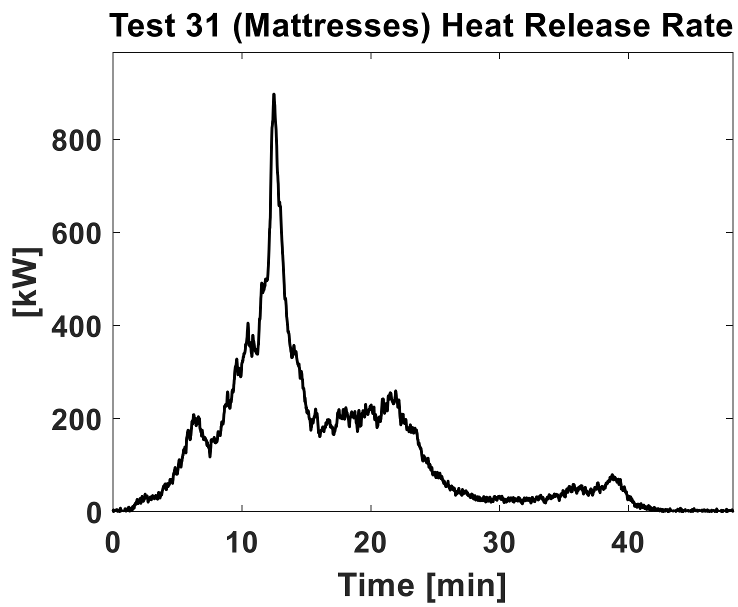


**Figure D 31: Heat Release Rate measurements during Test 31, a 15 cm (6'') thick queen size polyurethane foam mattress (Type B). Two pillows were placed on one end of the bed.**

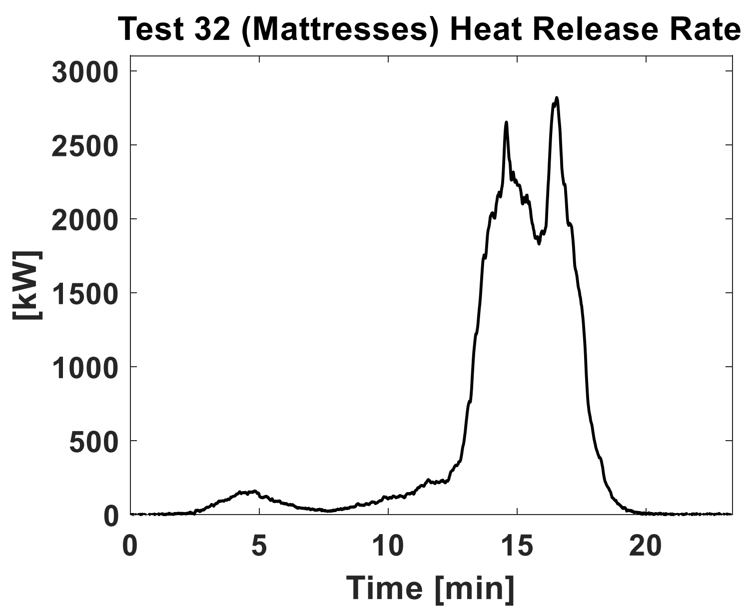


**Figure D 32: Heat Release Rate measurements during Test 32, a 30 cm (12'') thick queen size polyurethane foam mattress (Type C). Two pillows were placed on one end of the bed.**

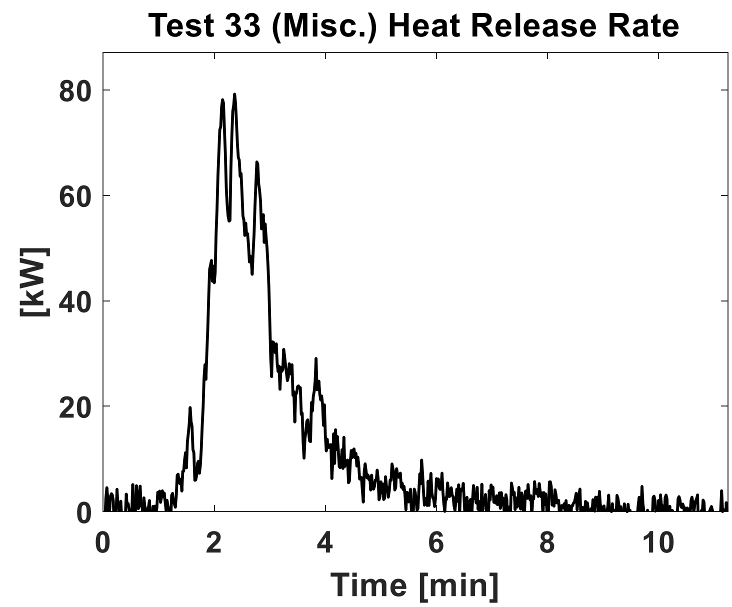


**Figure D 33: Heat Release Rate measurements during Test 33, a bookshelf with a pillow at the base.**

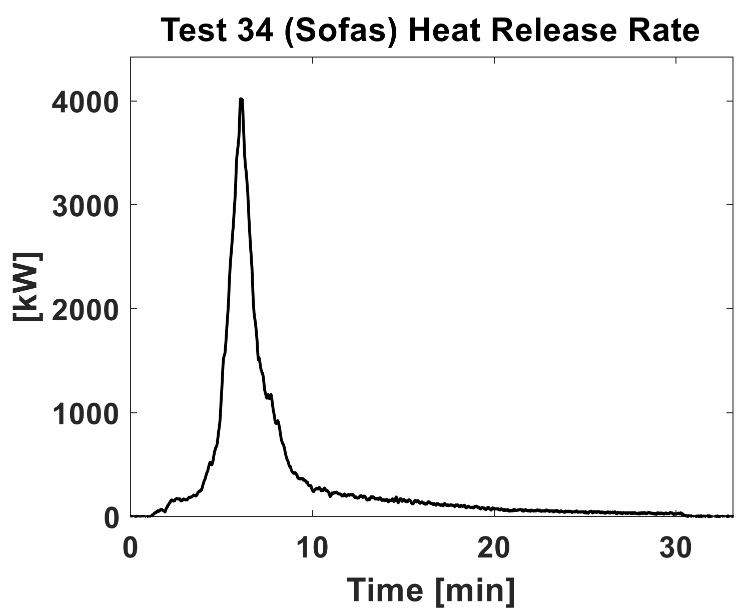


**Figure D 34: Heat Release Rate measurements during Test 34, Sofa C. Pillows rested on each of the arm rests.**

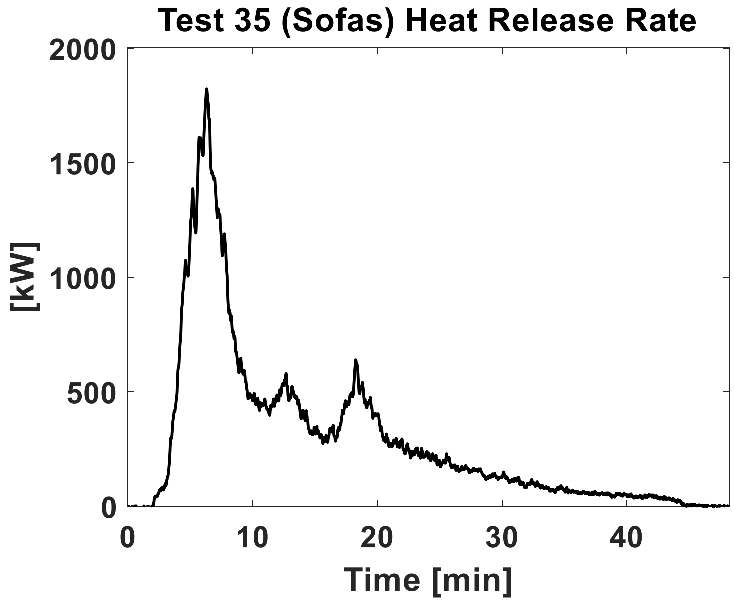


**Figure D 35: Heat Release Rate measurements during Test 35, Sofa A but with modified seat cushion inserts. Pillows rested on each of the arm rests.**

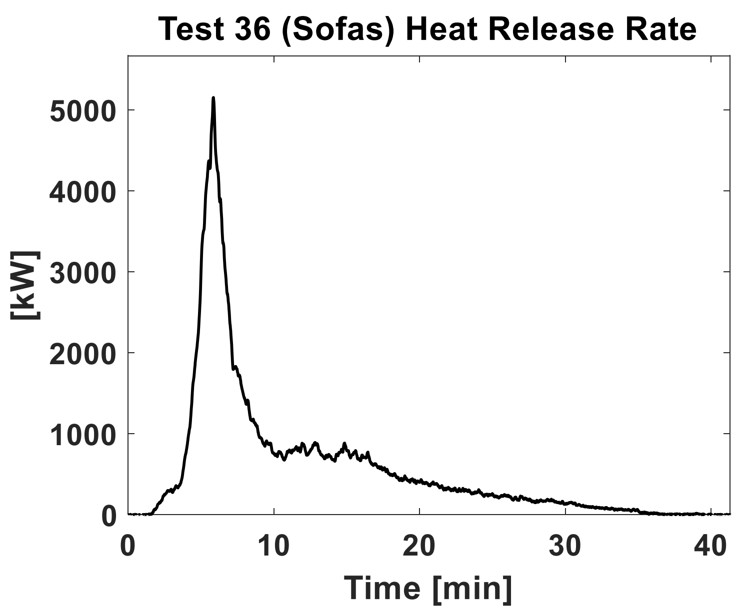


**Figure D 36: Heat Release Rate measurements during Test 36, Sofa B. Two Pillows rested on middle of the sofa adjacent to the back cushion.**

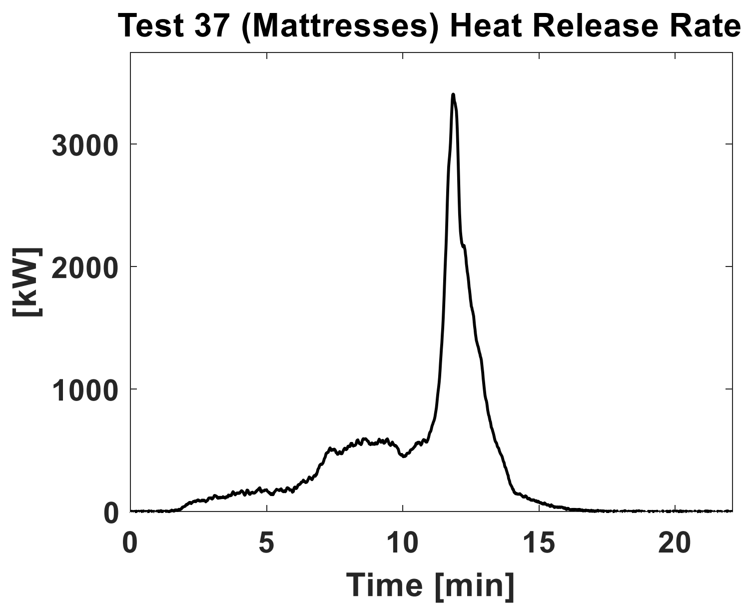


**Figure D 37: Heat Release Rate measurements during Test 37, a 15 cm (6'') thick queen size polyurethane foam mattress (Type B). The experiment was identical to Test 31 but the mattress was fitted with bedclothes including a polyester mattress cover, polyester top and bottom sheets, and a comforter with a polyester insert and cover. Two pillows were placed on one end of the bed.**

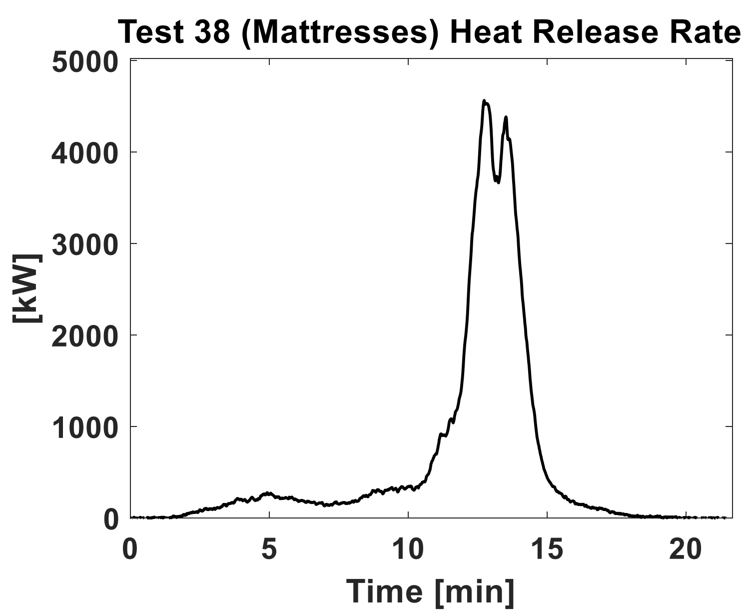


**Figure D 38: Heat Release Rate measurements during Test 38, a 30 cm (12'') thick queen size polyurethane foam mattress (Type C). The experiment was identical to Test 31, but the mattress was fitted with bedclothes.**

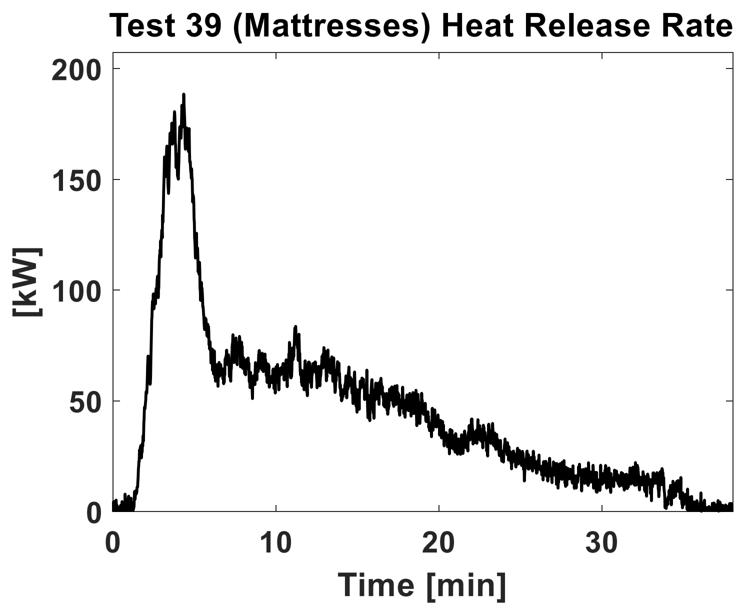


**Figure D 39: Heat Release Rate measurements during Test 39, a 15 cm (6'') thick queen inner spring mattress (Type A). The experiment was identical to Test 26, but the mattress was fitted with bedclothes.**

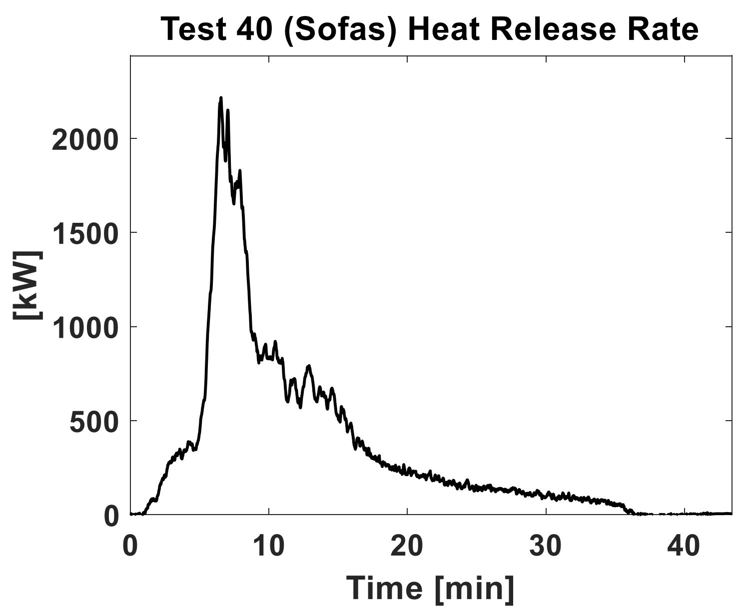


**Figure D 40: Heat Release Rate measurements during Test 40, Sofa A but with modified seat cushion inserts. Pillows rested on each of the arm rests.**

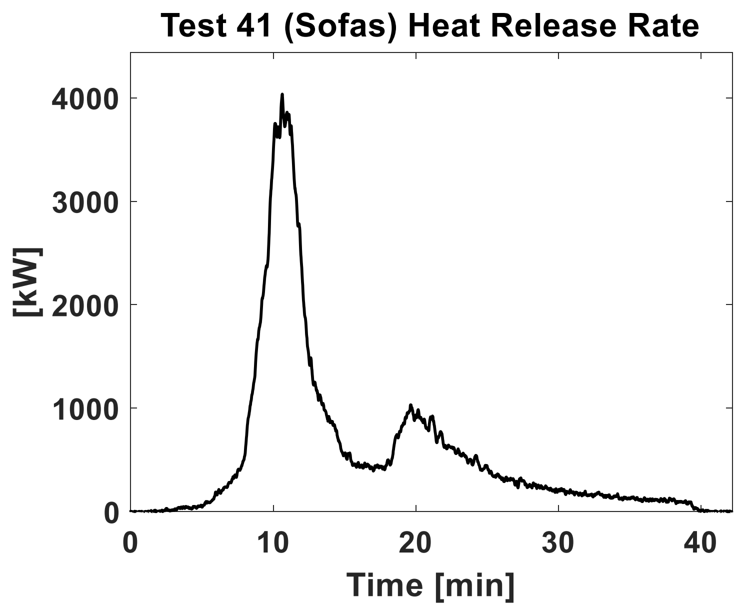


**Figure D 41: Heat Release Rate measurements during Test 41, Sofa B. One pillow rested on the left armrest and one behind the middle of the sofa on the floor.**

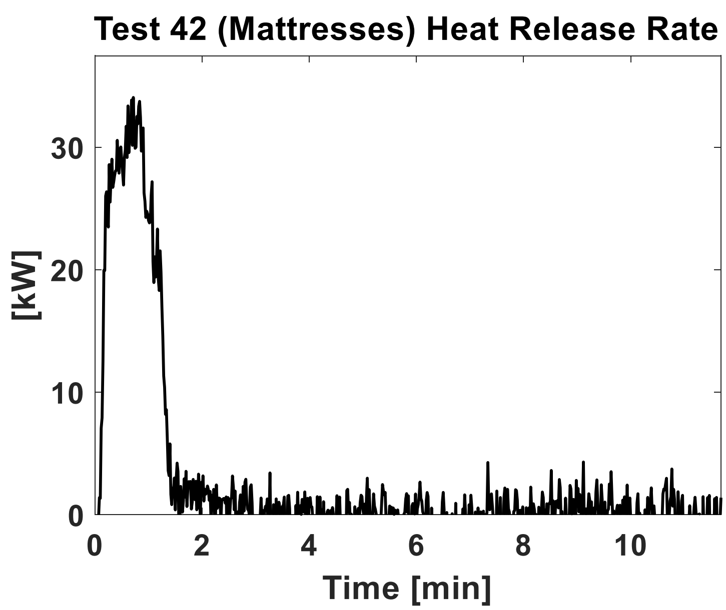


**Figure D 42: Heat Release Rate measurements during Test 42, a 30 cm (12'') thick queen size polyurethane foam mattress (Type C) undergoing the 16 CFR 1633 test protocol with top burner and side flame.**

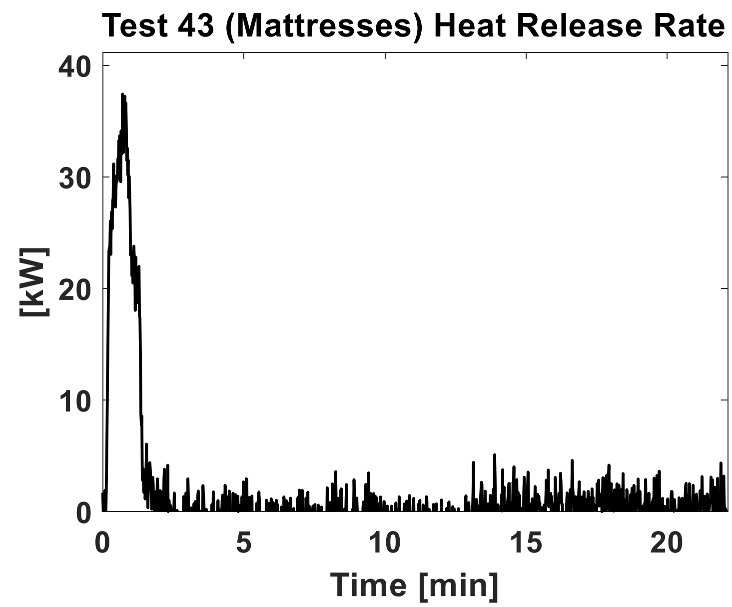


**Figure D 43: Heat Release Rate measurements during Test 43, a 30 cm (12'') thick queen size polyurethane foam mattress (Type C) undergoing the 16 CFR 1633 test protocol with top burner and side flame.**

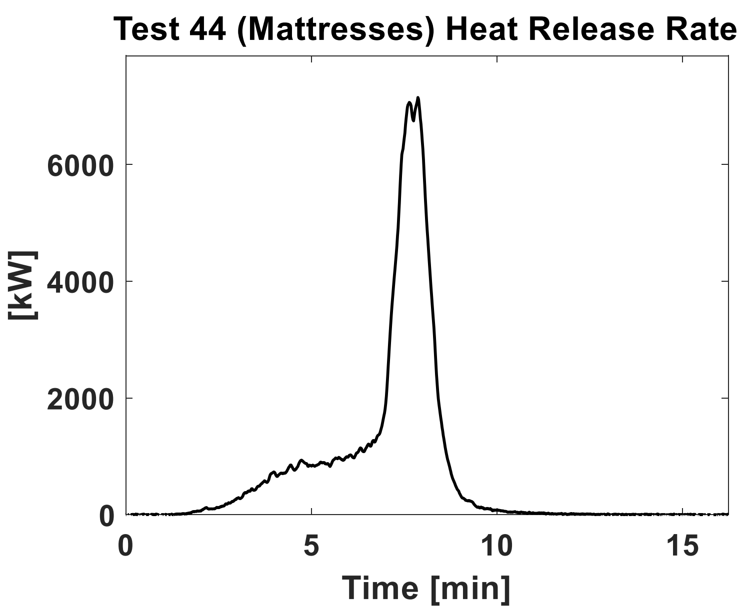


**Figure D 44: Heat Release Rate measurements during Test 44, a 30 cm (12'') thick queen size polyurethane foam mattress (Type C) with bedclothes with the mattress' FR sock removed.**

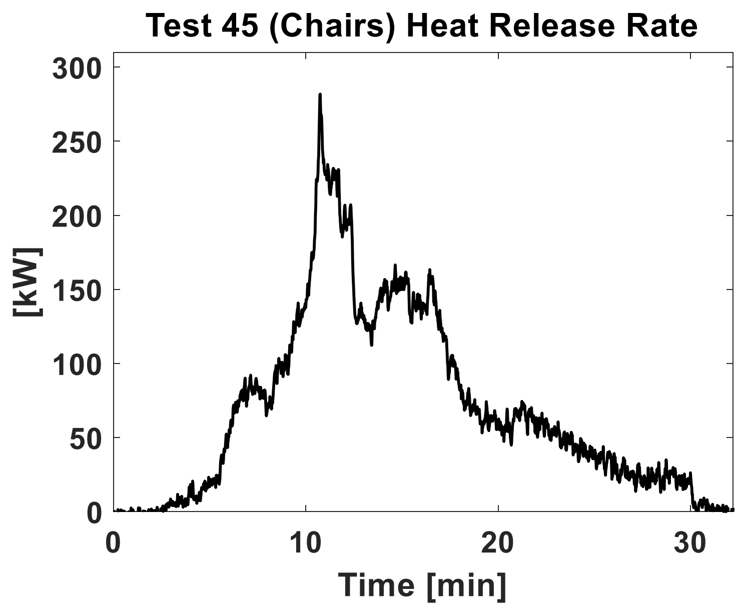


**Figure D 45: Heat Release Rate measurements during Test 45, a stack of chairs with polyurethane foam padding.**

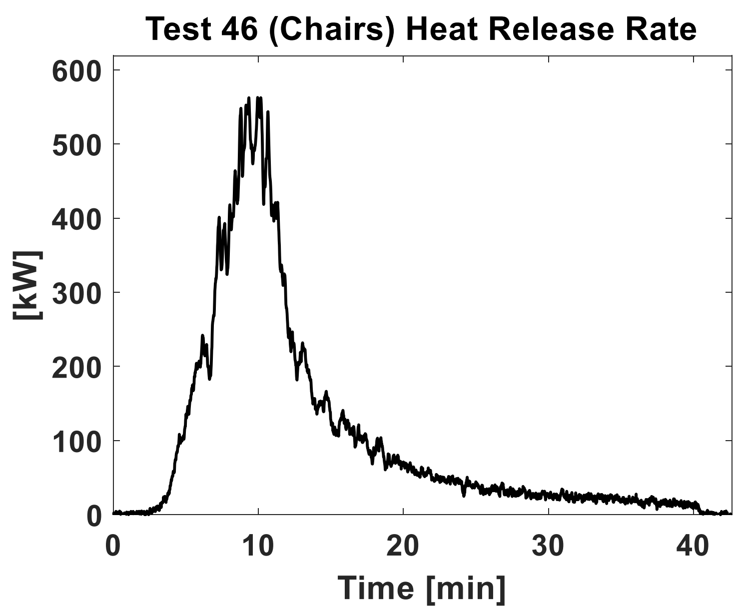


**Figure D 46: Heat Release Rate measurements during Test 46, an office chair with polyurethane foam padding.**

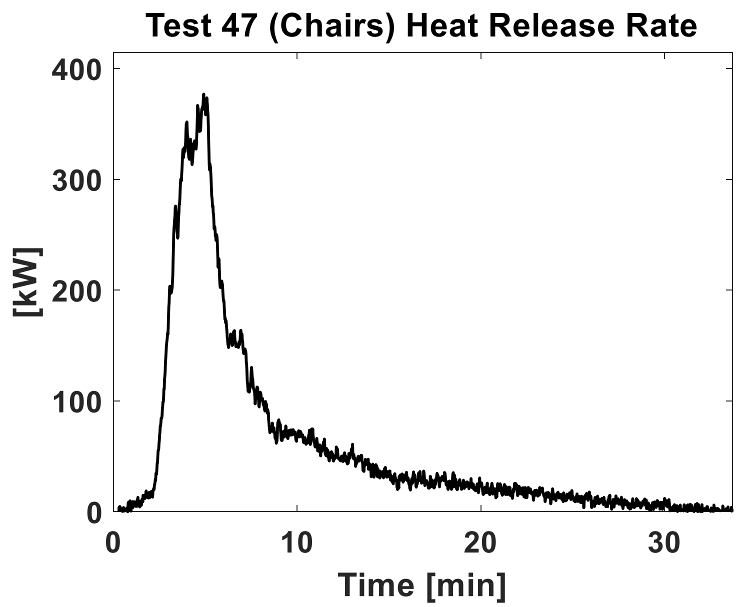


**Figure D 47: Heat Release Rate measurements during Test 47, a stack of three chairs with polyurethane foam padding.**

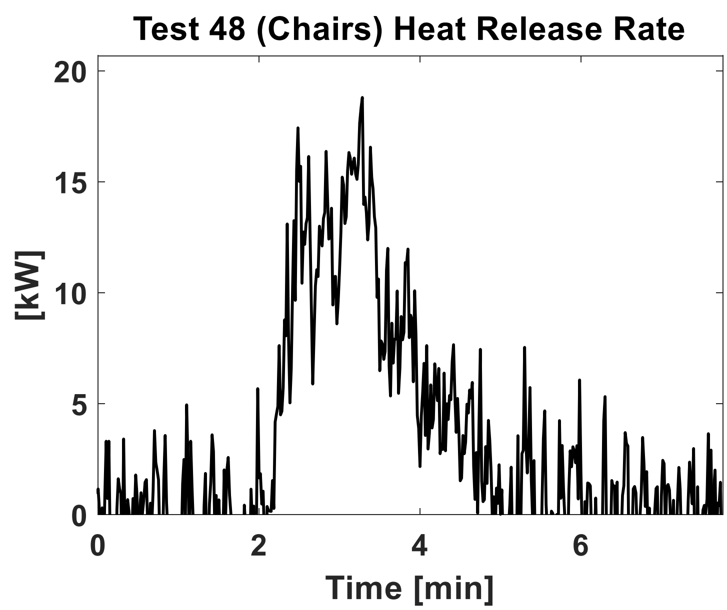


**Figure D 48: Heat Release Rate measurements during Test 48, an office chair with polyurethane foam padding.**